AD-A159 891 CONCEPTS FOR NEAR CONTINUOUS RECEPTION OF VHF (VERY HIGH FREQUENCY) SIGNA..(U) JAYCOR SAN DIEGO CA F FELBER ET AL. 15 JUL 85 JAYCOR-J200-85-875/2393 1/2

UNCLASSIFIED N00014-84-C-0730 F/G 17/2.1 NL

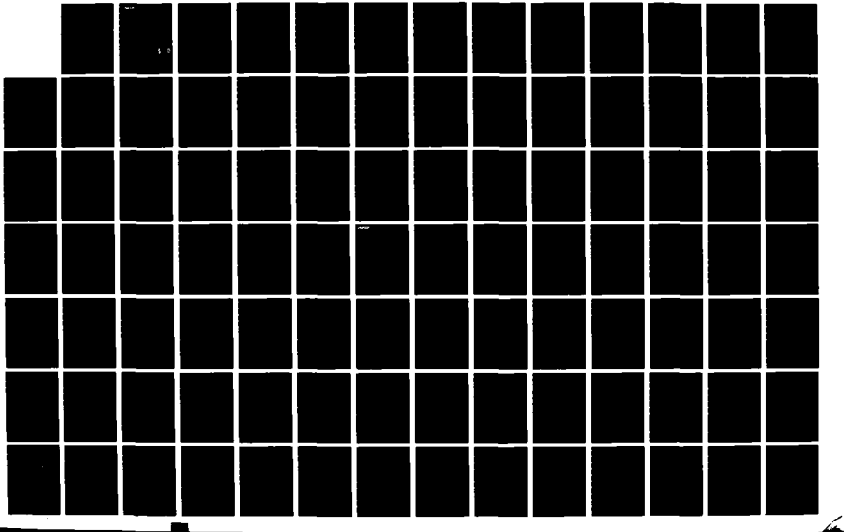

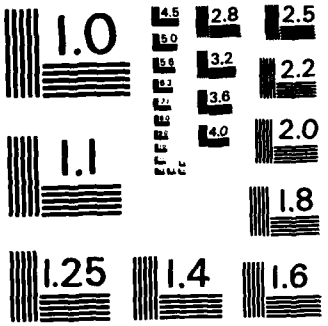

JAYCOR

(1)

FINAL TECHNICAL REPORT

CONCEPTS FOR NEAR CONTINUOUS RECEPTION OF VHF SIGNALS USING METEOR BURST PROPAGATION

by

F. Felber, H. Davis, R. Stahl, R. Wheeler, D. Wright

J200-85-875/2393

Submitted to:

Scientific Officer
Head, Electronics Division
Office of Naval Research
800 North Quincy Street
Arlington, VI 22217
ATTN: Dr. Fred W. Quelle
Ref: Contract Number: N00014-84-C-0737

15 July 1985

11011 Torreyana Road — Post Office Box 85154 • San Diego, California 92138-9259 • (619) 453-6580

CONTENTS

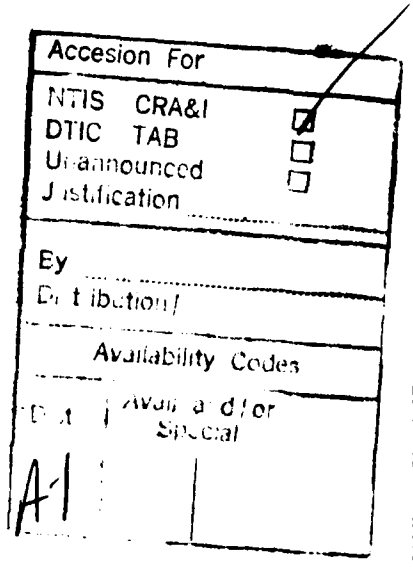

1.0 INTRODUCTION

This is the final technical report being submitted by JAYCOR to the Defense Advanced Research Projects Agency and Office of Naval Research under Contract N00014-84-C-0737, "Concepts for Near Continuous Reception of VHF Signals Using Meteor Burst Propagation."

This program has been sponsored by DARPA through the Office of Naval Research (Dr. Fred W. Quelle, Scientific Officer). The total cost and fixed fee estimated for this program was $240,057. The period of performance was from 18 September 1984 to 17 May 1985. The final report was due 16 July 1985. The program has been completed within budget and on schedule.

The objective of this program, as given in the original JAYCOR proposal, has been "to design experiments leading to the verification of diversity reception techniques for tactical C^2 signal collection." The results of this design effort are summarized in this final report. The experimental program that has been designed is referred to in this report as the VHF Reception Program -- Phase II. Similarly, the program that has just been completed is referred to as the Phase I program.

In the Phase I program, we have identified three key physics issues concerning diversity reception of meteor path propagation. These issues are:

- What is the gain vs. beamwidth tradeoff on a single receiver antenna?
- Can independent meteor propagation paths be obtained at a single location using multiple receiver antennas?
- What spatial separation is needed to obtain independent paths from a common volume?

We have determined in our Phase I program that these questions are the principal physics issues remaining to be resolved before a netted diversity reception system can be intelligently designed for testing of applications. The intended applications, which may include interception of noncooperative VHF communications from beyond the line-of-sight, will not be directly addressed by this program. To directly address applications would require a program designed with the parameters of the intended applications, and would require a much greater emphasis on signal processing and data

analysis. Such a program would attempt to demonstrate diversity gain (reliable signal from individually unusable signals), as well as network gain (simple combining of signals at a central processor) in a system closely resembling the system to be deployed in applications. Instead, the objective of Phase II experiments is to resolve the important physics issues with the simplest experiments and supporting modeling that can give a good understanding of the answers. If successful, the Phase II program would provide preparation sufficient to begin design of a full-scale demonstration of an efficient VHF diversity-reception network in some subsequent program.

Consistent with our perception of DARPA objectives, the Phase II program is the simplest that accomplishes the objectives without undue or unacceptable uncertainties in the results. The Phase II program features the following cost-saving measures:

- A single, central receiving site located on government property (GFE land use) within ten miles of the site where most of the manned test operations would be performed.
- Simple unmanned remote transmitter sites located on government property (GFE land use), and activated by telephone.
- Simple signal transmission, signal processing, and data analysis, avoiding a costly development program.

The Phase II experiments are conceptually simple. To address the gain vs. beamwidth tradeoff, one would use an array of eight receiving antennas at the receiving site to produce three distinct receiving beam patterns having widths of 10^{o}, 16^{o}, and 40^{o}. The corresponding antenna gains over isotropic are 18 dB, 16 dB, and 12 dB, respectively. Percent-copy would be measured for each beamwidth pointed at several locations with respect to the hot spot patterns. To address the question of independent meteor paths, one would operate several distinguishable transmitters simultaneously at distances from the receiver of 475 km up to 2000 km. The transmitters may be aimed at a common volume or at separate receiving sites. The correlation of the transmitted signals, which are just distinguishable tones on a continuous carriers of the same frequency would provide answers in the simplest manner to questions of spatial and angular diversity and path independence.

The independence of meteor paths is an unresolved issue because experiments to date have typically used beamwidths of 40^{o} to 50^{o}. With these wide beams it is known that even at distances of 35 km, antennas receive virtually identical information. The Phase II program would explore the possibility that narrow beams focussed on separate hot spots can receive uncorrelated information from independent meteor paths.

The gain vs. beamwidth tradeoff is unresolved for the same reason, namely, that narrow, high-gain receiving beams have not been tried in VHF meteor communications. The question is whether percent-copy can be enhanced by focusing a narrow beam onto a hot spot. Focusing reduces the solid angle subtended, but the higher gain increases the usable number of meteors per solid angle. In Phase II one would experimentally explore this tradeoff in order to determine the optimal receiving antenna configurations.

The model that we have developed in Phase I (see Section 2.2) has been exercised to simulate the Phase II experimental conditions. The model presently runs on an IBM PC and takes 5 to 8 hours per run. The runs have been done overnight at no direct cost to the Phase I program. Because the number of runs performed to date has been limited by time, the preliminary results are not comprehensive. The results of the code runs do suggest, however, that one may face some counter-intuitive surprises in Phase II.

At first we expected that by focusing with narrow beams on separate hot spots, we would obtain independent meteor paths from each hot spot. The code suggests, however, that there is a strong correlation between the hot spots, apparently owing to the effects of the antenna sidelobes.

We expect that based on the results of the experiments and further modeling in Phase II, it will be possible for communications systems designers to design the optimal receiving antennas and system configurations confidently for any application of VHF meteor communications.

Section 2 presents a technical discussion, which summarizes much of the Phase I work. The model developed by JAYCOR is described. Equipment requirements are delineated. A summary of our research on data correlation processing is presented, even though much of it will only be applied in a more advanced program that may follow a Phase II program. Section 3

discusses the technical issues that would be addressed by the Phase II program. Section 4 describes a program plan for Phase II.

2.0 TECHNICAL DISCUSSION

2.1 Meteor Communications/Background

As meteors enter the earth's atmosphere they form long columns of ionized particles. These columns diffuse rapidly and usually disappear after a few seconds. During their brief existence, however, the ionized columns will reflect radio signals, typically for hundreds of milliseconds, giving rise to what is variously referred to as meteor scatter, meteor propagation, or meteor burst communications. The radio waves can be scattered obliquely to provide beyond line-of-sight VHF radio communications over distances of as much as 2000 km (Villard et al., 1955). The frequency range for this mode of communication is 30 to 100 MHz (Oetting, 1980). The lower limit is the frequency at which the effects of ionospheric scatter become important. The upper limit is set by limitations of receiver sensitivity.

Meteor burst communications has a number of applications of potential value to the Department of Defense. One such application is the reception of noncooperative tactical VHF communications from beyond line-of-sight (BLOS), which is illustrated schematically in Figure 2.1. Depending on the percent-copy, or connectivity, the receiving system may be able to understand the message or context, or at least monitor communications traffic. Meteor burst communication systems have also been considered for jam-resistant and intercept-resistant applications, for determining the location of noncooperative transmitters, and for emergency communications networks. In this last regard, an important advantage of meteor burst communications is that "the nuclear surviviability of the meteor burst medium is superior to other BLOS media such as satellite and HF skywave..." (Oetting, 1980). Ionospheric disturbances associated with nuclear explosions often greatly increase D-layer absorption, which reduces the availability of HF communications relative to VHF.

Research in meteor burst communications has been sporadic in the past. The earliest report of a radio effect resulting from meteors was in 1931 (Pickard, 1931). However, it was not until 1946 that a clear correlation between radio signals and individual meteor trails was established (Hey and Stewart, 1946). Numerous field experiments on meteor burst communications were conducted during the 1950's (see Bailey et al., 1955, McKinley, 1961,

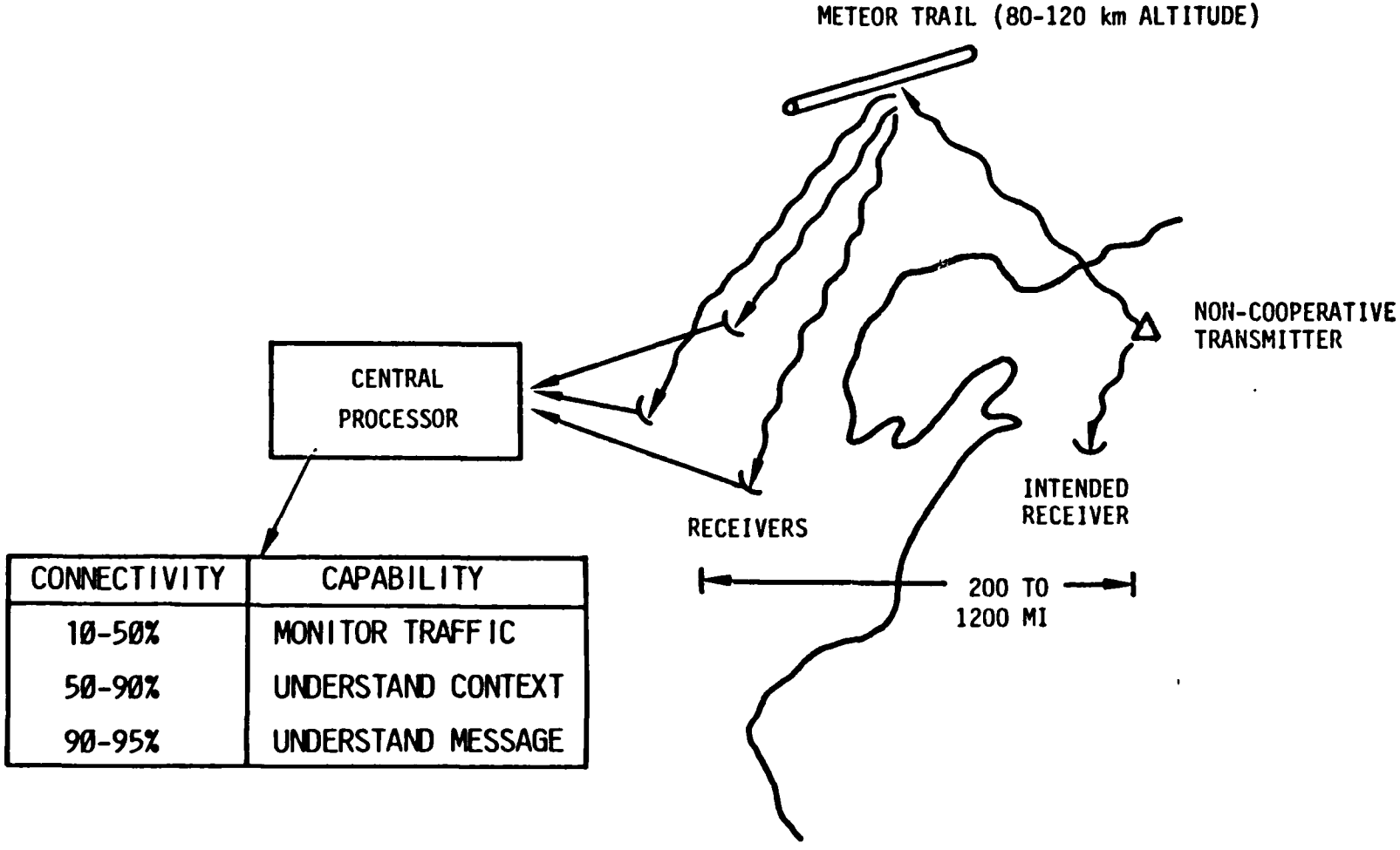

Figure 2.1. Schematic of VFH Reception Application

or Sugar, 1964 for brief histories). In the 1960's, the major investment in long range communications was in satellite systems, with meteor scatter development being largely disregarded. However, the advances in solid state and computer technologies in the 1970's resulted in meteor burst communication systems becoming competitive. The first large network, the Department of Agriculture's SNOTEL system, was developed to monitor 500 remote data acquisition stations by 2 master receiver stations using meteor burst communications (Vancil, 1984). Since then, numerous commercial message communication systems have been developed using meteor scatter (NOSC, 1980).

In any application, an improved percent-copy confers an advantage on the receiver. Near-continuous reception of noncooperative signals is not feasible with a single meteor-scatter receiver, because meteor burst communications involve inherently weak-signal systems. Typically, signal transmission and reception involves 90 dB attenuation of signal power, with another 80 dB or so lost upon scattering off a meteor trail.

The purpose of the Phase I program was to design an experiment to test systems in which percent-copy is improved by diversity reception. Diversity reception refers to any technique in which multiple antenna/receiver paths are utilized. Simple "network gain" is achieved through diversity reception by combining signals from all the receivers at a central processor. The processor gathers the received signals individually and "ors" the results. In this simple approach, no real diversity gain is achieved.

In Phase I, we assessed a more advanced approach to signal processing, in which "diversity gain" is achieved. "Diversity gain" is the extraction of a reliable signal from individually unuseable signals. This approach is described in Section 2.4. "Diversity gain" will not be demonstrated in Phase II, because the developmental effort required in data correlation processing was not deemed to be warranted until the significant physics issues have been resolved.

As a result of the experimental work done in the 1950's and early 1960's, there are numerous empirical approximations to the performance of meteor burst communication systems. Two approximations for the performance of systems are found in Oetting (1980) and NOSC (1980). Several computer codes are in use, such as the Department of Commerce Meteor Burst

Communications Model (Haakinson, 1983), which utilize these approximations to estimate the throughput of a system.

The empirical approximations to the performance of meteor burst communication systems are scaled results from existing experiments. This approach restricts the application of the approximations to systems similar to the experiments used as the baseline data, and from which the results are scaled. Consequently, only simple questions relating to parameters affecting the performance of a meteor burst communications system can be answered reliably using such an approach to modeling, and inter-relationships between parameters remain uncertain.

To help resolve physics issues and design effective meteor scatter experiments, a computer code was developed in Phase I to simulate meteor burst communication links realistically and reliably. This code, and the model upon which it is based, is described in the next subsection. The code should be upgraded and extensively implemented in a Phase II program.

2.2 Modeling

The Meteor Burst Communications Simulation (MBCS) code, developed by JAYCOR in Phase I, incorporates many details of a communications system to allow the Monte Carlo simulation of the response of this system by randomly generated meteor paths. The code operates on an IBM-PC or compatible microcomputer, and is self prompting. First, the user inputs into a file the horizontal beamwidth and offset angle for both the receiving and transmitting antennas and the vertical beamwidth and takeoff angle for both the receiving and transmitting antennas. (The code, as presently configured, assumes a standard dipole antenna radiation pattern.) Then, the code requests, in order:

- the latitude and longitude of the transmitter
- the latitude and longitude of the receiver
- the Greenwich Mean Time for which the simulation is to be performed
- the date for which the simulation is to be performed (only the month and day of month are required)
- the frequency (in MHz) at which the transmission is to be simulated
- the threshold at which the receiving amplifier will detect a signal (in Watts).

ıe computer code opens an ascii file labeled "mbrec.dat" which at the ɔmpletion of execution contains records of 100 valid meteor reflections. ıe record includes time of reflection, peak power, and duration of the ignal (time the signal was above the threshold). The code also simulates he arrival of meteors in the earth's atmosphere in a realistic manner hich reflects the effects of the day of the year, the time of day, atitude, etc., on the meteor arrival process. The output then is a time-ɔmain weighting that can be used, for any given input signal, to compute he received signal. With such a computer code, detailed questions elating to antenna design and orientation, diurnal effects, redundancy, andwidth, etc., and their inter-relationships, can be studied.

MBCS was developed to be transportable and readable. The code was eveloped in FORTRAN-77 on an IBM PC compatible computer. The only xception to the use of FORTRAN-77 was the random number generator, which ad to be developed in Assembler. However, the main code and the random umber generator will operate on any reliable IBM PC compatible computer. 'he code was further developed following the precepts of structured rogramming to make the code easily understandable.

This subsection describes the function and operation of MBCS and the 'eatures of the underlying model. The required upgrading of the code and ts implementation in Phase II will be discussed in Section 3.

Figure 2.2 illustrates the geometry used in the model. In this 'igure, the following lines and curves are illustrated: P_1 is the plane lefined by the scattering point M, the transmitter site T, and the receiver ;ite R. The geometrical condition of scattering is that the meteor trail, illustrated in the figure as m, be in a plane tangent to the ellipsoid lefined by the foci, R and T, and the point M. This plane is defined as P_2, and m is a ray in that plane. The ellipse E_1 is defined by the Intersection of the ellipsoid and the plane P_1. Clearly P_1 is ɔerpendicular to P_2. The scattering half angle is measured in the plane P_1. It is important to realize that the geometric condition of scatter loes not demand that P_1 be perpendicular to the earth's surface, S. If P_3 is defined as the plane including the verticals at R and T through R and T, :hen P_3 may be tilted with respect to P_1, as shown in Figure 2.2. The ɔlanes P_1 and P_3 intersect in a straight line through R and T.

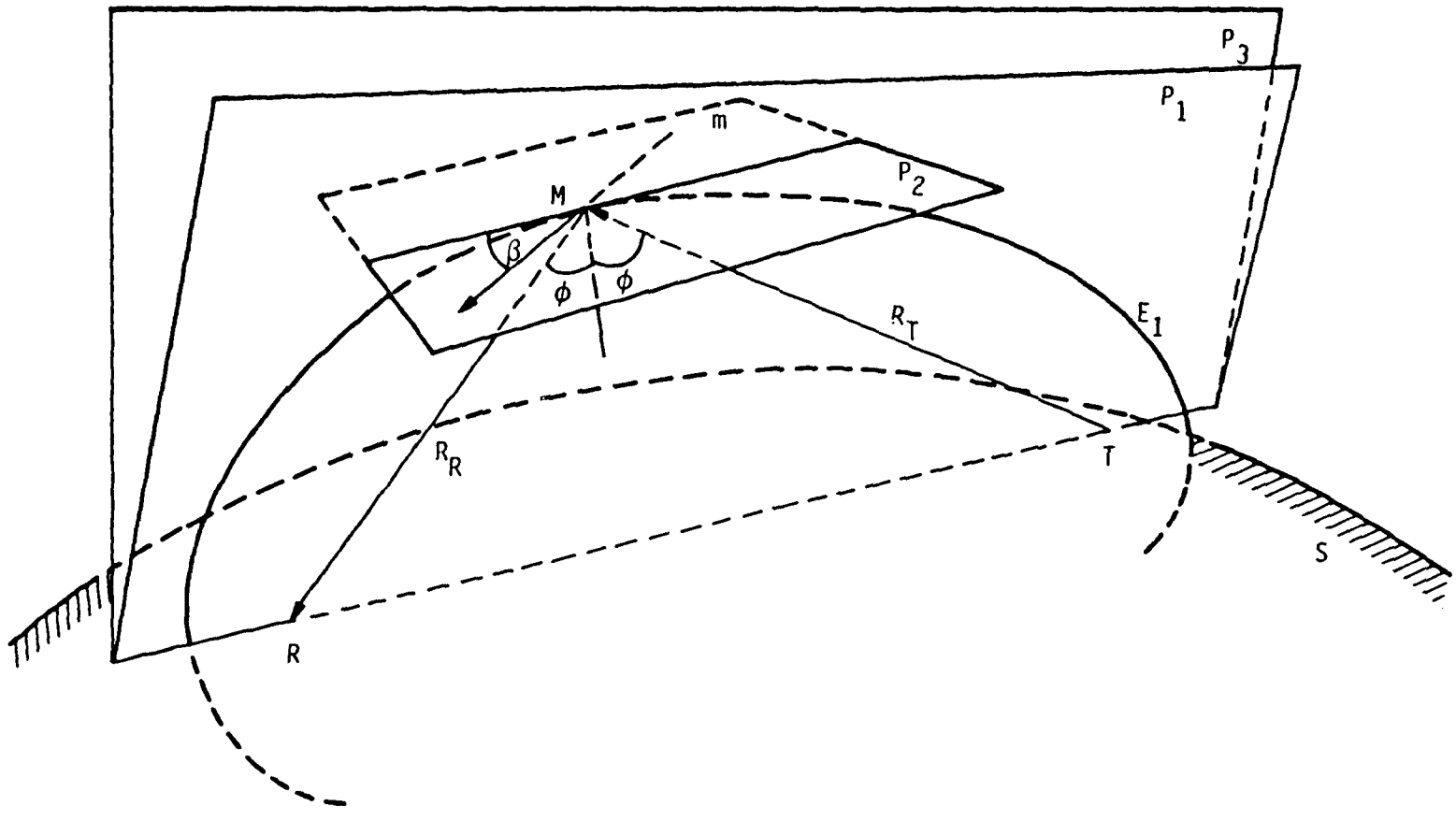

RE-08235

Figure 2.2. Scattering Geometries

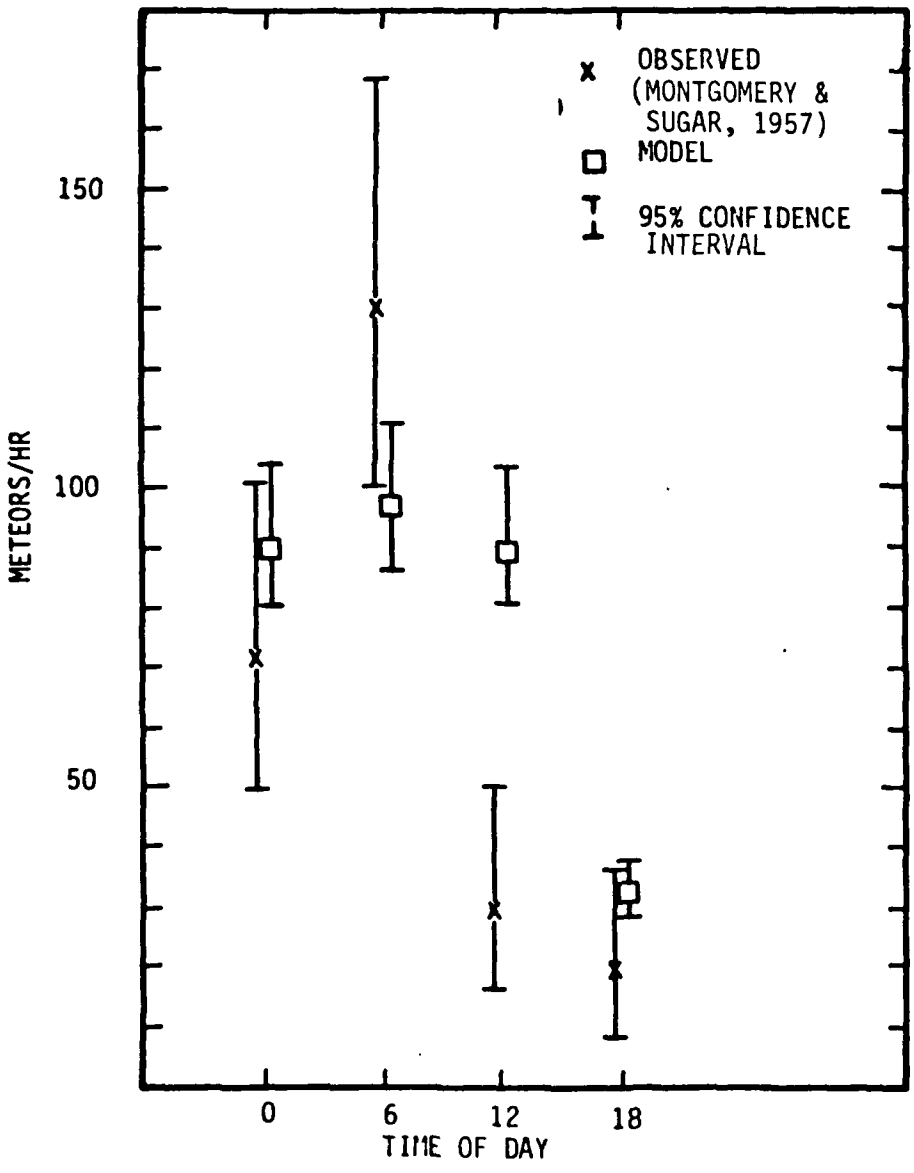

Figure 2.9. Comparison of Simulation Code with Experiments — Diurnal Variation

used rhombic antennas oriented along a line intersecting the two stations, with their main lobes intersecting at a point 100 km above the earth midway between the two stations. The European system used half-wave dipoles, with two receiving antennas at Winkfield so that phase differences could be used to infer the azimuthal bearing to the point of reflection. Data was collected for the European system at 37 and 70 MHz.

The first validation run studied the diurnal cycle effect. Daily data is published for the NBS system in Montgomery and Sugar (1957) for the time periods 6-7 May, 18-19 June, and 11-12 August, all in 1952. The Eta Aquarid meteor shower occurs during the 6-7 May period, and the Persid shower occurs during the 11-12 August period. Since no unusual meteor activity occurs during the 18-19 June period, these data were used to make comparisons. The NBS data were collected for 28 minutes, and extrapolated to an hourly rate. Assuming a Poisson distribution arrival process for the meteors during the 28 minute period, it is possible to compute confidence limits on the meteor rate published in Montgomery and Sugar (1957). Likewise, the meteor process generated by the computer code is simulated as a Poisson process, with the time required to generate 100 valid reflections (where the transmission link exceeded a given threshold) recorded, and so a confidence interval can also be generated for the computer code results. The observed and generated rates, with 95% confidence intervals, are presented in Figure 2.9. The only serious difference between the computer output and the observed data is for the 12:00 data. As the geometries for the noon and midnight periods are the same, comparable rates are usually observed for these two periods, which tends to validate the computer results and to suggest a possible equipment problem for the observed data.

The annual cycle in meteor rates was studied next. The annual cycle in meteor arrival rates most typically quoted is that of Hawkins (1956), which separates sporadic rates from shower rates. However, no information is given about how the data were collected, so it is not possible to construct confidence intervals about the Hawkins estimate of annual cycle. Since no information is given on the equipment used to gather the Hawkins' data, the NBS system was simulated with the meteor arrival rate adjusted to give the same annual mean number of meteors as reported in Figure 2.7. Figure 2.10 shows the meteor rate (daily average value of the meteors per hour) for mid-January, March, May, July, Sept., and Nov., as given in

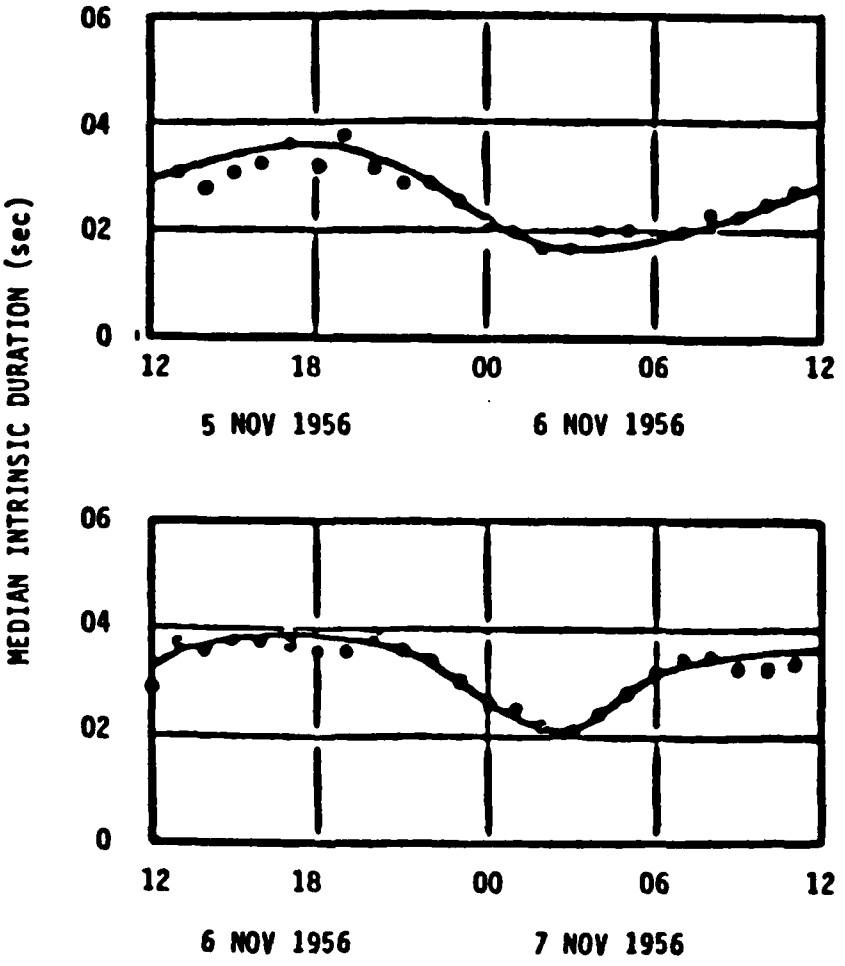

(From Sugar, Proc. IEEE, 1964)

Figure 2.8. Diurnal Variation of Duration of Underdense Meteor Bursts

the foci R and T (see Figure 2.2). A valid reflection will be received when the angle between that plane and the meteor path is less than

$$\psi_m = \frac{L(R_T + R_R)}{4R_T R_R \cos\phi}\,(1 - \sin^2\phi\cos^2\beta)$$

where L is the length of the meteor trail, and the remaining symbols are as defined in Figure 2.2 (Eshleman and Manning, 1954).

The initial radius of the trail is assumed to be 14 ionic mean free paths (Manning, 1958). According to this assumption, the initial radius varies exponentially from 1.3 cm at 80 km to 12.6 m at 120 km. While there is some empirical evidence that the initial radius may be larger at the lower altitudes (Sugar, 1964), the distribution of signal duration was found to better fit the data using the Manning hypothesis. The excellent agreement of the MBCS code with experiments on mean duration, which is about to be demonstrated, could only be obtained using the Manning hypothesis.

Once the trail is formed, it expands by diffusion at a relatively low rate, producing a radial distribution of material that is approximately Gaussian. The quantity $(4\,Dt + r_o^2)^{1/2}$ may be taken as the approximate radius of the trail after a time t. Here D is the diffusion coefficient and r_o is the initial radius of the trail. The mean daily value of D varies logarithmically from 1 m^2/sec at 85 km height to 140 m^2/sec at 115 km (Greenhow and Neufeld, 1955). As the variation in D is in fact due the variation in air density, there is also a small diurnal and annual variation in D, which has not yet been incorporated into the computer code. The diurnal variation in D contributes to a diurnal variation in the duration of meteor bursts, which is shown in Figure 2.8 (Sugar, 1964).

The JAYCOR MBCS code has been benchmarked by performing several simulations to compare the computer code results with published data. A difficulty that arose was finding quality data combined with adequate system details to perform a computer simulation. The two systems that were used, both of which involved some compromises, were the National Bureau of Standards system operating between Cedar Rapids, IW, and Sterling, VA (Montgomery and Sugar, 1957), and a system operating between Gibraltar and Winkfield, England (Bain, 1960). The NBS system operated at 49.8 MHz. It

coordinates but with magnitude 42 km/sec, and rejecting those meteors not moving towards the earth.

As a meteoric particle enters the earth's atmosphere it collides with air molecules, which then become trapped in its surface. The impact energy produces heat, which evaporates atoms from the meteor. The atoms move off with a velocity in the earth's reference frame that is substantially equal to that of the meteor. Collisions between these high velocity atoms and the surrounding air result in the production of heat, light, and ionization, distributed in the form of a long, thin, paraboloid of revolution with the meteoric particle at the head. The electron line density in the trail is proportional to the mass of the particle (see Figure 2.3 and Table 2.1). In the evaporation process each impact of an air molecule frees many meteoric atoms. Thus the total mass of air molecules striking the meteor is small compared to the meteoric mass. As a consequence the velocity of the meteor remains quite constant until the meteor is nearly completely evaporated (Sugar, 1964).

As a meteoric particle approaches the earth no appreciable ionization is formed until the particle enters the relatively dense air at heights below about 120 km. Above that height collisions of the particles with air molecules are not frequent enough to be of significance. As the particle traverses the region below 120 km, it vaporizes rapidly and most particles are completely evaporated before reaching 80 km. The higher velocity particles produce trails at slightly higher altitudes. Larger mass particles produce trails at lower altitudes. Paths with greater angle of incidence also tend to produce trails at higher altitudes (Greenhow and Hall, 1960).

The length of a meteor trail is primarily dependent on the mass of the meteoric particle and its angle of incidence onto the earth's atmosphere (zenith angle). The most likely length for a trail formed by a sporadic meteor is 15 sec(z), where z is the zenith angle (Eshleman, 1957). A more realistic distribution of lengths will be incorporated into future versions of the code.

The observability of the forward scattered reflection from a meteor trail is a function of whether the reflection is within the principal Fresnel zone. The center of the principal Fresnel zone occurs where a meteor path lies exactly within a plane tangent to the ellipsoid defined by

The computer code MBCS uses the inverse power distribution to randomly generate particle masses, but uses the relationship between mass and density given in Table 2.1.

To a reasonable approximation, the meteors can be treated as being isotropically distributed both in space and in velocity to simulate the meteor arrival process at a fixed time. Although there is some apparent variation in the spatial density of meteors along the earth's orbit, as depicted in Figure 2.6, this is a slowly varying annual cycle which will not change over any small segment of time. There is also evidence of a variation in the density of the meteors about the ecliptic, with the meteoric particles tending to lie in the same ecliptic plane about the sun as does the earth (Bain, 1960, Meeks and James, 1957). The former variation is significant, with as much as a factor of 2.3 increase in the density in July. Hence this factor is accounted for in the computer code as affecting the rate of meteor arrival as a function of date. The concentration of meteoric particles near the ecliptic has been found to be a minor effect, however, with the isotropic model giving an adequate fit to the data (Bain, 1960). The arrival of meteors in the earth's atmosphere is then modeled as a Poisson arrival process, with the rate of arrival a function of the day of the year. The number of valid reflections is further modified by other pertinent factors, as described below.

The meteors also can be modeled as isotropic in direction of travel; but tend to have velocities near 42 km/sec, which is the escape velocity for a particle leaving the solar system. The earth travels about the sun at a velocity of 30 km/sec, resulting in meteors entering the atmosphere with velocities ranging from 11.3 to 72 km/sec (Sugar, 1964). The computer code generates random velocity vectors uniformly on a sphere in velocity space of radius 42 km/sec, and then subtracts the earth's velocity vector to obtain a geocentric velocity vector for the meteoric particle. Those velocity vectors not directed towards the earth are then rejected. This method of considering a meteor's velocity relative to the earth's velocity, and rejecting all meteors not moving towards the earth, properly accounts for the diurnal cycle, latitude effect, and seasonal declination effect. The computer code accomplishes this by generating meteor locations uniformly on a sphere in configuration space of 100 km height above the earth's surface, generating the velocity vectors uniformly in polar

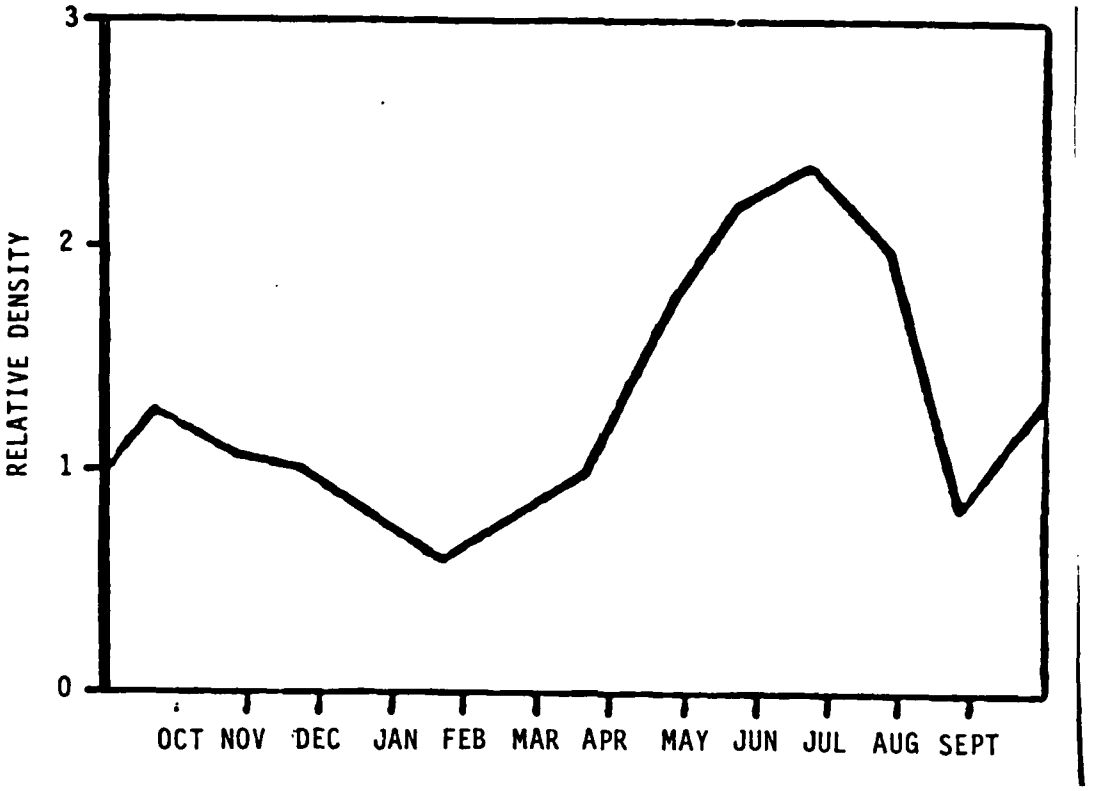

Figure 2.6. Variation in the Space Density of Meteors Along the Earth's Orbit

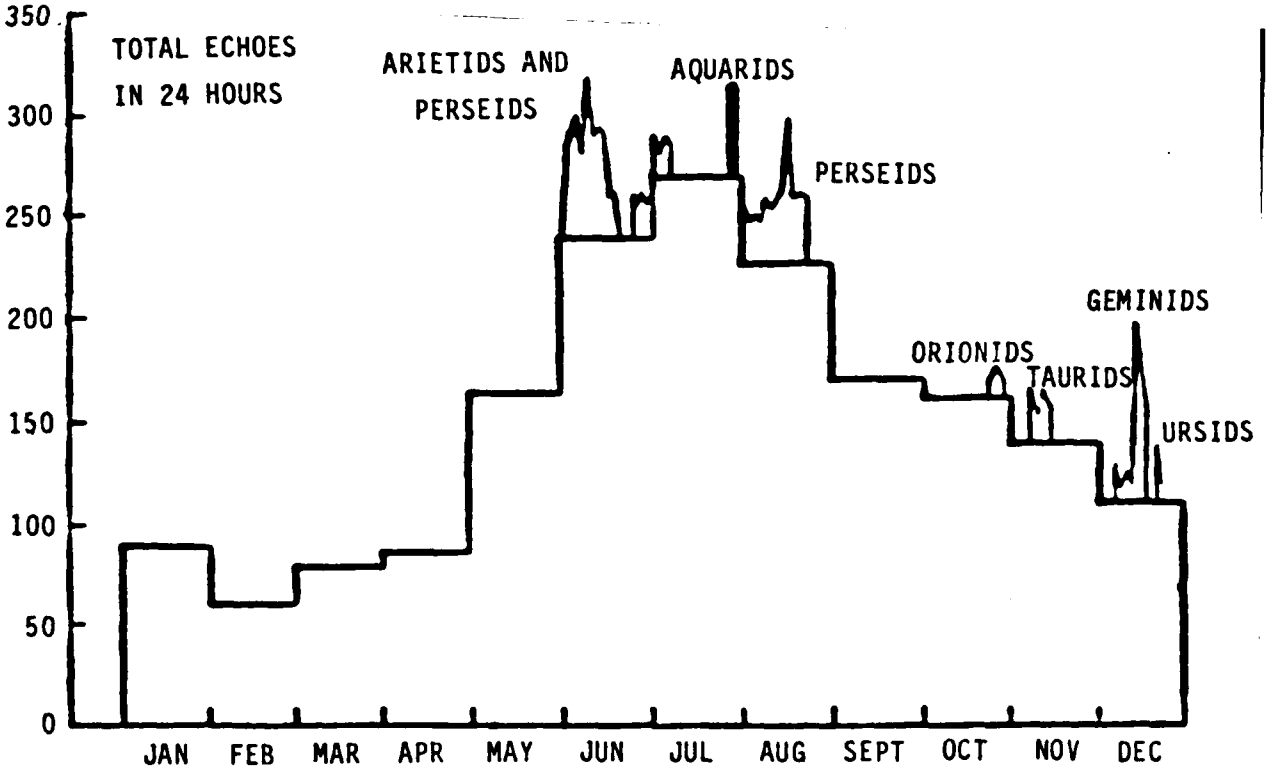

Figure 2.7. Annual Variation of Meteor Rates

The annual cycle is caused by two factors: the earth's tilt on its axis and a variation in the spatial density of meteors along the earth's annual path. The major factor is the tilt of the earth's axis relative to the ecliptic plane, and is similar to the comparable factor affecting the diurnal cycle. The relationship of a location to the earth's ecliptic plane is varied, which in turn affects the ratio of vertical to horizontally inclined trails and the number of angles of incidence giving valid reflections. The second factor, a variation in the spatial density of meteors, is illustrated in Figure 2.6 (Hawkins, 1956b). Figure 2.7 shows the annual cycle for sporadic and shower meteor rates (Hawkins, 1956).

The mass distribution of sporadic meteors is such that there are approximately equal total masses of each size of particle. The approximate relation between particle mass and daily rate is given in Table 2.1 (Sugar, 1964, Villard, et al., 1955), and is illustrated in Figure 2.3. A model for the probability distribution for the mass of meteoric particles which more closely agrees with the data is the "inverse power" distribution

$$F_M(m) = K\, m^{-k} ,$$

where k = 2 for sporadic meteors, and k = 1.5 for shower meteors (Eshleman, 1957). Note that Table 2.1 is equivalent to k = 1.

TABLE 2.1. ORDER OF MAGNITUDE ESTIMATED METEOR MASS DISTRIBUTION

MASS (grams)	DISTRIBUTION OF METEORS ENTERING EARTH'S ATMOSPHERE DAILY	ELECTRON LINE DENSITY
10	10^4	10^{18}
1	10^5	10^{17}
10^{-1}	10^6	10^{16}
10^{-2}	10^7	10^{15}
10^{-3}	10^8	10^{14}
10^{-4}	10^9	10^{13}
10^{-5}	10^{10}	10^{12}
10^{-6}	10^{11}	10^{11}

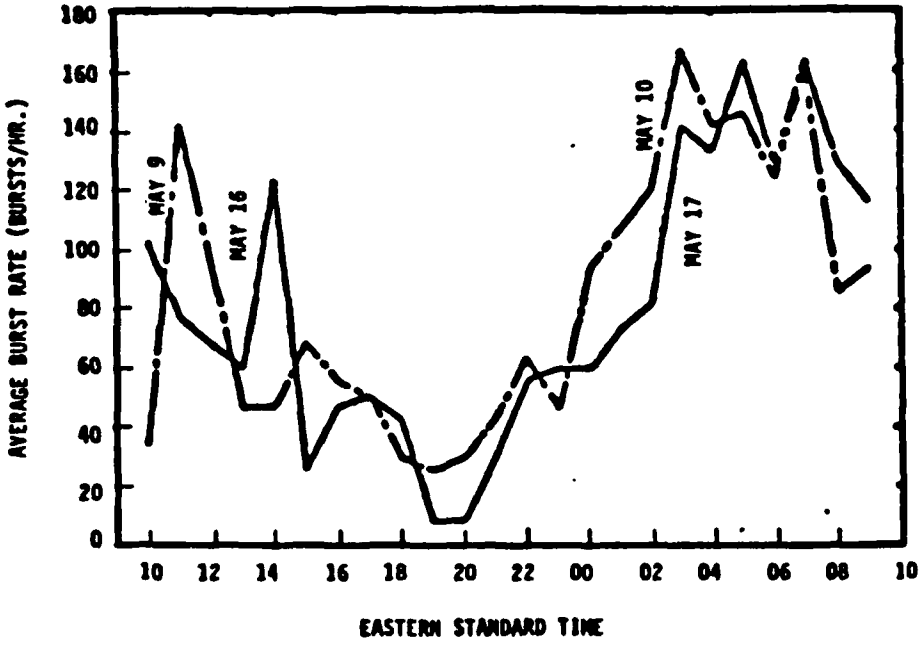

Figure 2.4. Observed Diurnal Variation of Meteor Burst Rates

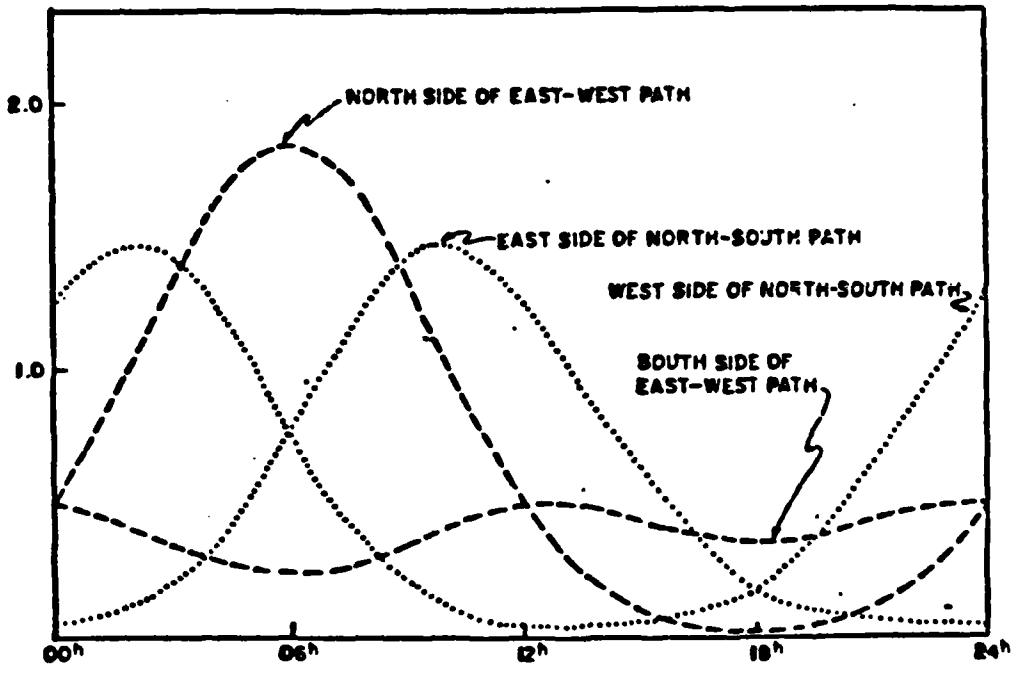

Figure 2.5. Predicted Diurnal Variations

Meteors can be divided into two classes, shower meteors and sporadic meteors. Shower meteors are collections of particles all moving at the same velocity in fairly well-defined orbits or streams around the sun. Their orbits intersect the orbit of the earth at a specific time each year. At these times the well known meteor showers are observed. The shower meteors account for only a small fraction of all meteors. It is the nonshower or sporadic meteors that comprise nearly all of the meteors of interest in radio propagation. Sporadic meteors do not have well-defined streams, but seem rather to move in random orbits. The computer code only simulates sporadic meteors, but can easily be modified to simulate shower meteors as well.

The rate of incidence of sporadic meteors at the earth is further modified by two cycles, a diurnal and an annual cycle. The first of these, the diurnal variation in meteor arrival rate, is due to several factors. The major factor in the diurnal cycle is meteors being swept up by the forward motion of the earth during the morning hours, and only those meteors overtaking the earth's motion entering the atmosphere during evening hours. This results in a maximum occurrence rate around 6:00 a.m. and a minimum rate around 6:00 p.m., as shown by typical data in Figure 2.4 (Montgomery and Sugar, 1957). This factor is further modified by the tilt of the earth's axis relative to the ecliptic plane, as this varies the location that is the leading point on the sphere, the effect of which varies with latitude. Finally, the orientation of the receiver-transmitter path determines whether the horizontally inclined meteor paths, which tend to occur at noon and midnight, are parallel or perpendicular to the transmission link. Analytically predicted diurnal variations, accounting for these effects are presented in Figure 2.5 (Hines, 1956).

The forward scattering cross section is that of a cylinder with effective radius

$$r_c = 4Dt\, \ell n \left(\frac{r_e q \lambda^2 \sec^2 \phi}{4\pi^2 Dt} \right)^{1/2}$$

The transmission equation is then

$$\frac{P_R}{P_T} = \frac{G_T G_R \lambda^2 \sin^2 a}{32\pi^2 R_T R_R (R_T + R_R)(1 - \cos^2 \beta \sin^2 \phi)} \left[\frac{4Dt}{\sec^2 \phi}\, \ell n \left(\frac{r_e q \lambda^2 \sec^2 \phi}{4\pi^2 Dt} \right) \right]^{1/2}$$

This equation applies until approximately a time

$$T = \frac{r_e q \lambda^2 \sec^2 \phi}{4\pi^2 D}$$

after which the relation for underdense trails is applicable.

It is interesting to note at this point a violation of reciprocity for transmission in both underdense and overdense cases. The power received in both cases is proportional to $\sin^2 a$, where a is the angle between the electric polarization vector at the meteor trail and the reflected ray. This term appears because an electron reradiates an amplitude pattern of a Hertzian dipole, which McKinley (McKinley, 1961) describes as a circle rotated about a tangent, or a holeless doughnut. The axis, along which there is no scattered field, is coincident with the electric vector. Upon interchange of the transmitter and receiver, the bilateral symmetry of the transmission equations is in general broken by a difference in the angle a. For example, for vertically polarized signals, the received signal vanishes for meteor bursts directly over the receiver, but has maximum strength for bursts over the transmitter. The orbital motion of the earth and diurnal variations can skew the number of meteor impacts over a transmitter and receiver, particularly on east-west paths, so that the percent-copy will differ if receiver and transmitter are interchanged. Preliminary tests using MBCS suggest that, upon interchange, the difference in the power ratio P_r/P_t is typically of order 10 to 20%, but can be much higher under certain circumstances.

$$2\left[\lambda R_T R_R/(R_T + R_R)\ (1-\cos^2\beta \sin^2\phi)\right]^{1/2},$$

where

λ is the wavelength,

R_T is the distance from the transmitter to M,

R_R is the distance from the receiver to M,

β and ϕ are as defined in Figure 2.2.

As the trail expands by diffusion, the phase difference of the contributions from the electrons on opposite sides of the trail increases, so that the received power decreases.

The complete transmission equation for the underdense case is

$$\frac{P_R}{P_T} = \frac{G_T G_R \lambda^3 q^2 r_e^2 \sin^2 a}{16\pi^2 R_T R_R (R_T+R_R)(1-\cos^2\beta\sin^2\phi)} \exp\left(-\frac{8\pi^2 r_o^2}{\lambda^2 \sec^2\phi}\right) \exp\left(-\frac{32\pi^2 Dt}{\lambda^2\sec^2\phi}\right)$$

where

P_T and $P_R(t)$ are respectively the transmitted and received power,

G_T and G_R are respectively the power gains of the transmitting and receiving antennas relative to an isotropic radiator in free space,

λ is the wavelength in meters,

$r_e = 2.8178 \times 10^{-15}$m is the classical radius of the electron,

r_o is the initial trail radius,

q is the line density of the trail in electrons per meter,

a is the angle between the electric polarization vector and the reflected ray,

D is the diffusion coefficient in square meters per second, and

t is time measured from the formation of the trail in seconds.

For overdense trails, the assumption that the incident wave passes through the trail essentially unmodified is no longer valid. For this case it is assumed that the wave penetrates the trail until reaching a surface of sufficiently high electron density to be reflected. The model used is that of an expanding cylindrical reflector of radius r_c. After a time the electron density everywhere falls below the critical value and the underdense model is once more applicable. However, by this time the radius is quite large and the signal contribution is rather small.

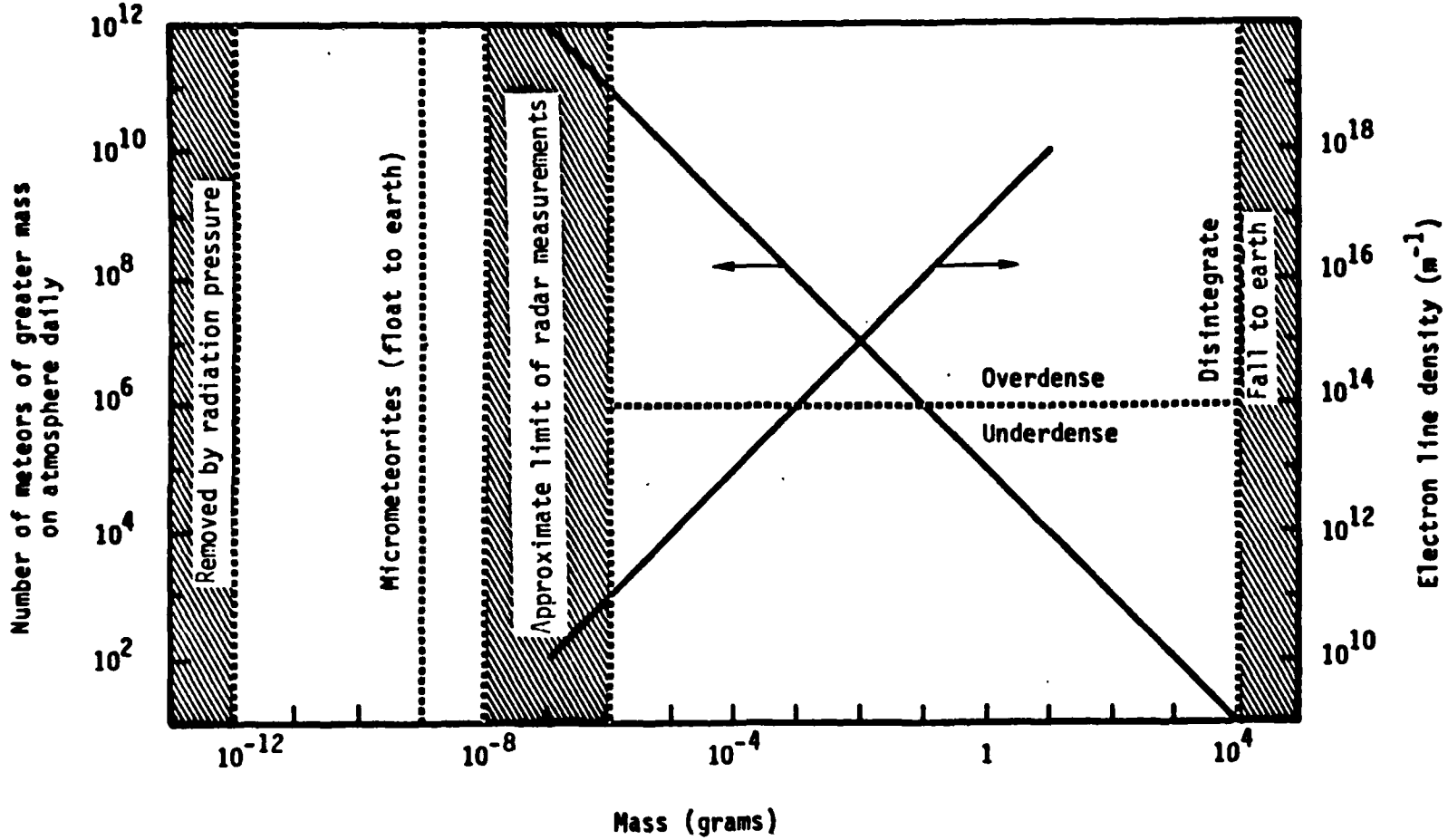

RE-07371

Figure 2.3. Mass Distribution and Electron Density of Sporadic Meteors

The distribution of energy reflected by a meteor trail is a function of many variables. The ionization density distribution across and along the trail, the orientation of the trail, the VHF wavelength, the polarization of the incident wave relative to the trail, the motion of the trail either as part of the process of formation or due to ionospheric winds, and the straightness of the trail are all significant (Sugar, 1964). In discussing the reflection properties it is convenient to divide the trails into two classes, underdense trails and overdense trails. Underdense trails are those in which the electron density is low enough so that the incident wave passes through the trail, and for which the trail can be considered to be an array of independent scatterers. Overdense trails are those in which the electron density is high enough to prevent penetration of the incident wave. Waves reflect from overdense trails in the same sense that they reflect from solid conducting cylinders. At the long wavelengths considered by this code, the effective duration of a trail is long compared to the time it takes the trail to form, and the trail may be considered to have a cylindrical shape.

The mass distribution of meteors incident daily on the earth's atmosphere is shown in Figure 2.3. The approximate electron line density (in electrons/meter) produced by meteors of given masses is shown by the right-hand scale in this same figure. The line density demarcating underdense and overdense trails is commonly taken to be q 10^{14} electrons per meter (Sugar, 1964), as shown in Figure 2.3. The code treats both underdense and overdense trails.

For underdense trails, the model assumes that the trail is an infinitely long right-circular cylinder of electrons whose diameter is very small compared to the wavelength, and that the trail electron density is low enough that the incident wave passes through the trail without major modification (Sugar, 1964). The signal received can be computed by summing the energy backscattered by each electron in the trail while taking proper account of the phase relations of these contributions (Lovell and Clegg, 1948). When this is done it is found that the principal contribution of energy from a trail is from its first Fresnel zone, a region of length

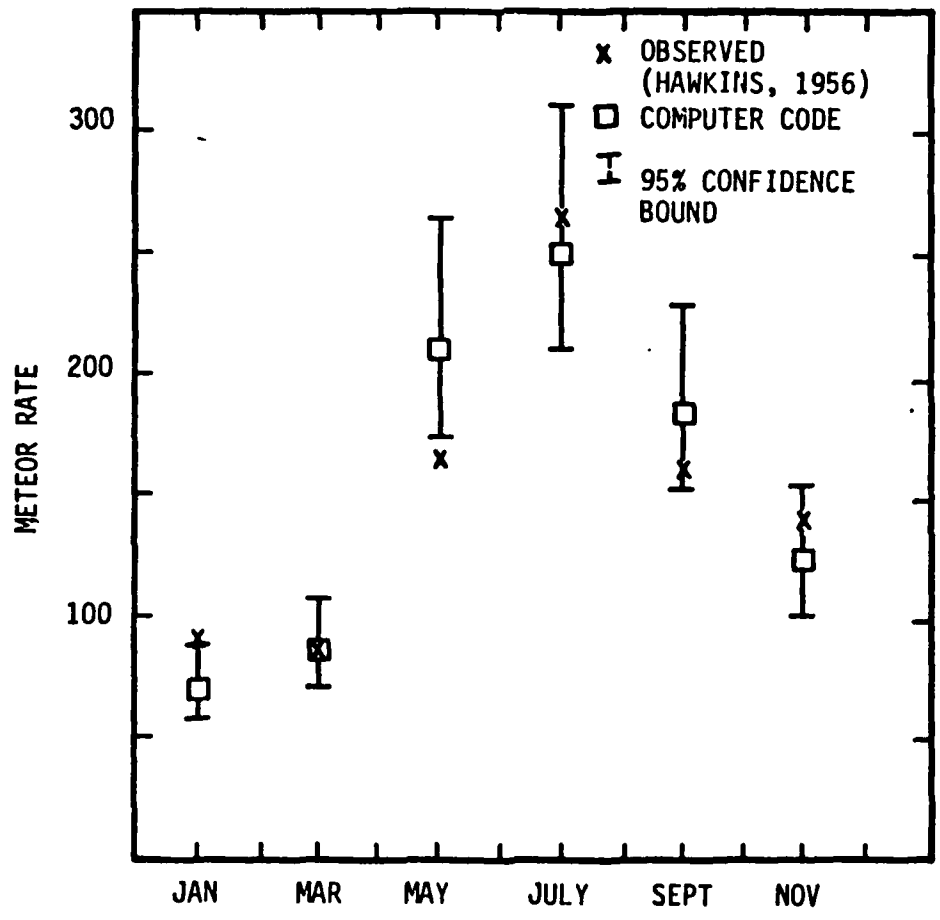

Figure 2.10. Comparison of Simulation Code with Experiments — Annual Variation

Hawkins (Figure 2.7) and from the computer code. The 95% confidence interval has also been plotted for the computer-generated results. There seems to be acceptable agreement between the published and computed annual cycles.

The peak amplitude distribution for several reception thresholds (in microvolts) is presented for the NBS system by Montgomery and Sugar (1957). The distribution of peak amplitudes generated by the computer code is compared with the published distribution in Figure 2.11. Again, generally good agreement is obtained between the computer code and published data.

The duty cycle of signal transmission (length of time the transmission link remains above the threshold) is also studied. Montgomery and Sugar (1957) present the distribution of time the transmission link is above the threshold for the NBS system. The comparison of the NBS results to the computer code is presented in Figure 2.12. Furthermore, for the time period used in the study (June 18-19), the NBS system had a mean duration of 1.4 sec. while the computer code had a mean duration of 1.33 sec. with a standard deviation for the mean of .13 sec. (This agreement provided the rationale for using the Manning hypothesis for radius size, as opposed to the observed data reported by Sugar).

A critical variable for some applications of meteor scatter communications and for the Phase II experiments is the "hot spot" phenomenon. The hot spot effect is evinced by a higher density of valid meteor reflections off of the line between transmitter and receiver than on the line. This effect is illustrated in Figure 2.13. Virtually all meteor paths in the earth's atmosphere are oriented with a velocity vector pointed towards earth. A reflection occurs at that point on a meteor trail where the path to the meteor trail is orthogonal to the lateral component to the meteor direction, which for a meteor entering the earth's atmosphere will only be on the center line if the meteor's lateral path is exactly horizontal, which seldomly occurs. The hot spot effect makes other variables such as beamwidth and antenna locations (if there is more than one receiving antenna), as well as diurnal and annual variations, very important. It is also important in the case of diversity reception systems with several independent receiving antennas oriented towards the same transmitter to learn the effects of path direction and diurnal effects.

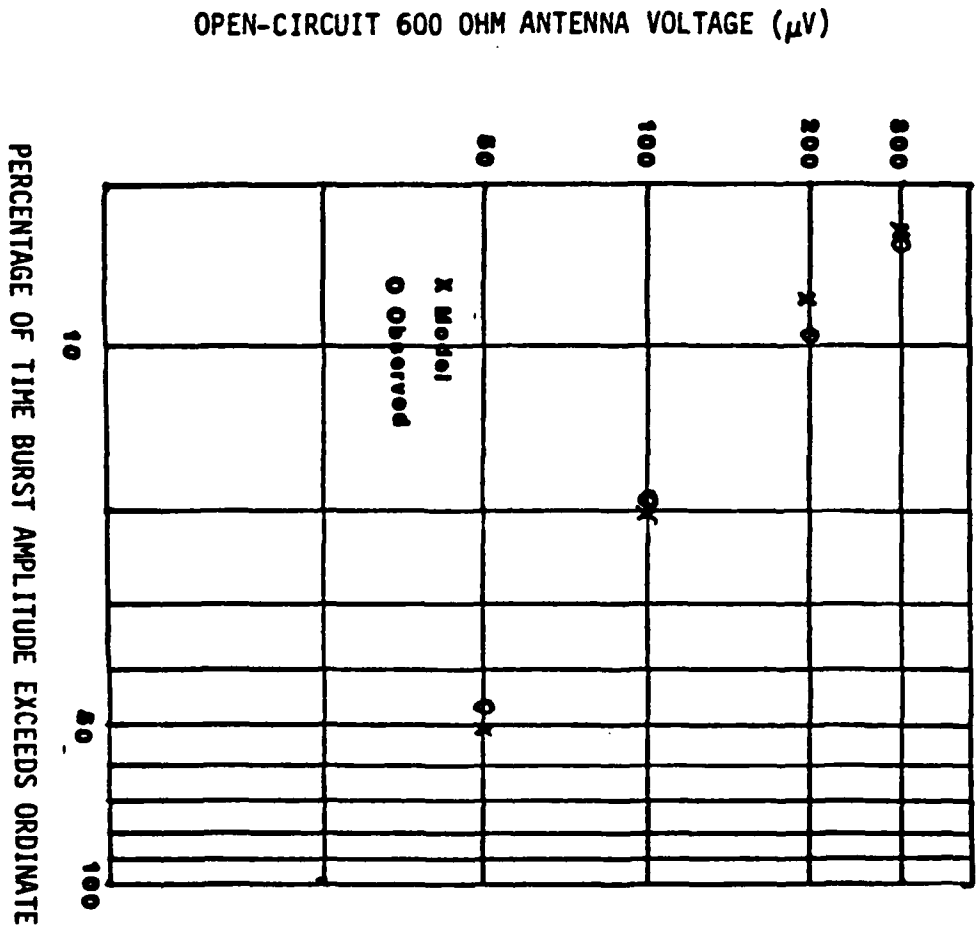

Figure 2.11. Comparison of Simulation Code with Experiments — Peak Amplitude Distribution

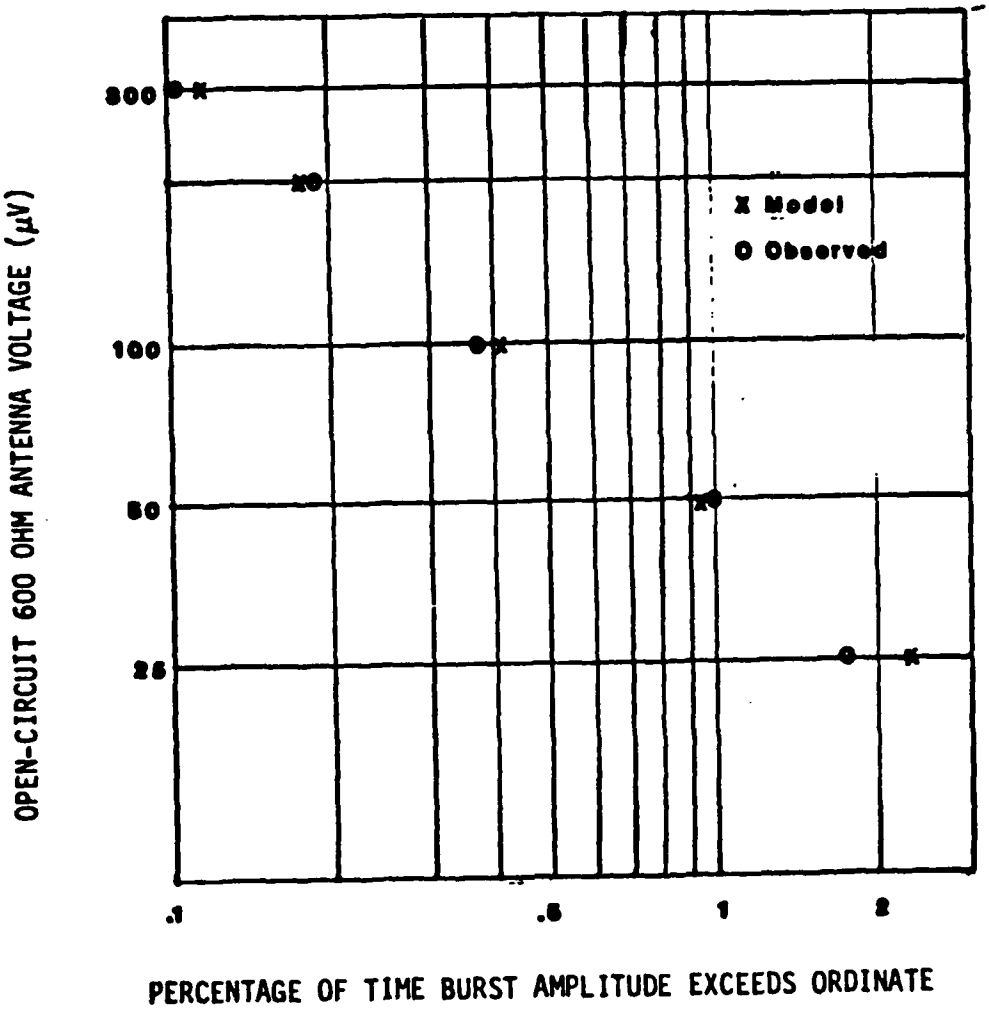

Figure 2.12. Comparison of Simulation Code with Experiments — Duty Cycle

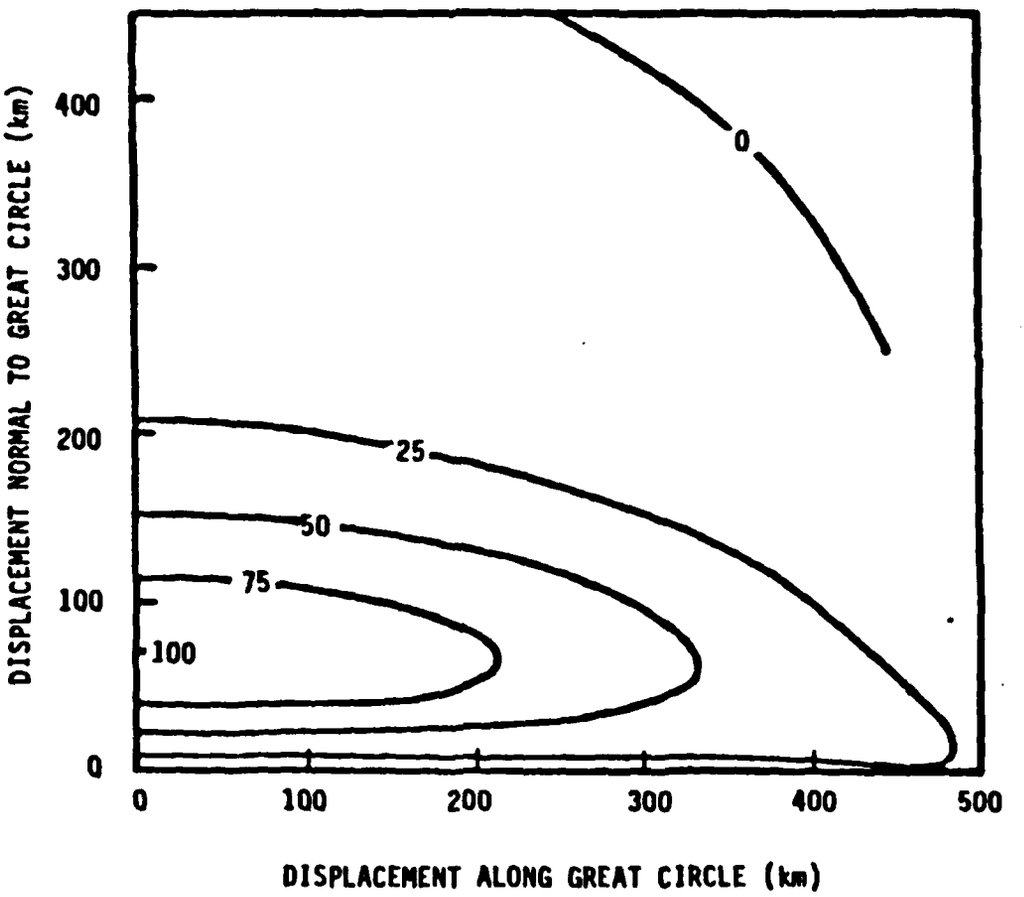

(From Canad.J.Phys. 34)

Figure 2.13. Relative Signal Contributions from Various Parts of Meteor Region for 1000 km Path

Consequently, the detailed predictions of the hot spot effect possible with MBCS is one of the most important capabilities of the code.

The hot spot effect is studied in detail by the European system described in Bain (1960). The European system had two receiving antennas separated by a moderate distance to allow phase differences to be used to estimate the bearing to the point of meteor reflection. Very definite diurnal effects were found in the hot spot locations. Figure 2.14 shows the published and computed densities of bearings to meteor reflections for midnight, 6:00 a.m., noon, and 6:00 p.m. The diurnal hot spot effect is a dynamic one, but the data had to be collected over an interval of time during which the hot spot is changing. Consequently, the distribution of bearings for the 3 hour periods before and after the times simulated by the computer code are shown in Figure 2.14. This allows one to develop a picture of the dynamic effect observed, and compare this with the effect computed for a fixed time using the computer code. An acceptable agreement between the observed and computed diurnal hot spot effects is seen in Figure 2.14.

The above comparisons are meant to be a benchmarking rather than a definitive validation of the MBCS code. Much is not known about the data sets used. A more comprehensive comparison is needed using data collected with known systems. However, this preliminary comparison between published and simulated data is certainly encouraging, and suggests that the Meteor Burst Communications Simulation code is a promising tool for the design of meteor burst communications systems and experiments.

2.3 EXPERIMENT DESIGN

2.3.1 Experiment Objectives

The evaluation of the VHF diversity reception concept has brought into focus basic questions concerning VHF meteor path reception characteristics. The objective of the experimental program that has been designed is to address these questions relating to the variation of reception duty cycle along a single path as a function of the receiver antenna gain and beamwidth, and the relative independence of meteor path signals as a function of the angular and spatial separation of the propagation paths in multiple source reception.

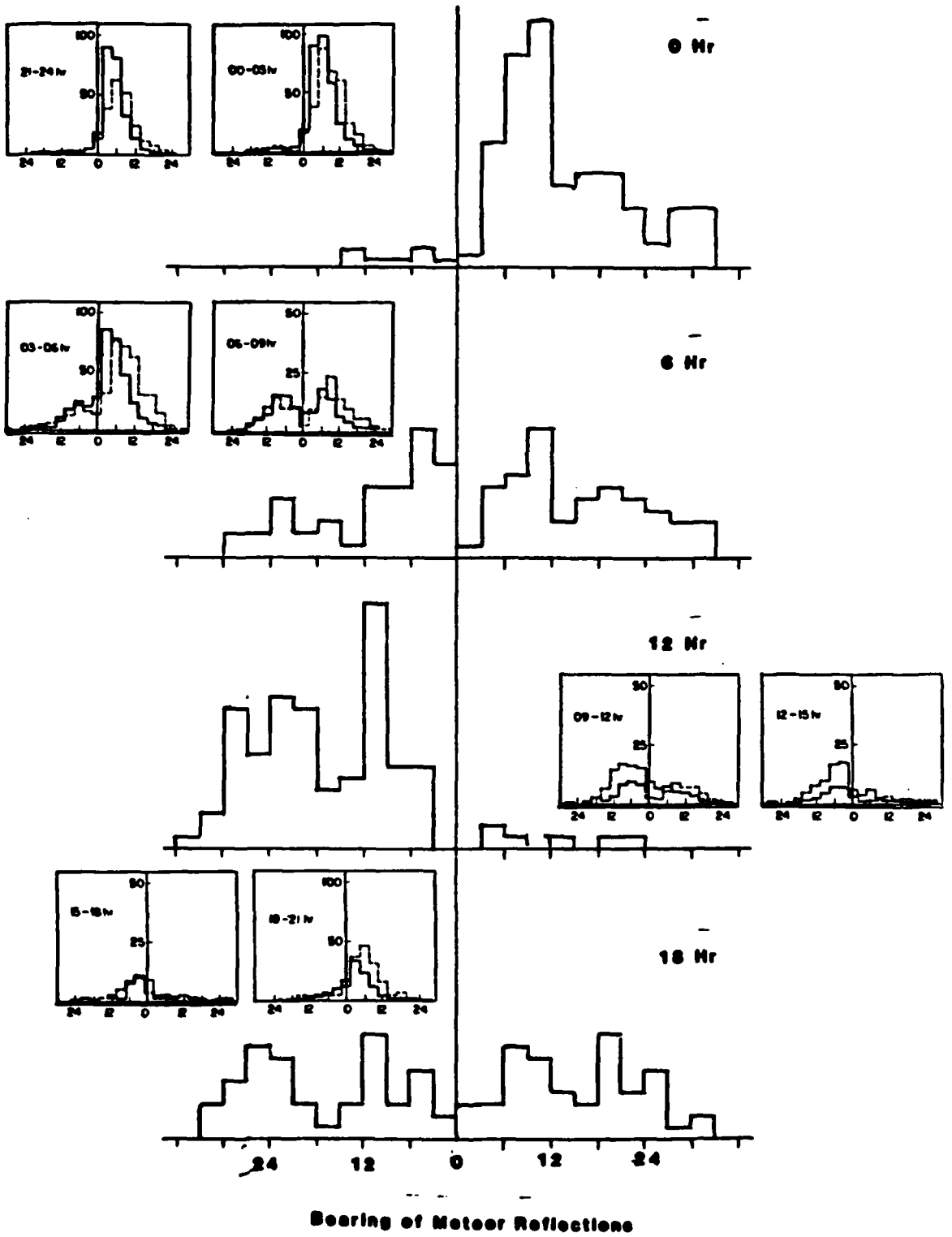

Figure 2.14. Comparison of Hot Spots Simulation Code with Experiments

2.3.2 Experiment Features

The experiment will provide a capability to evaluate these issues by allowing a variety of configurations to be employed using realistically achievable gain/beamwidth receiving antennas at a centrally located site, and (by invoking reciprocity) a number of separated and remotely controlled transmitters at a variety of distances and angular separations from the receiving site. (See Figure 2.15).

This approach allows for the complexity of antenna array reconfigurations needed to vary gain, beamwidth and pointing direction of the directive antennas to be done at the central manned receiver site. The central site will include the needed data acquisition, recording and processing analysis efforts. Transmitter sites will be relatively simple and can employ transmitters controlled via a commercial dial-up telephone line to each location (see Figure 2.16 for network control diagram).

A unique feature of the proposed system is to have three transmitters placed at some combination of four to seven licensed locations all operating on the same RF carrier frequency, but using a single-side-band, surpressed carrier, with each transmitter radiating a distinct audio tone as an identifier. This approach allows all signals to be received on one common receiver by combining signals from different antennas. Data will be recorded as audio tones (one for each transmitters) on a simple analog recording unit.

2.3.3 Candidate Site Locations

A receiving site that has been considered is Camp Elliot near Miramar Naval Air Station, San Diego. This area, north of the city (within ten miles of JAYCOR headquarters in San Diego) is government property under the control of the Commander NAS Miramar. A request for use of space and facilities for the receiver site and the large multi-element antenna arrays has been made. A response from the Public Works Office at Miramar gives preliminary approval of the request pending detailed selection of a specific site and clarification of environmental and operational constraints. (See attached letters at end of Subsection 2.3, JAYCOR to NAS Miramar and NAS Miramar to JAYCOR.)

Four prospective transmitter site locations have been identified which have the features of being appropriate distances from the receive site (400 to 1400 km) and lying on different angular paths (north-south to east-west)

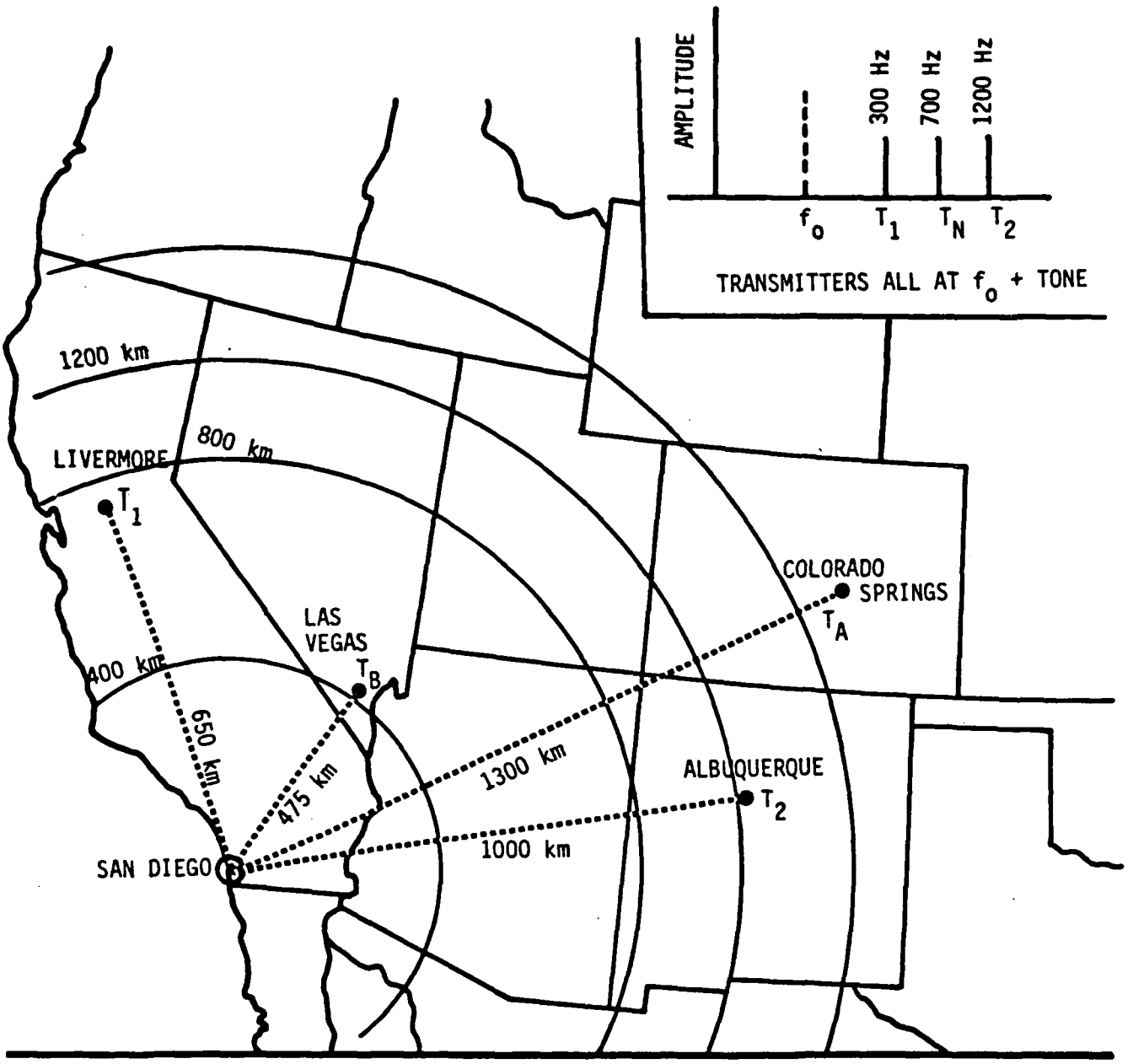

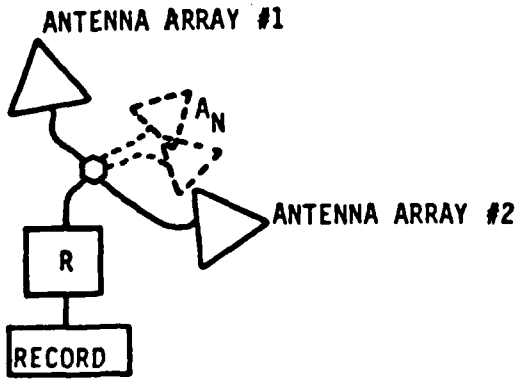

RECEIVER SITE WITH ANTENNA FARM

3 ARRAYS DIRECTED AT

1) T_1

2) T_2

3) T_N

RE-08288 **Figure 2.15. VHF Reception Program — Phase II, Experiment Configuration**

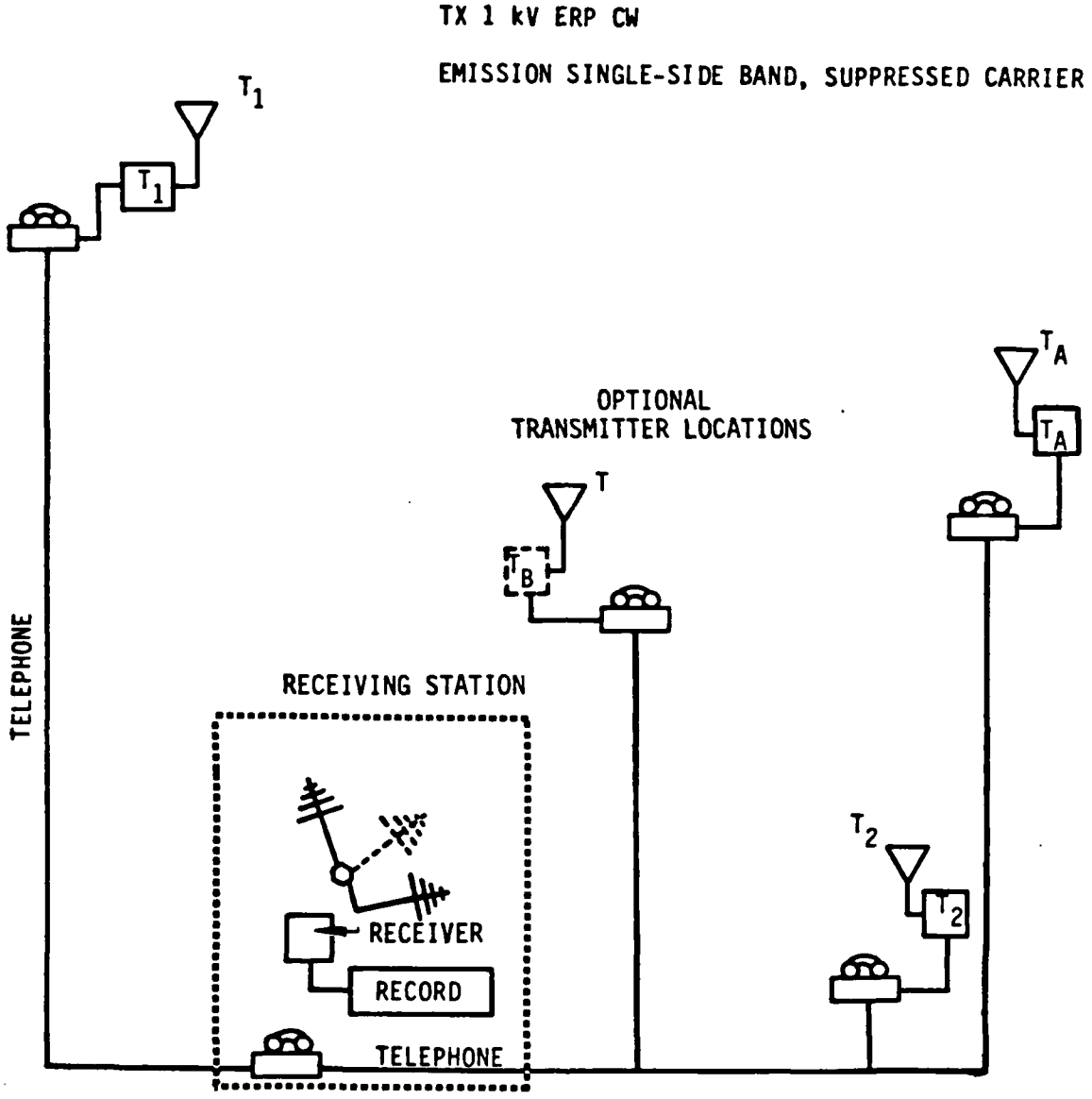

Figure 2.16. VHF Reception Network Control

Direct-dial telephone to each transmitter site from the receiver site activates and deactivates transmitters.

from San Diego. These sites are also easily accessible to facilitate repair or maintenance service. Additional transmitter sites should be licensed to be available for the temporary placement of a transportable transmitter to increase diversity of distance/angle data. The four primary candidates transmitter sites (see map in Figure 2.15) and their ranges from San Diego are:

Location	Distance from San Diego
Camp Parks (Livermore, CA)	800 km
Nellis AFB (Las Vegas, NV)	475 km
Fort Carson (Colorado Springs, CO)	1300 km*
Kirtland AFB (Albuquerque, NM)	1000 km

Criteria for additional transmitter site locations are:

1) A site colinear with an existing site but at different range.
2) A site within a few angular degrees of an existing site.
3) A site to evaluate maximum viable range (i.e., 1500-2000 km).

Prospective transmitter sites, which can be selected from existing Army/Navy/Air Force and government property, will require a minimum of space and support facilities. An example of the present facilities operated by the Air Force is shown in Figure 2.17.

2.3.4 Frequency Selection and Allocation

The potential application of the proposed concept is for the lower VHF band from about 30 to 100 MHz. Below 30 MHz there is a high probability of long-range ionospheric propagation. Fortunately, the solar cycle is at a low for the next few years, and should minimize low VHF ionospheric path signals. The desired frequency for this experiment is in the 30-50 MHz range. Above 50 MHz, the duty cycle is much lower than in the low VHF range.

This low VHF band is assigned in one to two megahertz segments to the U.S. Government and non-government agencies and is primarily used for

---

* A letter of tentative approval from Fort Carson is attached at the end of Subsection 2.3.

local-area master-station communications to multiple, remote (often mobile) sites. The Federal Government frequency assignments are administered by the intradepartmental Radio Advisory Committee (IRAC) (ref. Telcon with Mr. John Caufey 202/724-3346) in coordination with the FCC. Selected segments of the low VHF band, i.e., 33-34 MHz, 37-38 MHz, 40-42 MHz are devoted to military tactical radio and some known government meteor communication users such as the Department of Agriculture SNOTEL network, the Federal Emergency Management Agency (FEMA) civil defense system, an Alaska Meteor Burst Communications System for federal bureaus during auroral disturbances, a commercial Northern Natural Gas of Omaha Oil Pipeline Communication System in the midwest, and a Canadian Meteor Burst Store and Forward System (JANET) initiated in the mid 50's.

A frequency search of the non-government Master Frequency List was made on the microfiche list at the San Diego field office of the FCC. All frequencies in the lower VHF band appear to be assigned to low-power unscheduled users such as city, county, and state governments and private users for network communications between a central office and remote stations and a variety of police, sheriff, civil defense and fire department communications on the FM channels assigned. A single frequency often has a number of different users. The government Master Frequency List is maintained at area regional centers and is a classified document.

2.3.5 Procedure for Authorization of U.S. Governmental Frequency Assignment

Assignment of a frequency to perform a government sponsored experiment is initiated by submitting a government form DD 1494 from the sponsoring agency through an area FCC office. The information required on this form includes specifics of the transmitter locations, transmitter power (ERP), antenna types, modulation bandwidth, operating schedules, etc., and a list of the equipment types to be used in generating and radiating the RF signals. Discussions with the Western Area Frequency Coordinator, Mr. Turkiewcz at Pt. Mugu California (805/989-7983) and with the San Diego FCC Coordinator, Mr. Wayne Smith, Navy Comm. Station, SD (619/696-5621) indicate frequency coordination and assignment typically take from 90 to 180 days, and frequency assignment is based on a priority system assigned to the government sponsoring agency. (See sample DD 1494 in attachments at end of 2.3.) Because this experiment would employ multiple transmitters

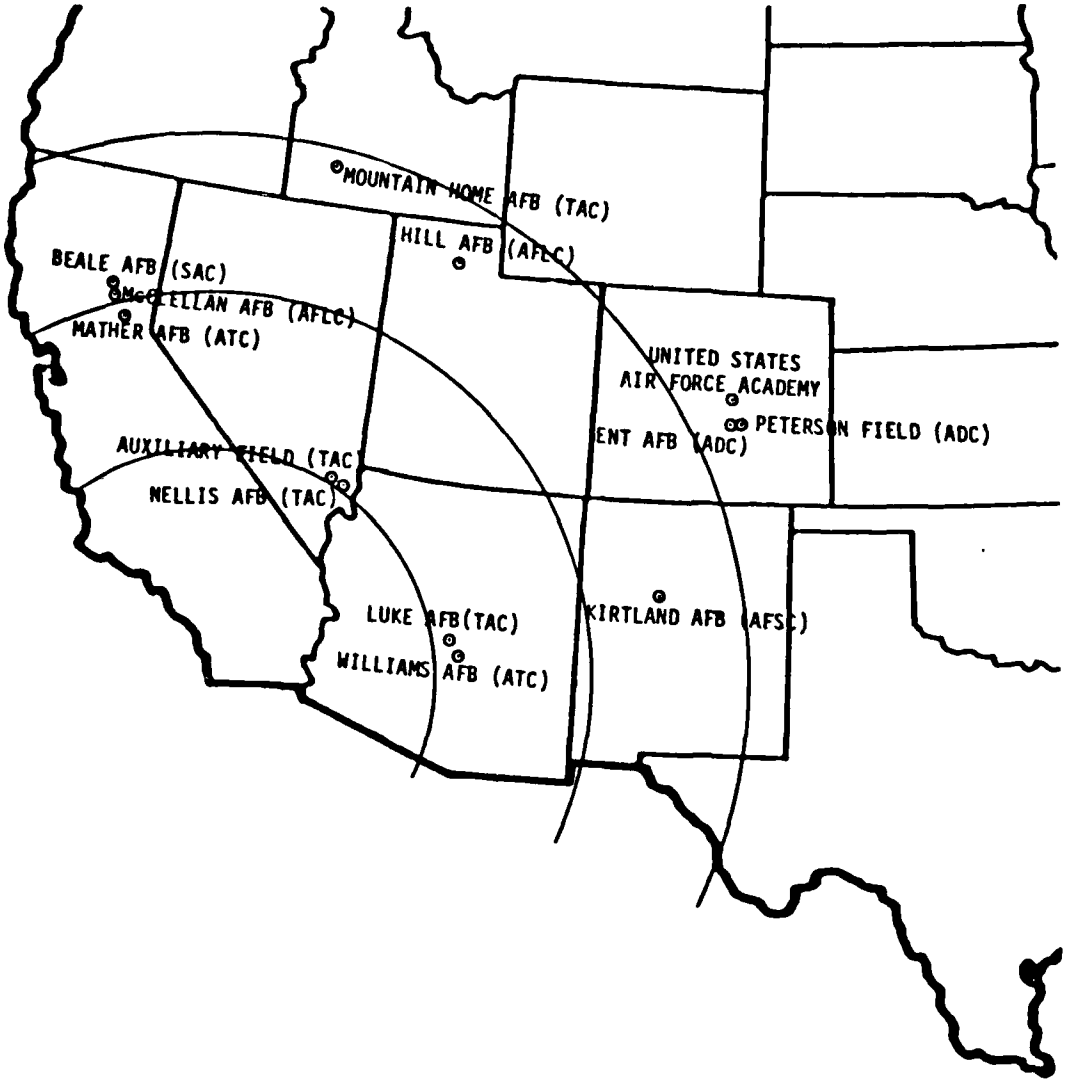

Figure 2.17. Prospective Transmitter Sites, Air Force Facilities

operating on the same frequency at widely dispersed locations (typically one in each of 3 to 5 western states), frequency coordination may be fairly complex, and assignment processing time may be greater than normal. Authorizations will be sought for the prospective locations previously mentioned and for alternate locations in the event that frequency conflicts arise.

2.3.6 Experiment Plan and Configuration

The experiment will involve collecting data periodically to measure both diurnal and seasonal effects of three different VHF meteor path configurations. These three experiment configurations and the corresponding test objectives and implementations are briefly described below and refer to figures and sketches which describe the antenna features, propagation paths, and network configurations.

1. Gain vs. Beamwidth (Figure 2.18)

   Objective: Determine the signal reception duty cycle as a function the gain/beamwidth of a receiving antenna when directed towards an over-the-horizon signal source.

   Approach: Gain/Beamwidth variations (see sketches of antenna configurations, Figure 2.19).

Forward Gain	Horizontal (azimuthal) Beamwidth
12 dB	40^{o}
16 dB	16^{o}
18 dB	10^{o}

   Data Base: Record detected signal received during specified period of time (duty cycle). Data taken at same times each day from two different transmitter stations to acquire two independent sets of data.

2. Angular Diversity (Figure 2.20)

   Objective: Determine the dependence/independence of signal reception of two signals in the same geographic area when antennas look at different meteor path volumes.

APPLICATION FOR FREQUENCY ALLOCATION	CLASSIFICATION:	PAGE 4 OF PAGES	FORM APPROVED: OMB 22-R 0248

F. ANTENNA EQUIPMENT CHARACTERISTICS

1. TRANSMITTING ☐ RECEIVING ☐ TRANSMITTING AND RECEIVING ☐

2a. NOMENCLATURE, MANUFACTURER'S MODEL NO.	2b. MANUFACTURER'S NAME.
3. SYSTEM NOMENCLATURE	4. TYPE:
5. FREQUENCY RANGE	6. POLARIZATION
7. GAIN (a) MAIN BEAM _____ (b) SIDE LOBE _____	8. SCAN CHARACTERISTICS. (a) TYPE _____ (b) VERTICAL SCAN _____ (1) MAX ELEV _____ (2) MIN ELEV _____ (3) SCAN RATE _____ (c) HORIZONTAL SCAN _____ (1) SECTOR SCANNED _____ (2) SCAN RATE _____
9. BEAMWIDTH (a) HORIZONTAL _____ (b) VERTICAL _____	

10. REMARKS

CLASSIFICATION

APPLICATION FOR FREQUENCY ALLOCATION	CLASSIFICATION:	PAGE 3 OF PAGES	FORM APPROVED: OMB 22-R 0248

E. RECEIVER EQUIPMENT CHARACTERISTICS

1a. NOMENCLATURE, MANUFACTURER'S MODEL NO.:	1b. MANUFACTURER'S NAME:
2. SYSTEM NOMENCLATURE	3. RECEIVER TYPE
4. TUNING RANGE:	5. METHOD OF TUNING
6. RF CHANNELING CAPABILITY	7. FREQUENCY TOLERANCE
8. EMISSION TYPE(S)	9. RF SELECTIVITY: ☐ CALCULATED ☐ MEASURED (a) -3 dB _____ (b) -20 dB _____ (c) -60 dB _____ (d) TYPE OF PRESELECTION USED _____
10. IF SELECTIVITY (a) 3 dB _____ (b) -20 dB _____ (c) -60 dB _____	
11. MAXIMUM BIT RATE	12. MAXIMUM POST DETECTION FREQUENCY
13. DE-EMPHASIS AVAILABLE ☐ YES ☐ NO	14. MINIMUM POST DETECTION FREQUENCY
15. IF FREQUENCY (a) 1st _____ (b) 2nd _____	16. SENSITIVITY: (a) _____ dBm (b) CRITERIA _____ (c) NOISE TEMPERATURE _____ °Kelvin
17. OSCILLATOR TUNED (a) ABOVE TUNED FREQUENCY ☐ (b) BELOW TUNED FREQUENCY ☐ (c) EITHER ABOVE OR BELOW THE FREQUENCY ☐	
18. SPURIOUS REJECTION	19. IMAGE REJECTION
20. REMARKS	
CLASSIFICATION	

APPLICATION FOR FREQUENCY ALLOCATION	CLASSIFICATION	PAGE 2 OF PAGES	FORM APPROVED OMB 22-R 0248

D TRANSMITTER EQUIPMENT CHARACTERISTICS

1a NOMENCLATURE, MANUFACTURER'S MODEL NO	1b MANUFACTURER'S NAME
2 SYSTEM NOMENCLATURE	3 TRANSMITTER TYPE
4 TUNING RANGE	5 METHOD OF TUNING
6 RF CHANNELING CAPABILITY	7 FREQUENCY TOLERANCE
8 EMISSION TYPE(S)	9 EMISSION BANDWIDTH ☐ CALCULATED ☐ MEASURED (a) 3 dB _____ (b) 20 dB _____ (c) -40 dB _____ (d) -60 dB _____ (e) Occupied Bandwidth _____
10 FILTER EMPLOYED (a) ☐ LOW PASS (c) ☐ BAND PASS (b) ☐ HIGH PASS (d) ☐ NONE	
11 MAXIMUM BIT RATE	12 MAXIMUM MODULATION FREQUENCY
13 PRE-EMPHASIS ☐ YES ☐ NO	14 DEVIATION RATIO
15 POWER (a) CARRIER _____ (b) MEAN _____ (c) PEAK ENVELOPE _____	16 PULSE CHARACTERISTICS (a) RATE _____ (b) WIDTH _____ (c) RISE TIME _____ (d) FALL TIME _____ (e) COMPRESSION RATIO _____
17 OUTPUT DEVICE	
18 SPURIOUS LEVEL	19 HARMONIC LEVEL (a) 2nd _____ (b) 3rd _____ (c) OTHER _____
20 FCC TYPE ACCEPTANCE NO	

21 REMARKS

CLASSIFICATION

APPLICATION FOR FREQUENCY ALLOCATION	CLASSIFICATION	PAGE 1 OF PAGES	FORM APPROVED OMB 22-R 0248

I. SYSTEM REVIEW

A. GENERAL INFORMATION

TO	FROM

1 SYSTEM NOMENCLATURE

2 STATUS OF ALLOCATION

☐ STAGE 1 ☐ STAGE 2 ☐ STAGE 3 ☐ STAGE 4

3 PURPOSE OF SYSTEM

4 INFORMATION TRANSFER REQUIREMENTS

5 ESTIMATED TERMINATION DATE

6 ESTIMATED INITIAL COST OF THE SYSTEM

7 TARGET DATE

8 SYSTEM RELATIONSHIP AND ESSENTIALITY

9 REPLACEMENT INFORMATION

10 RELATED ANALYSIS DATA

11 LINE DIAGRAM

12 REMARKS

B. TERRESTRIAL SYSTEMS

1 STATION CLASS(ES)	2 NUMBER OF UNITS

3 STATION LOCATIONS AND/OR AREAS OF OPERATION	4 FREQUENCY REQUIREMENTS

5 PROPOSED DATE OF ACTIVATION

C. SPACE SYSTEMS

(PROVIDE ATTACHMENT IN ACCORDANCE WITH INSTRUCTIONS)

DOWNGRADING INSTRUCTIONS	CLASSIFICATION

DEPARTMENT OF THE ARMY
HEADQUARTERS, FORT CARSON
AND
HEADQUARTERS, 4TH INFANTRY DIVISION (MECHANIZED)
FORT CARSON, COLORADO 80913-5000

REPLY TO
ATTENTION OF

June 6, 1985

Facility Management

Mr. George F. Ross
Senior Engineer
JAYCOR
Hilton Parkway 12
4570 Hilton Parkway
Colorado Springs, Colorado 80907

Dear Mr. Ross:

With reference to a phonecall on June 4, 1985 between yourself and William Davis, Chief, DEH Facility Management, Fort Carson would entertain a proposal to temporarily site your project on this installation. In all probability the land could be made available, but an available enclosed, lockable building that has electrical power to it may prove more difficult to provide.

I would ask that you contact Mr. Davis at 579-3038 to set up a meeting here at Fort Carson to further discuss the details of your proposal and to visit potential sites.

Sincerely,

Henry T. Brown, Jr.
Colonel, Engineer
Director of Engineering and
Housing

DEPARTMENT OF THE NAVY
NAVAL AIR STATION MIRAMAR
SAN DIEGO, CA 92145

IN REPLY REFER TO
11011
Ser 1832C/8418
JUN 14 1985

Mr. Ralph M. Wheeler
JAYCOR
11011 Torreyana Road
P.O. Box 85154
San Diego, CA 92138-9259

Dear Mr. Wheeler:

We are in receipt of your letter of 16 May 1985 requesting space and limited facility support for a temporary antenna farm located on East Miramar land. Your request has been reviewed and is satisfactory in principle to this command, however, additonal information must be considered before final approval can be granted.

At your convenience, I would like to request a meeting between your staff and mine to discuss items such as site location, utility requirements, environmental impacts, aircraft navigational constraints, security and license agreements. Please contact either Ms. Merrily Severance or Mr. Rene Trevino of my staff at (619) 271-3321, to arrange for this meeting.

As standard practice, we also request that you have the Office of Naval Research contact us to verify your government contract.

Sincerely,

C. J. GUILD
CDR, CEC, USN
Public Works Officer
By direction of the Commanding Officer

AC power: 120 volts AC, 1000 watts maximum.

Operational schedule: 2-3 hours per day, 5 days per week, for up to 12 months.

Security classification: UNCLASSIFIED.

Physical security: Locked room for receiver equipment.

Maximum number of personnel involved: Normal operation, 2 people; installation and set up, 3 to 5 people.

Program proposed under government contract N00014-84-C-0737.

Office of Naval Research

Arlington, VA 22217

Contract Monitor: Mr. Fred Quelle

Telephone: (617) 451-3171

Upon your approval, we would select the preferred building and site and would coordinate our test activity with your representative.

A response to this request and any questions regarding this effort should be directed to me.

Yours truly,

Ralph M. Wheeler

VHF Experiment Director

(619) 453-6580 ext. 220

RMW:sb

JAYCOR

May 16, 1985

Capt. Gary E. Hackanson
Commanding Officer
Naval Air Station, Miramar
San Diego, CA 92145

Dear Sir:

A concept to evaluate the reception of VHF (40 mHz) signals from over-the-horizon is being investigated by JAYCOR under a government contract. An experiment is planned in which we would listen (receive only) to a far-off transmitter (100's of kilometers). Special antennas would be used which require a space about the size of a football field. Available government space and some limited facilities support (AC power and housing for radio equipment) was suggested by our government contract monitor in order to keep costs of the program to a minimum.

At the suggestion of your public works people, an examination of useable areas at Camp Elliot was made. The following facilities and space appear to satisfy our requirements:

Building E-137 and the open land to the north
Building E-133 and the open land to the north
Building E-131 and the open land to the south.

We request your approval to propose the use of one of these locations for conduct of this experiment. We feel confident that this experiment could be successfully completed on a "no interference" to NAS activities. The following requirements are stated for your evaluation of this request:

Receive only operation (no transmitted RF signals would be radiated.
Equipment quantity: 1 or 2 receivers
Receive antenna features:

Array of 2 to 6 antennas with maximum length 50 feet and width of 150 feet. Maximum height 35 feet (This is lower than the local power lines in the requested area).

Inside space required: 200 to 300 square feet of warehouse or office space.

ATTACHMENTS TO SUBSECTION 2.3

- Letter JAYCOR to NAS Miramar
- Letter NAS Miramar to JAYCOR
- Letter Fort Carson to JAYCOR
- DD Form 1494

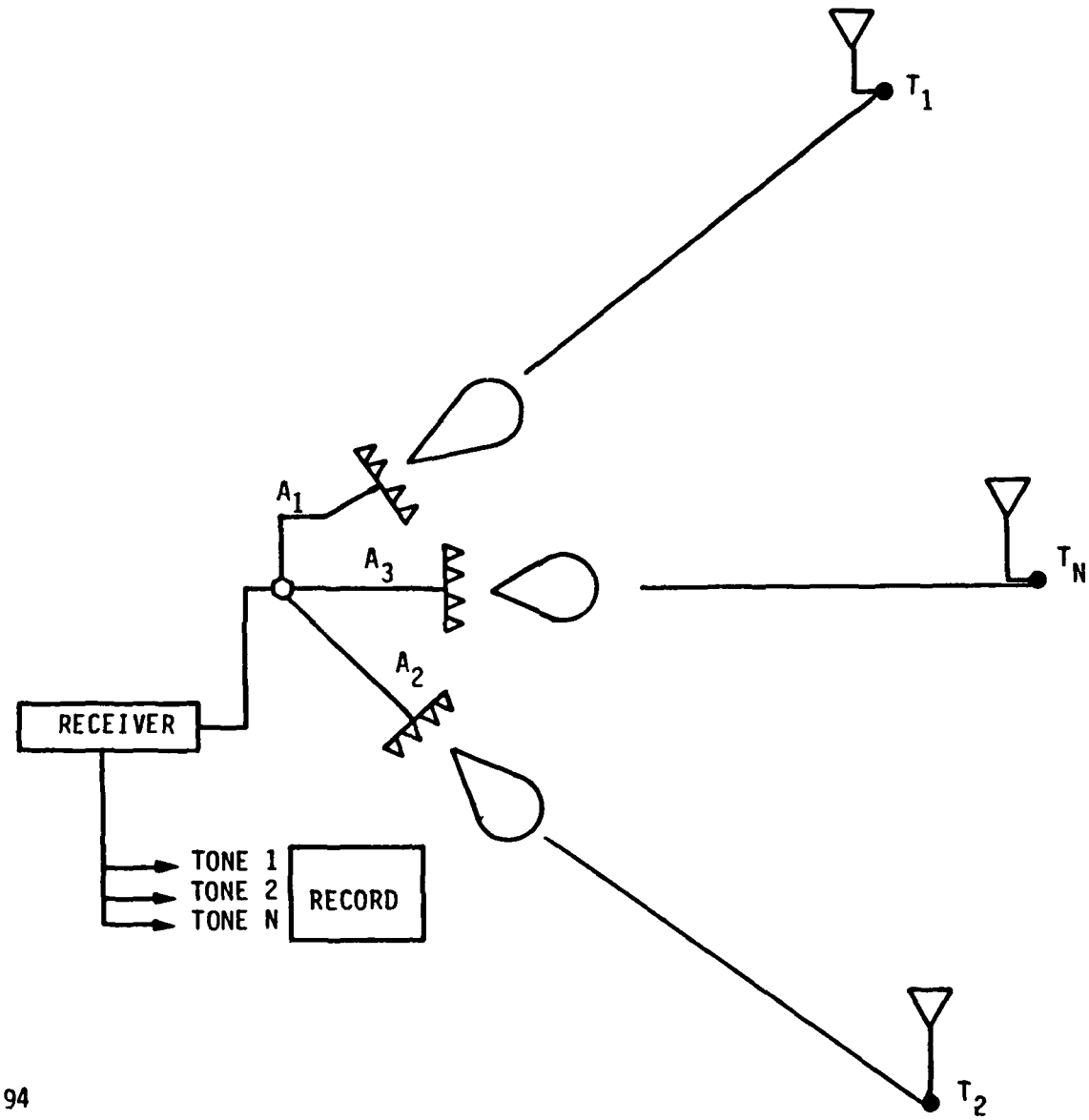

Figure 2.21. Spatial Diversity Experiment

Approach: Use directive antennas to point at different hot spots. Antenna beamwidth will be less than 1/2 the angular separation of the optimum hot spots. Two receivers (one rented for 2 months) will be used in this experiment with an offset in frequency to differentiate signals.

Data Base: Time related comparison of received signals from each source.

3. Spatial Diversity (Figure 2.21)

Objective: Determine the dependence/independence of signal reception of signals located at various distances and angular separations from the central receiver location.

Approach: Use narrow beam antennas to point at optimum hot spots on each link from sources located at different angles and distances from the reception point.

A_1 : 4 ANTENNA ARRAY , GAIN = 16 dB, BEAMWIDTH = 16^o

A_2 : 4 ANTENNA ARRAY , GAIN = 16 dB, BEAMWIDTH = 16^o

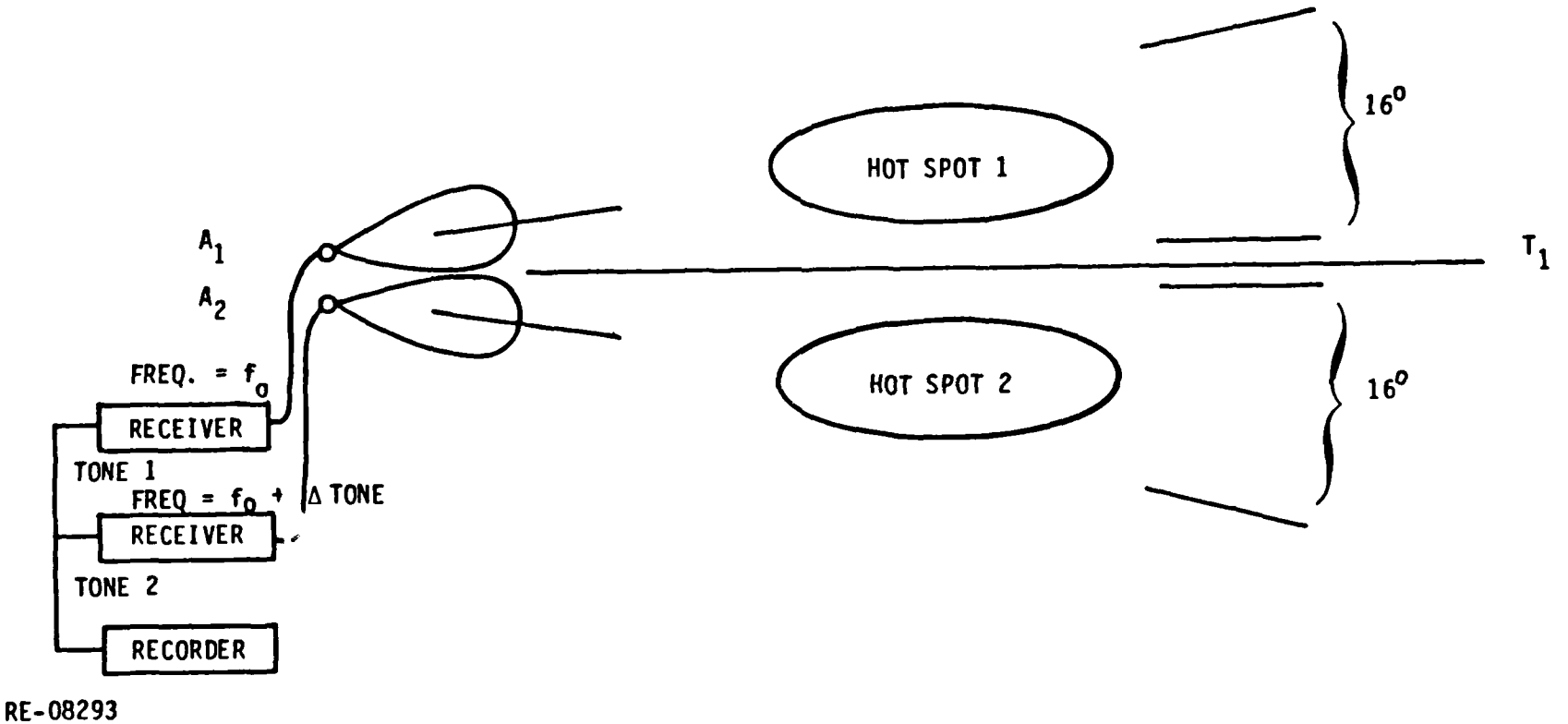

Figure 2.20. Angular Diversity Experiment

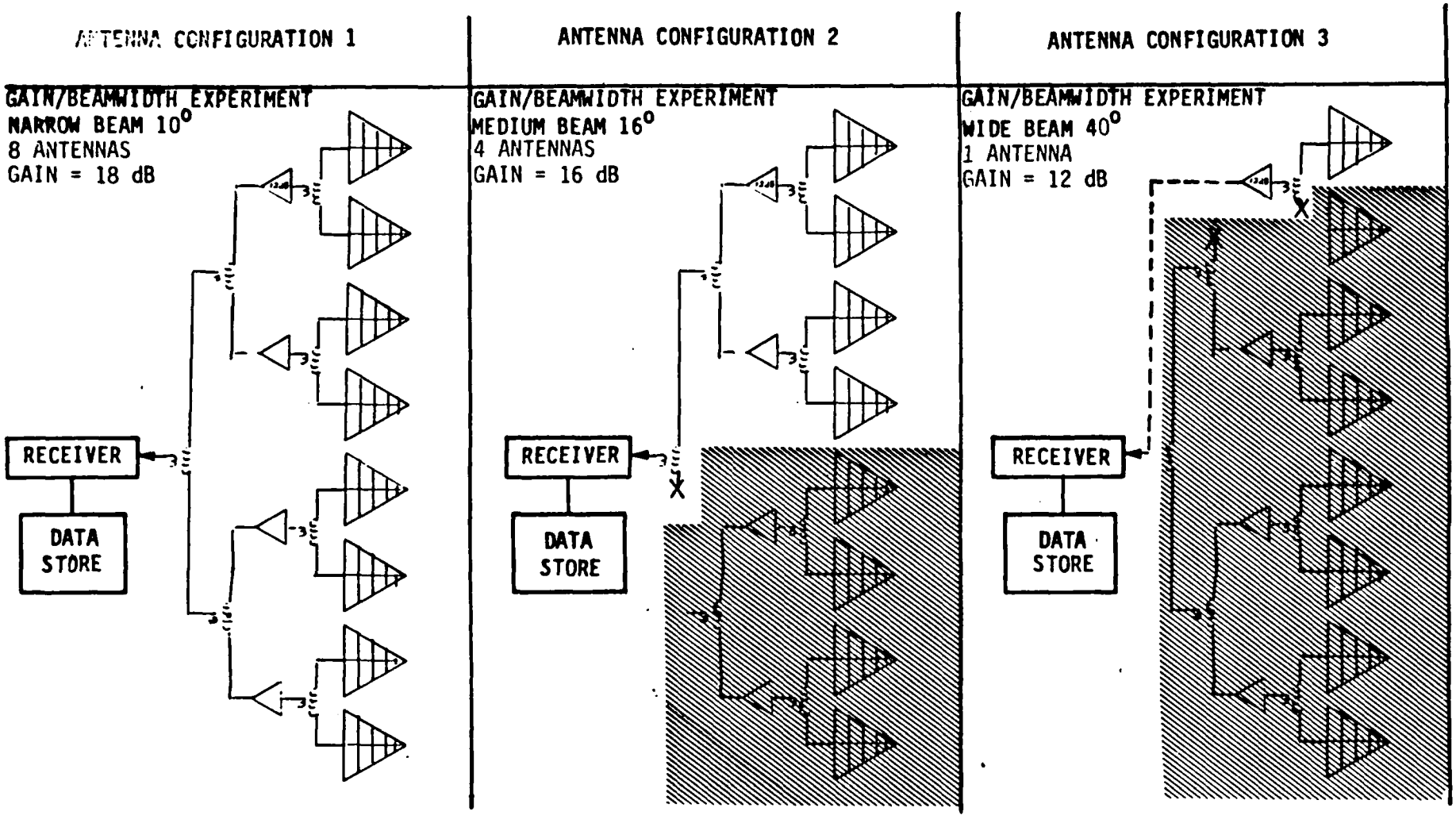

RE-08292

Figure 2.19. Gain/Beamwidth Antenna Array Configurations

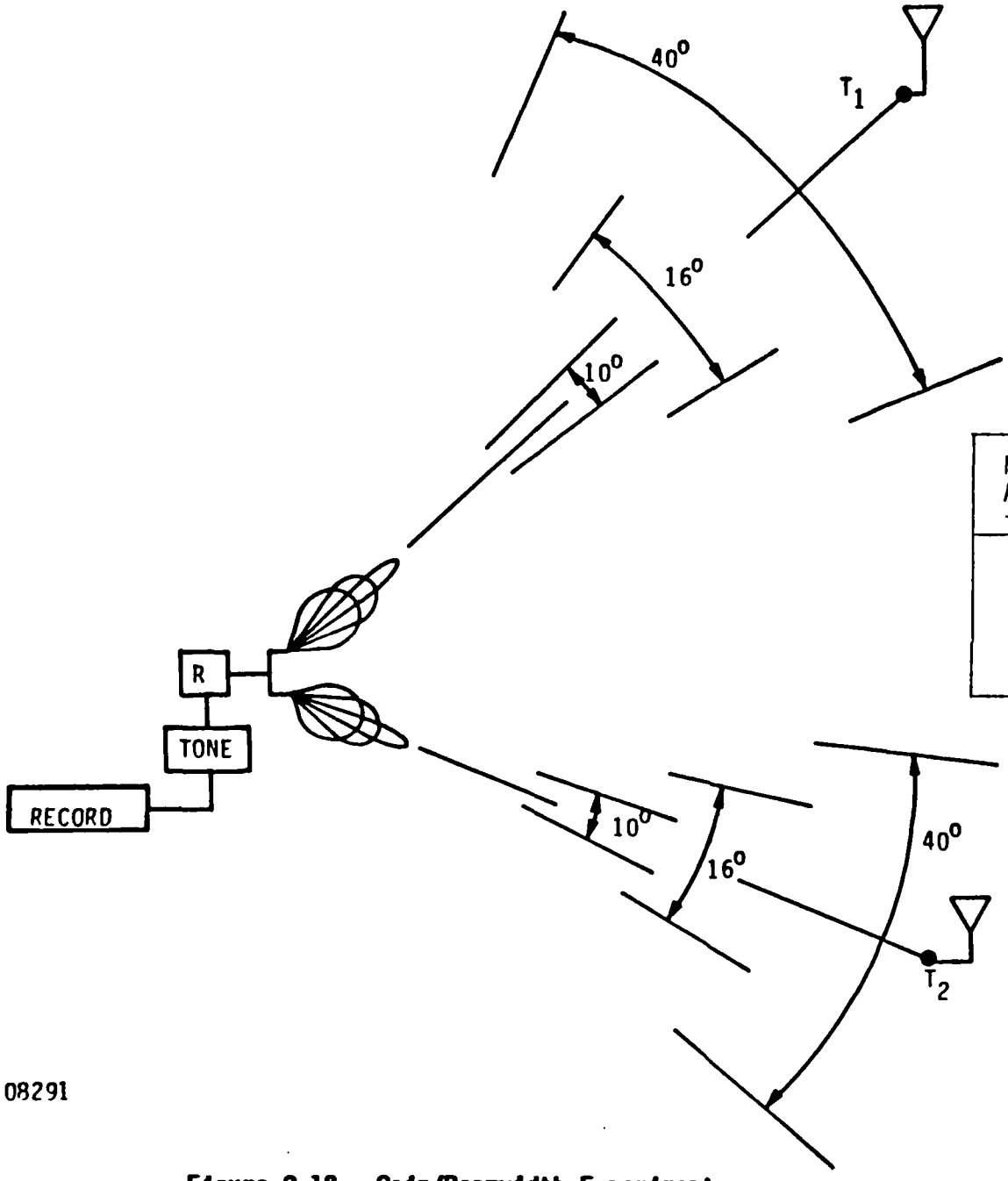

Number of Antennas in Array	Gain	Beamwidth
1	12 dB	40°
4	16 dB	16°
8	18 dB	10°

Figure 2.18. Gain/Beamwidth Experiment

Two data sets from two separate sources

APPLICATION FOR FREQUENCY ALLOCATION	CLASSIFICATION	PAGE 5 OF PAGES	FORM APPROVED OMB 22-R 0248

II. EQUIPMENT USAGE

A. TARGET STARTING DATE FOR EACH STAGE.

STAGE 1 _____ STAGE 3 _____

STAGE 2 _____ STAGE 4 _____

B. TYPE OF SERVICE:

C. EXTENT OF USE:

D. GEOGRAPHICAL AREA FOR:

STAGE 2

STAGE 3

STAGE 4

E. NUMBER OF EQUIPMENTS IN INITIAL STAGE:

F. NUMBER OF EQUIPMENTS PLANNED FOR OPERATIONAL USE.

G. NUMBER OF EQUIPMENTS OPERATING SIMULTANEOUSLY IN THE SAME ENVIRONMENT

H. TRANSMITTER INSTALLATION.

I. RECEIVER INSTALLATION

J. PREVIOUS J/F 12 APPLICATION NUMBER TO BE

☐ CONTINUED, UNCHANGED J/F 12/ _____

☐ SUPERSEDED J/F 12/ _____

☐ RELATED J/F 12/ _____

☐ NONE

K. IS AN ECP SPECTRUM SIGNATURE BEING SCHEDULED FOR THIS EQUIPMENT IN ACCORDANCE WITH MEASUREMENT PROCEDURES DESCRIBED IN MIL-STD-449 ( )? ☐ YES ☐ NO

L. DESCRIBE BRIEFLY ANY OTHER MEASURED DATA BEING OBTAINED IN LIEU OF OR IN ADDITION TO PROCEDURES SET FORTH IN MIL-STD-449 ( )

M. EQUIPMENT SPECIFICATION NUMBER(S)

N. APPLICABLE SERVICE CONTRACT NUMBER(S)

O. NAME AND OFFICE SYMBOL OF — TELEPHONE NUMBERS

PROGRAM MANAGER Commercial _____ Autovon _____

PROJECT ENGINEER Commercial _____ Autovon _____

P. REMARKS

CLASSIFICATION

2.4 SIGNAL DESIGN AND PROCESSING

2.4.1 Introduction

An objective of the Phase I program has been to consider means for optimizing diversity reception of VHF communications. Signal processing can provide a means for substantially improving percent copy in diversity communications systems by producing a reliable signal from multiple signals that may be unusable individually. In Phase I we have devoted considerable attention to this matter, which promises to be of significant utility in applications of diversity reception of non-cooperative VHF transmitters. Although the Phase II program emphasizes the resolution of outstanding physics issues rather than signal processing issues, we feel that it is important to summarize our work in signal design and processing here, so that it might be available for future development of diversity reception communications systems.

It is well known that the ionization trails produced by small meteors as they disintegrate in the high atmosphere result in short-term communication channels, which are usable in the spectral region from, roughly, 30 to 100 MHz. Since the formation of these trails is a random process, the characteristics of the meteor burst communication link between two given points are also random processes. As a simplification, we may think of the channel as being either on or off with typical behavior being a few hundred "on" periods per hour, with each period being a few hundred milliseconds, and with a representative duty cycle being a few percent. The actual value depends on the characteristics of the sender and the receiver, the time of year and of day, geographic position, etc.

While these duty cycles permit useful traffic transfer between cooperating stations, any workable system for monitoring must have only a few percent of "off" periods. Such a large increase in duty cycle may be achieved by forming parallel observation paths and combining signals from these multiple paths. That is, several antenna/receivers may be oriented towards the location to be monitored and their output relayed to a central signal processing location which analyzes them jointly to produce an optimum estimate of the content of the monitored signal.

Two methods of providing multiple observation paths are conceivable:

- Angular diversity where many co-located narrow beam antennas (plus a receiver per antenna) partition the volume of meteor occurrences into several high gain regions.
- Spatial diversity where several distributed stations with moderate-beamwidth antennas provide signals from distinct volumes of space.

The two approaches are illustrated in Figure 2.22. The concept of spatial diversity is self evident. Since angular diversity partitions the regions of meteor trails, each beam sees fewer events of a given strength. However, the increased gain in each beam permits lower intensity meteor trails to be distinguished (from the noise floor) so that the duty cycle of the narrower beams is affected by conflicting factors. We assume here that it remains constant as the beam is narrowed.

In either approach then, we have available multiple paths that are at least partially independent in terms of the signal propagation mechanism and are essentially independent in terms of noise impairment. The signals are independent when they arise from distinct meteor trails and are dependent when a single trail gives rise to a receivable signal in multiple paths. Both phenomena give rise to increased throughput. The improvement is self evident for independent signals. With dependent signals the additional signal power from multiple observations can be exploited to extend the usable duration of the burst. These improvements require that the receivers' direct observables be brought to a central processing facility so that the combining can be optimized. In the angular diversity case such joint processing is readily achieved since all receivers are co-located. With spatial diversity, however, some form of a collection network is required to bring the various observables together for joint processing.

The signal design and processing methods described in the following are viable with either diversity method. The combining procedure will allow not only the detection of all signals that could have been detected individually, but also may permit the combination of individually unusable signal remnants into a composite signal that can be used.

2.4.2 Channel Description

For applications of a diversity reception communication system, multiple propagation paths may be used to monitor a single sender. Each

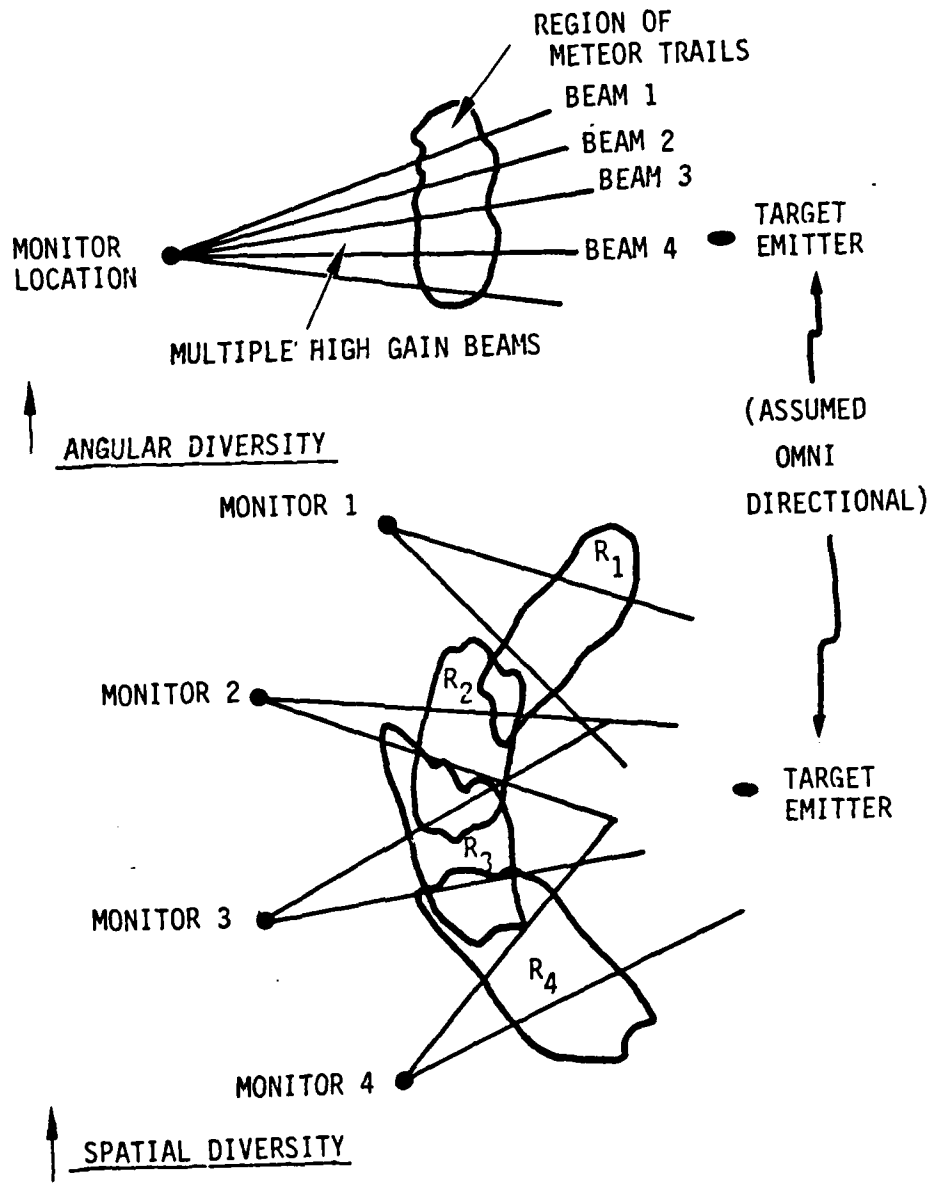

Figure 2.22. Diversity Strategies for VHF Monitoring via Meteor Bursts

such path includes the transmitter being monitored, a meteor burst transmission channel and a receiver (including an antenna). A diagram of the overall monitoring network for certain applications, such as non-cooperative reception, is shown in Figure 2.23.

These multiple paths will each yield an observation process of the sender's communication activity which has a low to moderate duty cycle. If the paths are configured to yield more or less independent responses, then the joint output of the ensemble of receivers may be processed to give a diversity combined output which includes the combined parallel propagation effects of the multiple paths.

If these paths are independent, then each path's propagation is the result of distinct meteor events. Returning to the "on-off" conceptual model of the last section, it is evident that a parallel path monitoring network would result in a combined channel which is the logical OR of the set of individual channels. Let the probability that any given path is in the "on" state be P1. Then, assuming independent paths and identical individual duty cycles, the probability that the set of N combined paths is in the "on" state is $PN = 1-(1-P1)^N$. Expanding this with the binomial theorem yields:

$$PN = \sum_{n=1}^{N} \binom{N}{n} P1^n$$

The union bound of probability theory, $PN < N*P1$, suggests that the duty cycle of the combined channel is no better than N times the duty cycle of any one path. Moreover, even this level of improvement depends strongly on the channels being statistically independent. In the extreme case where the same meteor phenomenon is the causal mechanism for every path, then the performance of the combined parallel path is no better than the performance of any one path.

The results of the previous paragraph are unduly pessimistic, however, since the behavior of each meteor burst channel is more complex than simple "on-off" conditions. Noise is present at the input to each of the receivers in Figure 2.23 so that each channel would be "on" only in a probabilistic sense, even when a meteor burst exists. A more precise view is that each receiver produces a continuous random variable "r(t)". If we ignore for the moment the effects of variations in the length of the

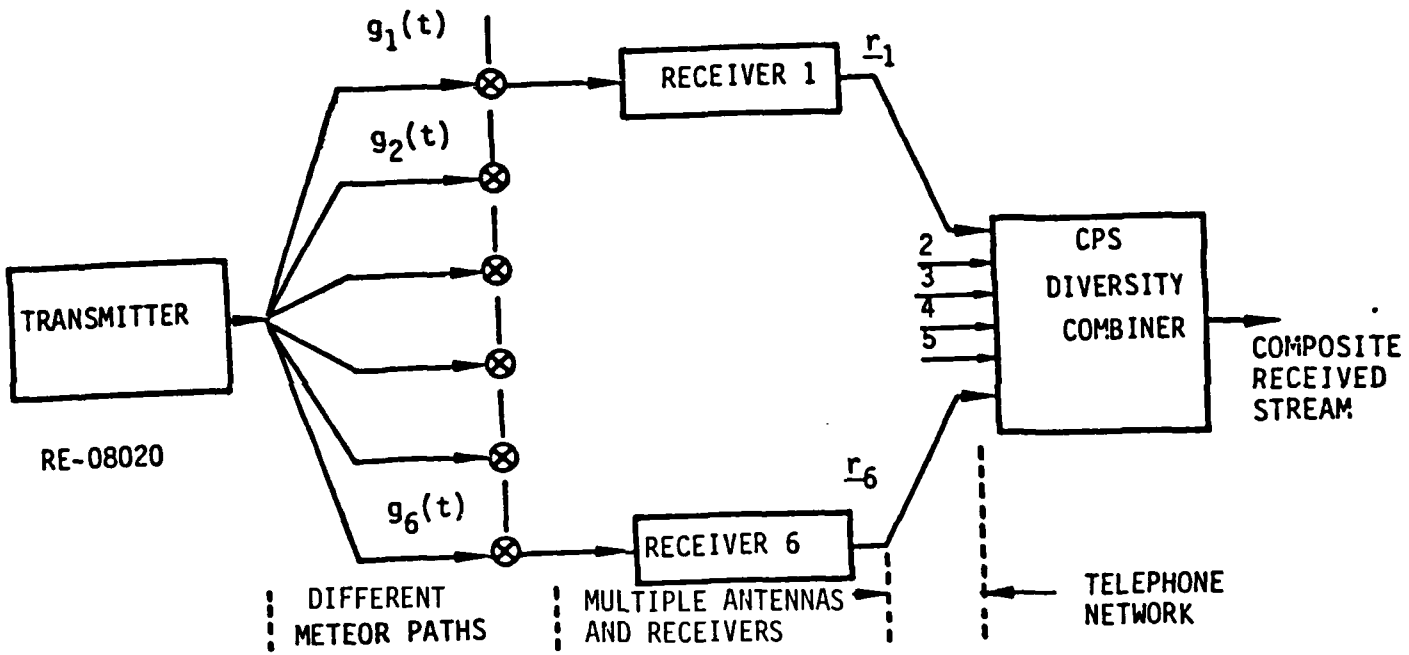

Figure 2.23. Network Concept for Applications of Diversity Reception (Reciprocal of the Phase II Program)

propagation path, then r(t) will be a scalar variable which is the sum of a noise process and of a signal whose amplitude is a random process generated by meteor bursts.

We assume in the following that the receiver input noise has a uniform spectrum over the frequency band of interest and that it has a Gaussian distribution so that an additive white Gaussian noise (AWGN) description is appropriate. The observation process from each of the receivers is then of the form:

$$r(t)=s(t)+w(t)$$

where "w(t)" is white Gaussian noise with a mean of zero and a (one-sided) power spectral density of N_o. The signal process "s(t)" consists of the transmitter's baseband signal "m(t)" modulating a carrier of angular frequency as seen after passage through a meteor burst channel. This channel may be characterized by its instantaneous gain "g(t)" and propagation delay "d(t)". Thus the signal observed by a receiver has the form:

$$s(t) = g(t)m[t-d(t)]\cos[\omega(t-d(t))]$$

At first glance the gain process, g(t), exhibits the typical meteor burst behavior. That is, it is zero much of the time (i.e. burst absent) and exhibits random (Poisson distributed) bursts of finite gain. These bursts usually have a very sharp onset, corresponding to the rapid formation of an ionization trail, followed by an exponential decay of gain as the cylinder of ionization diffuses. This rate of decay is reasonably small compared to the symbol rate of transmission of the source being monitored so that the function g(t) may be approximated as a constant over the symbol interval for symbols of the order of 10 milliseconds or shorter. The delay process, d(t), may be considered a constant, to a first approximation, during the course of a given meteor burst (i.e. a non-zero g(t) episode). The delay will vary from one burst to another, however, depending on the actual location of the ionization trail. Consider for example, a receiver which is 1000 km from the transmitter. Then a meteor burst occurring at an altitude of 100 km above the mid-point between the transmitter and the receiver results in a propagation delay of about 3.40 ms. For a burst at the same altitude but above a point 200 km at right angles from the mid-point, the transit time increases to 3.65 or about 0.25 milliseconds more. For symbols of the order of 10 ms duration, the

propagation time may therefore be treated as constant without serious error in symbol timing (error of the order of a few percent). Propagation time variations of a few hundred microseconds are very significant on the time scale of the carrier signal, however, since this time interval spans a few thousand cycles of the carrier. From another perspective, the wavelength of a carrier in the 30-100 MHz range is a few meters while the bursts occur over a region that is hundreds of kilometers in extent so the path length of two different meteor bursts may be expected to exhibit a carrier phase which varies randomly over 360 degrees. There may also be some variation in the path length (and hence of the carrier phase) during the course of the burst as a result of displacement of the ionization trail by ionospheric winds. Such motion results in the received carrier appearing to have a slightly different frequency than the sender's - for wind speeds of less than 70 mph (30 meter/second) the proportional frequency shift will be 0.1 parts per million or, equivalently, a few Hertz. This degree of frequency uncertainty in the received burst signals can be removed by carrier tracking of the incoming signal phase so long as the symbol period is short enough that the phase change is small. (This will be the case for symbol rates of a few tens of Hertz or higher).

Putting all this together we arrive at a first view of the received signal as:

$$s(t) = g_n m(t)\cos(\omega t + \theta_n) \qquad nT \leq t \leq (n+1)T$$

The above expression denotes the signal during the nth symbol interval and states that the channel gain is a random variable which is treated as constant over the symbol interval and that the signal is received with a random carrier phase. For simplicity, the gross delay is ignored and the expression is written in the time frame of the receiver.

This model of the signal process is simplistic in the sense that it is premised on either a single relatively strong burst or no burst at all. While these strong bursts constitute the usual dominant transfer mode for a meteor burst channel, the nature of the meteor phenomena is such that there is also a background of weaker but much more frequent meteor trails. A more complete model of the network which accounts for this additional background signal activity would then depict a scattered background activity with a Rayleigh amplitude and a fluctuating phase. This background is interspersed with occasional episodes of much stronger amplitude

and coherent phase. In the context of the network model of Figure 2.23, the incoherent background may be of particular importance since the background signals in the multiple channels may be combinable to yield a useful monitoring of the transmitter during intervals when no major burst is in progress.

It should be emphasized that the preceeding signal model ignores variations in the transmitter-to-receiver transit time. As argued above, this is justifiable in the context of low symbol rate transmission. However, for monitoring of a higher speed data transmitter (e.g. 4800 bps or more), the time-dispersion resulting from path length variation will present additional signal processing challenges to deskew the multiple transmission paths. The signal processing methodology described in the following avoids this complicating factor by addressing only low speed symbols. This limitation of the monitoring method should be kept in mind.

In earlier paragraphs, the issue of channel independence was raised in the context of the "on-off" channel model. In that simple context, signals in multiple channels from a common meteor could not enhance the duty cycle above that for the single channel. Commonly observed signals can however, be processed to yield a superior duty cycle in the more complete model since (largely) independent noise - if not signal - is present at each receiver's input and since, with proper processing, the signals from the parallel paths may be combined coherently. This results in a stronger signal which will have a longer lifetime before dropping beneath the noise floor.

The performance of the network model may then be summarized as follows:

- The multiplicity of paths provides for the observation of more meteor burst trails since a larger region of space is observed (spatial diversity) or several regions are observed with enhanced gain (angular diversity).
- The multiplicity of paths may permit the incoherent background activity of low level meteorites to be exploited for enhanced duty cycle.
- The multiplicity of paths can result in an array gain for those meteor trails which are observed in more than one beam.

2.4.3 Experimental Signal Set

From the discussion of the channel model above, it is evident that the experimental signal set should have two key properties. First it should have a low symbol rate to avoid the time dispersion difficulties alluded to in the above section. Second, it should be robust with respect to the random phase characteristic of the channel.

Binary frequency shift keying at 100 symbols/second is the recommended signal set for an experiment that would address signal processing issues. The symbol interval of 10 mS is long with respect to the dispersion of propagation time so this signal set satisfies the first criterion. If the two frequencies of a binary signal pair are each integer multiples of the symbol rate, then the two signals in the set are orthogonal over the symbol time. An orthogonal signal pair may be distinguished incoherently (i.e. without knowledge of the carrier phase) so this signal set also satisfies the second criterion. Such a set can also be processed coherently, of course, with significant performance advantage under low contrast conditions.

We propose then, that the signal set be comprised of 100 and 200 Hz tones each of duration 10 ms. Representative waveforms in this class are shown in Figure 2.24. Mathematically, this signal set is defined as:

$$m_n(t,j) = A\sin(2\pi f_j\ (t-nT))$$

where:

- n denotes the symbol epoch (n=0,1,2, ...)
- T is a symbol interval (10 milliseconds)
- j_n represents the choice of frequency for epoch n and is binary (0 or 1).
- f is the instantaneous frequency during the symbol interval, and is one of two choices f_0=100 Hz or f_1=200 Hz.
- A is the amplitude of the signal set and is a constant.

Fortuitously, a signal set with these properties seems to be representative of operational traffic of interest for monitoring via a VHF reception network.

The proposed signal set has certain other advantages for experiment. The low symbol rate results in a relatively large energy-to-noise ratio for moderate carrier powers so that many meteors should give rise to usable signals. Concommitantly, the low rate signal has a narrow, concentrated,

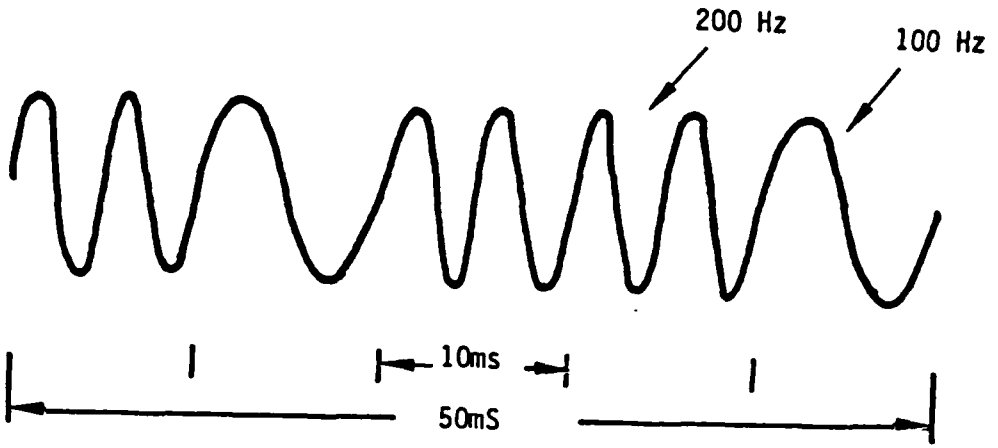

Figure 2.24. Representative Signal a Signal-Processing Experiment

spectrum which minimizes out-of-band spectral emissions. The constant amplitude waveform of these signals will minimize the consequences of any nonlinearities in amplifiers through which the signal is processed. Of considerable importance to the experiment, these low rate signals lend themselves to processing by general purpose micro-computers, thus minimizing program cost and maximizing program flexibility.

The data content of the signal depends on the stream of binary letters (the "j_n" in the equation above). For the experiment this data stream should be a clearly definable pattern so that the outputs of individual receivers and of the central diversity combining can be readily checked for correctness. On the other hand, the transmitted data pattern should appear more or less random so that good balance occurs between logical 0 and 1 and so that the potential for biases in the signal processing is minimized. The so called psuedo-noise (PN) sequences have these properties and are very easy to implement. Recommended for a signal-processing experiment is a PN sequence of periodicity 8,388,607 which may be generated by a linear feedback shift register of length 23. A suitable recursion relation to generate a PN sequence of this type is:

$$S_{n+23} = S_n + S_{n+3} \qquad \text{(modulo 2 addition)}$$

Note that the periodicity of this sequence is very nearly one day for a bit rate of 100 per second.

2.4.4 Modulator Organization

The modulator will generate the PN data sequence and map this sequence into the frequency shift keyed waveform described above. These operations will be implemented in a small general purpose computer equipped with a digital-to-analog convertor. The technique will be to produce a quantized version of the FSK waveform using a sampled construction which includes many samples per symbol of the experimental waveform. A sample rate of 16 times or more the bit rate is appropriate and easily realizable. After passage through low pass filtering to remove the high frequency artifacts of the sampled reconstruction, the resultant signal will closely follow the signal set described above. Note that this signal set is equivalent to a single sinusoidal cycle per symbol or two such cycles and that exact lock will be maintained between the symbol timing and the FSK tone frequencies so that all transitions are continuous.

The modulator's output will be presented to the VHF transmitter which operates single sideband. Thus, the actual transmitted waveform will also be in constant envelope FSK format with 100 Hz separation between its tones and with a 100 Hz symbol rate.

A top level block diagram of the modulator hardware in shown at Figure 2.25. A WWV interface has been posited in the diagram as a means of locking the modulator to a standard timing source. The structure of software to generate the experimental signals is shown in Figure 2.26. Note that in this and other software diagrams to follow, it has been assumed that the transmitter and receivers operate under the control of a central processing site via telephone lines. Some form of packet protocol has been assumed as the means of exchanging information on this wireline system. Provisions are also indicated in Figure 2.26 for a man-machine interface at the transmitter equipment.

2.4.5 Demodulator Organization

The use of a microcomputer for signal processing is a feature of the demodulator also. A signal processing interface consisting of A/D and D/A convertors is an essential adjunct to the microcomputer for this purpose.

Before exploring the actual implementation structure, however, it is worthwhile here to further consider some fundamental signal processing issues. When a meteor burst occurs, the signal arriving at the demodulator has a random phase. While it is not essential to recover the carrier phase to demodulate an FSK signal, there is a performance advantage to demodulating coherently where possible. We propose to preserve the potential for coherent detection in the demodulator design by projecting the received signal onto quadrature components (I & Q) as the first processing step in the demodulator. Since this is a reversible step, no loss of optimality results even if the exact phase relation is unknown. (There is an assumption, however, that the carrier frequency of the transmitter is known within a small uncertainty so that the projection of the signal onto the phase space of the receiver may be done without rapid change of phase).

With reference to Figure 2.27, which shows a top level block diagram of the demodulator, the resolution of the I and Q components is performed in the block labelled "audio synchronous mixers". The structure of this block appears in more detail in Figure 2.28, which shows that the operation consists of two down-conversion frequency translations using orthogonal

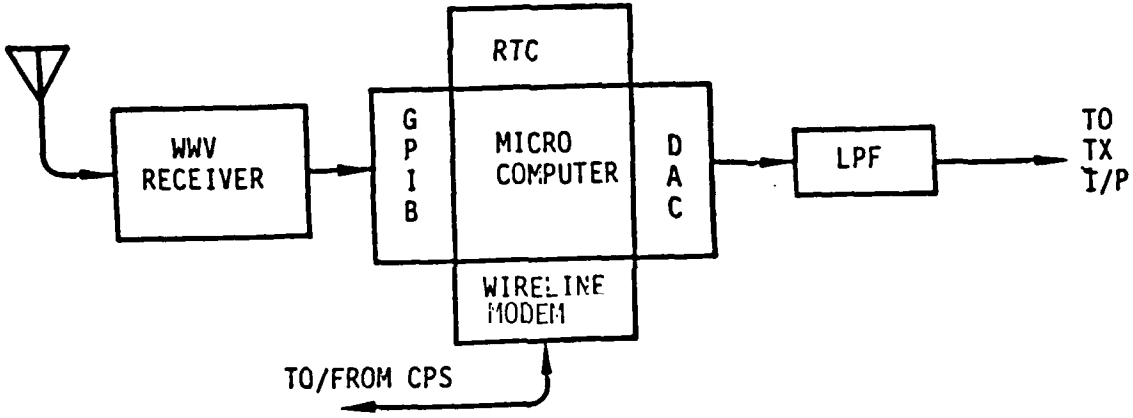

Figure 2.25. Modulator Hardware Organization

received observables on a long-term storage medium (magnetic tape) is made so that the data may be processed using advanced combining algorithms if and when they become available.

obtained. Such intermediate level signals may still be detected incoherently on the basis of the relative energy in the correlators for each of the two tones. (That is, by forming the sum of the square of the I and the Q correlators for each frequency). The CPS may then combine the energy estimates for each frequency from each of the monitoring network's parallel paths into a combined decision variable for each of the two tones. This diversity combining should weight the various components according to the current quality of meteor propagation for the various paths. Thus, the observable from a stronger path would receive more credance than that from a weaker path. Such weighting requires a procedure for estimating the relative quality of moderate to weak meteor burst propagation paths, however. Both this channel assessment procedure and the combining algorithm require further system analysis as well as software development and hence are appropriate for some later program exploring signal processing issues.

The top level organizations of the CPS hardware and software are shown in Figures 2.32 and 2.33, respectively. Packets containing the various paths' received observables will arrive at the CPS from the telephone network or from direct connection with the network's receivers. Since each of the propagation paths will have a specific average delay, the components from the various receivers must be aligned (or de-skewed) before they can be combined. (This deskewing should not be thought of as taking out the variation in any one path due to differences in that path's length from one burst to the next. It simply removes the average difference between the propagation time for two distinct paths). Also, the apparent signal strength must be assessed so that the appropriate diversity combining and detection algorithm may be employed. In the case of strong signals, the phase trajectory of the signal is determined beforehand to permit coherent detection to be done. Detection proceeds by whatever algorithm is most appropriate to the quality of the data and yields a composite network decision as to the monitored source's data bit. The relative quality of these decisions is appended to them and the result is output to a network operator.

The CPS will be fitted with additional software to permit an operator to control remote receivers. Additional features permit an operator to review the overall performance of a network. Provision to record all the

composite observable (i.e. six vectors of four components each). In the terminalogy of detection theory, a maximum aposterior probability (MAP) decision is required. For equally likely 0's and 1's at the transmitter, this requirement readily maps (through Bayes' Rule) to an equivalent requirement for a maximum likelihood (ML) decision. That is, the CPS's task is to find the binary value which satisfies

$$\text{Max}_{j_n = 0 \text{ or } 1} \quad P[r_1, r_2, r_3, r_4, r_5, r_6 \mid j_n]$$

With reference to the subsection on demodulation, above, it may be recalled that the four components of each of these vectors are comprised of a signal component plus a noise component. The noise may be treated as independent and identically distributed Gaussian random variables. The signal components of the two correlators which are matched to the tone that was actually sent have means of the form $g_n A\cos(\theta_n)$ and $g_n A\sin(\theta_n)$ while the other two components have means which are zero. Both g_n and θ_n are random variables (as a result of meteor burst activity) but may be treated as constants over the period of one symbol.

From a practical point of view it may be difficult to make decisions in a space of this high dimensionality. A sub-ideal but more readily implementable approach involves pre-processing each receiver's signal vector to establish if any of them are experiencing a strong meteor burst. When such a burst is in progress on a path, this path will be the predominate factor in reaching a network decision.

To keep initial software development from becoming too complex, the initial phase of the CPS should use this approach to signal processing. That is, it should assess which of the six receiver inputs have strong bursts in progress and ignore the rest. For those with strong bursts, the CPS should estimate the carrier phase and phase rate for the current propagation path. With a reliable phase estimate, the sequence of four dimensional observations from the receiver can be reduced to two dimensions. If more than one channel is responding to a strong burst in a given symbol interval then these two dimensional representations may be added coherently to produce a better equivalent signal-to-noise ratio prior to detection.

At the next level of complexity the CPS should be enhanced to process weaker signals which are not sufficiently strong for a phase estimate to be

of angular diversity, the receivers may all be situated in the same location so this interconnection may be very straightforward - a direct RS232 interface for example.

For spatial diversity, individual receivers may be scattered over a wide region. An approach to interconnection in this case is to use the public telephone network with medium speed wireline modems at the receiver sites and the central processing site. The observable vectors are transferred from the receivers to the central processor as they are received. Recalling that the signalling rate is 100 per second and that each vector contains four components, there are 400 such components per second to transfer for each receiver. If the sampling/processing resolution of 16 bits per sample indicated in Figure 2.30 is preserved for the interconnection, then the resultant data rate is some 6400 bits per second. This data transfer rate is above the limits of low cost wireline modems and of unconditioned voice lines. With some reduction in resolution (e.g. 12 bits/sample) and a 50% discard rate by the weak signal detection algorithm, the rate drops to 2400 bits/second which may be handled with moderate price equipment and lines.

2.4.7 Central Processor Organization

Once all the signals from the parallel components of the network are brought to a common location they can be processed jointly to achieve some diversity and/or array gain. The detailed approach to joint processing will require further development during the next phase of the project. However, some general issues are evident at this time and are discussed here. (For the sake of definiteness in the discussion, six paths are assumed. This number may be greater or less depending on the detailed design of an experiment. Clearly, at least two paths are required).

For each signalling interval of the transmitter being monitored, the central processing site (CPS) will be represented with six observable vectors, one from each receiver, with each vector having four components. (See the preceding sections for a description of these observables). For observations which seemingly have no useful signal content, no data is forwarded to the CPS by the receiver involved: the CPS will treat these as pure noise.

In an ideal sense the problem facing the CPS is to decide which of the binary hypothesis is more probable to have been transmitted given the

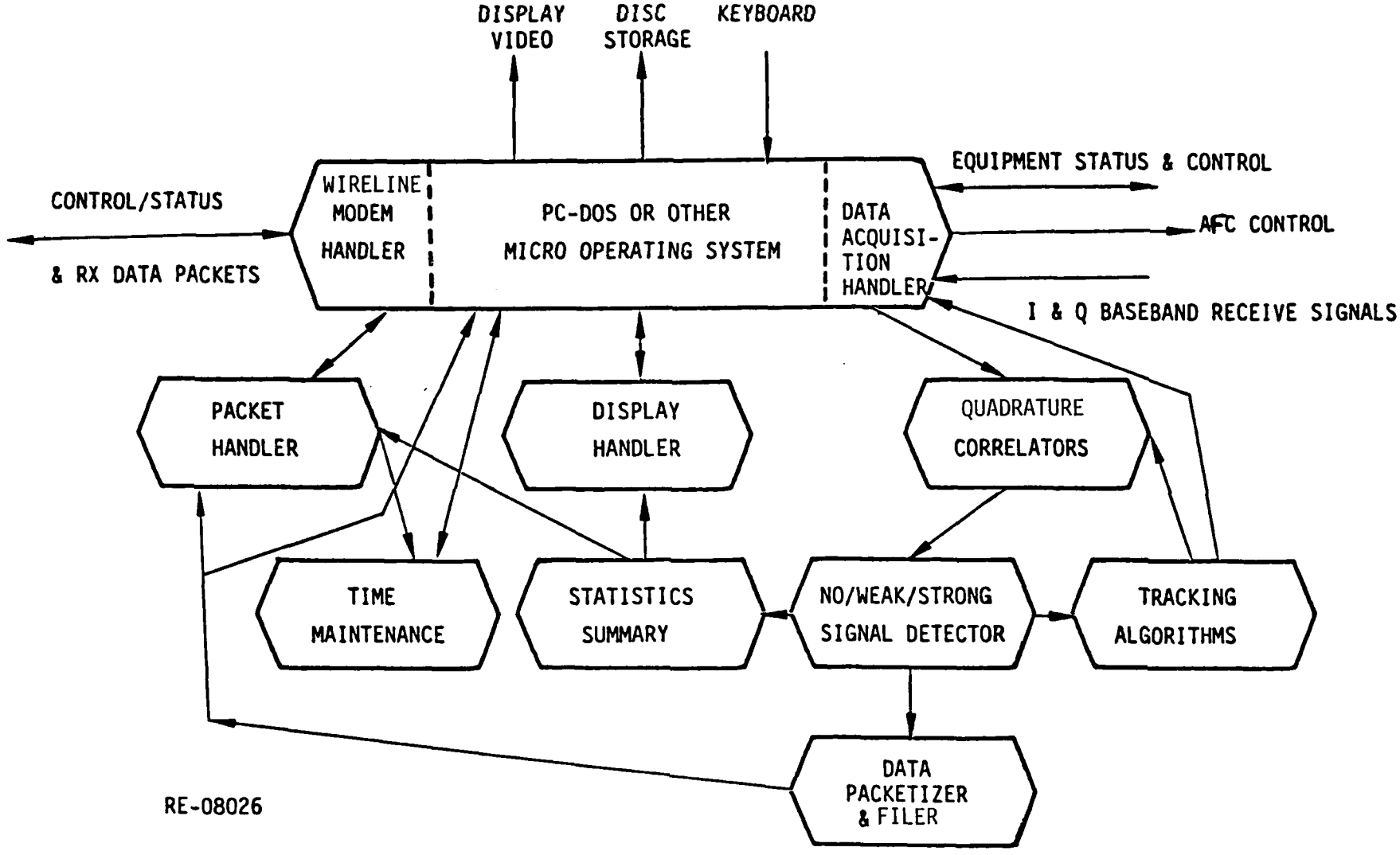

Figure 2.31. Demodulator - Software Organization

as by oscillator differences, it is important to keep the corrective changes to the local oscillator heavily damped to avoid unnecessary jitter in the frequency tracking.

The other major housekeeping function is symbol timing tracking. Note that the proposed algorithm for maintaining this timing depends heavily on the relative stability of the transmitter's and the receiver's symbol clocks and the presence of an occasional strong meteor burst to refresh the alignment of these clocks. To assess the reasonableness of this approach consider that it is not difficult to provide a clock stability of 1 ppm at each end of the path. At a symbol rate of 100 symbols/second (360,000 per hour) the maximum slip rate is less than one symbol position per hour. Since there are typically many tens to a few hundred strong meteor bursts per hour, these should provide ample opportunity for correction of the receiver's symbol timing to within a small fraction of a symbol interval. As for AFC, the symbol timing correction algorithm is engaged only during the presence of strong signals and is decision directed. The algorithmic basis will be an early-late gate which compares the relative content of each tone (100 or 200 Hz) in a window which the algorithm attempts to center on the transition time from one symbol to a next.

As noted earlier, a symbol period is assumed to be long relative to the variation in the propagation time as a result of differing path lengths. Such is the case for the 100 bit per second signals proposed for the experiment. A more complex symbol timing algorithm will be required, however, if the signalling speed is made substantially higher.

The organization of software to perform the demodulator tasks within a microcomputer is shown in Figure 2.31. Many of the blocks of this diagram relate directly to the preceding discussion of the demodulator. Additional blocks include provision for organizing the observable vectors into packets for transmission to a central processing site, for man-machine interactions, for recording the observed data on mass storage (e.g. a hard disc), and for keeping the time-of-day in unison with the central processing site.

2.4.6 Interconnection of Receivers

For either of the two types of diversity discussed in this subsection, there is a need to bring together the receiver output signals from the multiple paths to a common location for diversity combining. In the case

it may be desirable to limit the transfer of receiver observables to those which appear to be at least marginally useful. Thus each receiver will run a weak-signal-present algorithm to differentiate between unusable noise outputs and those with sufficient signal remnant to warrant transfer to the central processing site. The basis of the algorithm will be the ratio of the apparent relative energy in the 100 Hz correlators to that in the 200 Hz correlators.

The operation of the demodulators may then be summarized as being a set of four correlators which provide matched filtering for each of the two tones in each of the quadrature phases of the received carrier. These yield a four component vector observable at each symbol time. Preliminary processing of the observables is done to cull noise-only outputs from possible signal present observables which are forwarded to a central processing site. Housekeeping functions essential to demodulator operation include correction of the demodulator's symbol clock to keep it synchronous with the transmitter's and correction of the demodulator's local oscillator frequency to compensate for frequency differences between the transmitter and the receiver.

Both of these housekeeping algorithms are engaged only when a strong signal component is manifestly present - i.e. when a strong meteor burst is in progress. (Detection of the presence of strong signals is a simple extension of the weak signal algorithm previously discussed). The automatic frequency control (AFC) algorithm will be based on the rate of change of phase of the detected bit stream. That is, the four component correlator output will be comprised of a strong signal component in the output of either the 100 or 200 Hz correlators and of noise only in the other pair of correlators. Suppose, for example, that a 100 Hz tone is sent in the nth symbol interval and that a strong burst is in progress. Then the outputs of the 100 Hz correlators in the I and Q channels will be of the form $g_n A\cos(\theta_n)$ and $g_n A\sin(\theta_n)$, respectively (plus some noise). The ratio of the Q to I correlator outputs produces an estimate of $\tan(\theta_n)$. From several such estimates in succession an estimate of the rate of change of the phase angle per symbol interval can be made and used to generate a corrective signal to the local oscillator to bring the rate of change to zero. Since the apparent frequency of any incoming burst is influenced by Doppler shifting from motion of the ionization trail as well

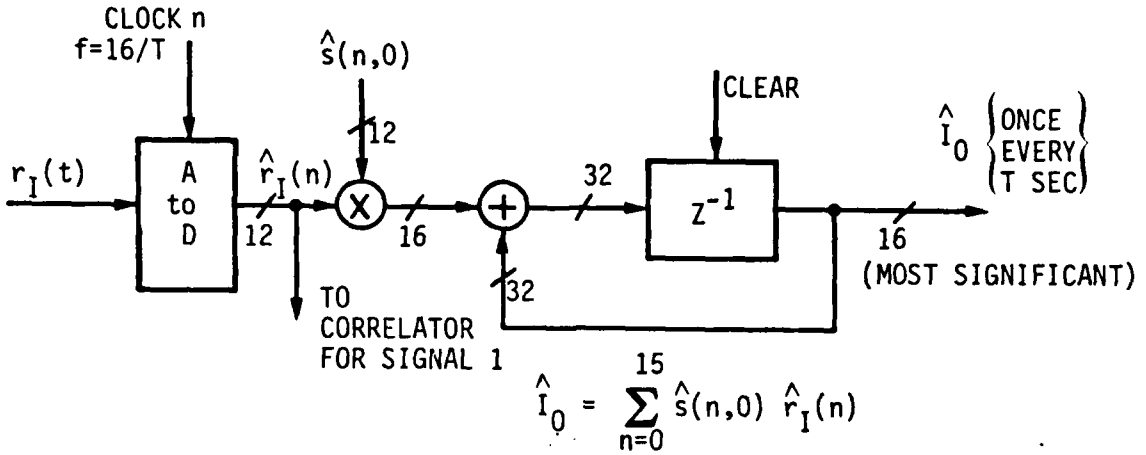

RE-08305

Figure 2.30. Demodulator - Implementation of Correlators

$$r_n = (I_{0,n}, I_{1,n}, Q_{0,n}, Q_{1,n})$$

All the information that is useful in making a decision as to the transmitter's nth binary input (i.e. j_n) is preserved in this observation vector. For a one-path observation of the monitored transmitter, a decision on j_n would be made on the basis of this observation vector alone. For an acutal signal-processing experiment, many concurrent observations of the transmission will be available. Optimum decisions for the network as a whole require that these observations be processed jointly. Hence in an ideal sense it is not appropriate for each receiver to infer a decision on j_n from r_n so each receiver will simply pass along these observation vectors to a central processing site.

Several remarks are apropos here. First, it should be clearly noted that an implicit assumption was made that the receiver is aware of the time frame of the transmitter to a sufficient degree of accuracy to carry out the correlation. (The correlation integration proceeds across the span of a symbol time and must be synchronously aligned). This assumption will be justified presently. Second, the ideal correlation operation shown in Figure 2.29, is difficult to implement exactly. A close approximation is shown in Figure 2.30 which implements the correlator digitally in discrete time and discrete amplitude. This digital correlator super-samples the analog waveform with a quantizer (A to D converter) to an appropriate resolution (12 bits is achievable at low cost), weights these by the template of the prototype signal and then carries out a simple digital integration. (A super sampling rate of 16 times the symbol rate is assumed here: the exact value is flexible.) Third, there are housekeeping functions that the demodulator must perform which are best implemented on a "decision - directed" basis. (These include symbol timing tracking and automatic frequency control). Thus under some conditions, the demodulator will further process r_n to obtain a best estimate of j_n. This estimate is only used locally for these housekeeping functions, however, and the network estimate of j_n is based on the set of r_n from all receivers. Fourth, while the ideal requires that all receiver's observables should enter into a network-wide decision variable, the reality is that signals below some minimum level are of negligible value in reaching a composite decision. Since the transport of this data from a remote receiver to a central processing site requires communication capacity (e.g. on a wireline modem)

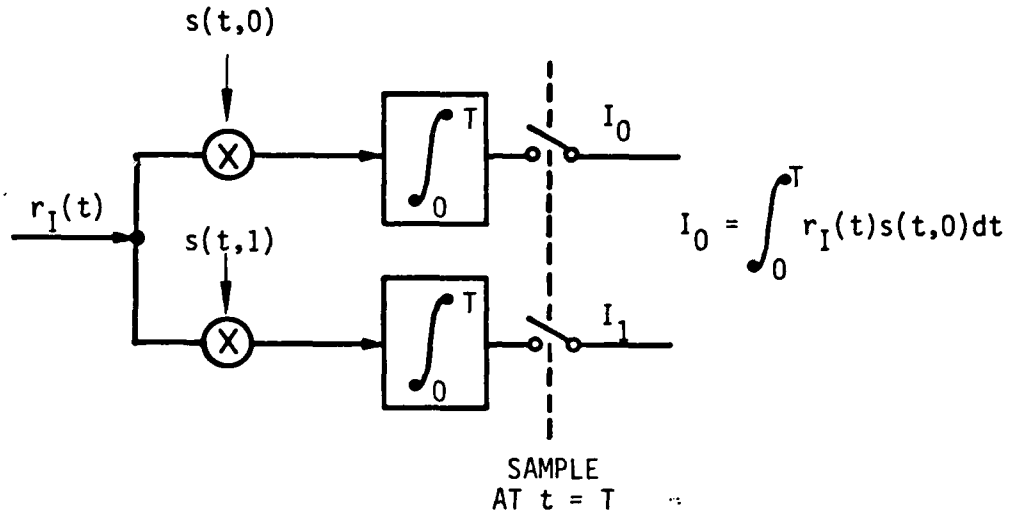

RE-08304

Figure 2.29. Demodulator - Ideal Correlations

(sine and cosine) variants of a local oscillator output. It should be noted here that the SSB transmitter and receiver are assumed to be tuned to slightly different center frequencies - a difference of 1800 Hz has been assumed for discussion. The output of the receiver is then, nominally, an FSK signal with frequencies of 1900 and 2000 Hz. The audio synchronous mixers down convert to the original FSK process (of 100 & 200 Hz) as an integral part of the quadrature projection activity. Note also that the local oscillator in the audio synchronous mixers is electrically tunable. This feature is exploited subsequently in the demodulation to complete an automatic frequency control loop which is used to compensate for any frequency differences between the VHF radio at the transmitter and the receiver.

After low pass filtering to remove the high order mixing frequencies, the quadrature components are presented to the demodulator's microcomputer where they are sampled and correlated. The signals have thus been reduced to their original baseband form, except that they are rotated in phase space by an arbitrary phase angle and are corrupted by additive noise. Mathematically, these inputs are:

$$r_I(t,n) = g_n A \sin(2\pi f_{j_n}(t-nT))\cos(\theta_n + w_I(t))$$

$$r_Q(t,n) = g_n A \sin(2\pi f_{j_n}(t-nT))\sin(\theta_n + w_Q(t))$$

Here the representation is for the nth symbol interval of T (= 10) milliseconds, the frequencies f_{j_n} are either 100 or 200 Hz, the unknown phase angle is θ_n for the nth symbol time, g_n is the response of the meteor burst channel for this interval, and $W_I(t)$ and $W_Q(t)$ are independent white noise processes.

It is well known that each of these time waveforms may be converted to binary decision scalars by correlating the waveform against each of its possible causal antecedents (i.e. the 100 Hz or 200 Hz tone). (Observe that the effect of the unknown phase is to simply scale the signal magnitude by a trigonometric function.) While this transformation (correlation) is not reversible, only irrelevant portions of the noise are lost in the operation. The correlation operation is diagrammed at Figure 2.29 for the "I" channel. An identical structure is required for the "Q" channel. At the end of each symbol interval, there are two scalar outputs from each of the I and Q correlators to yield a four component observation vector which we denote for the nth symbol interval as:

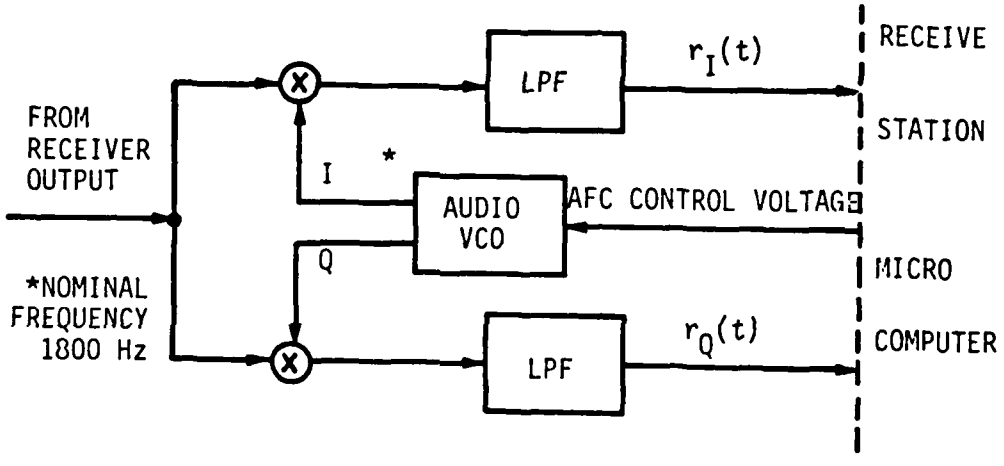

RE-08303

Figure 2.28. Demodulator Audio Synchronous Mixer

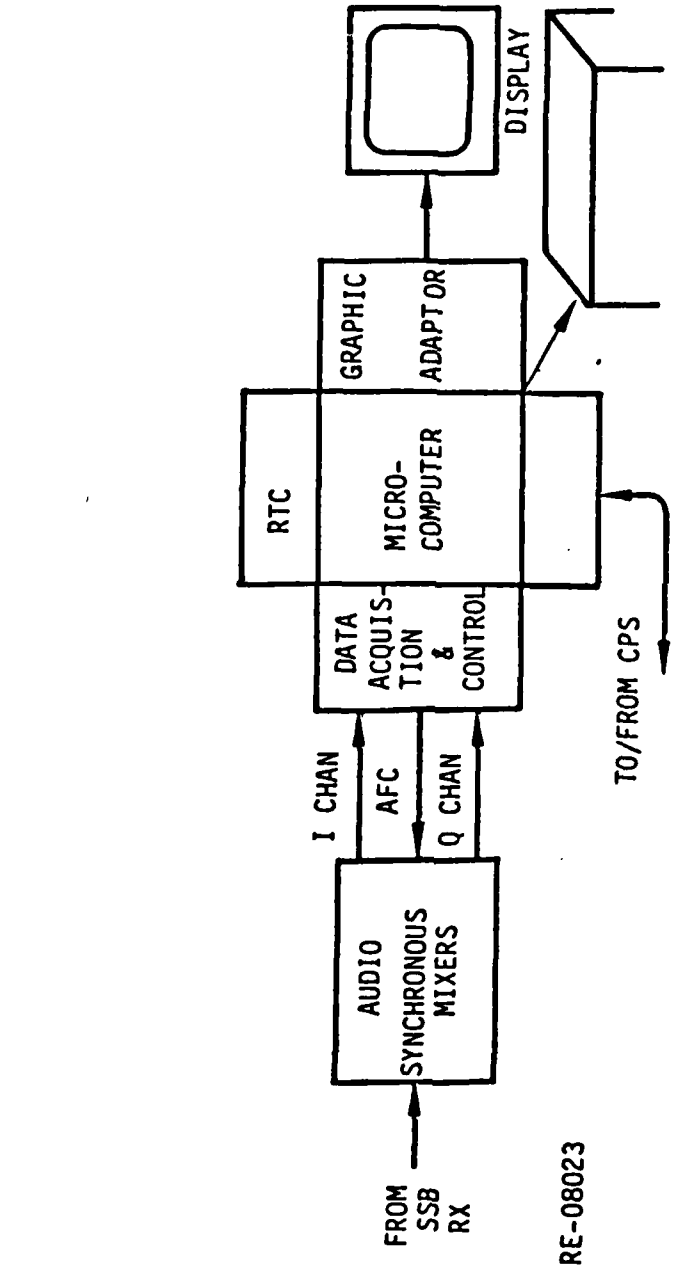

Figure 2.27. Demodulator Hardware Organization

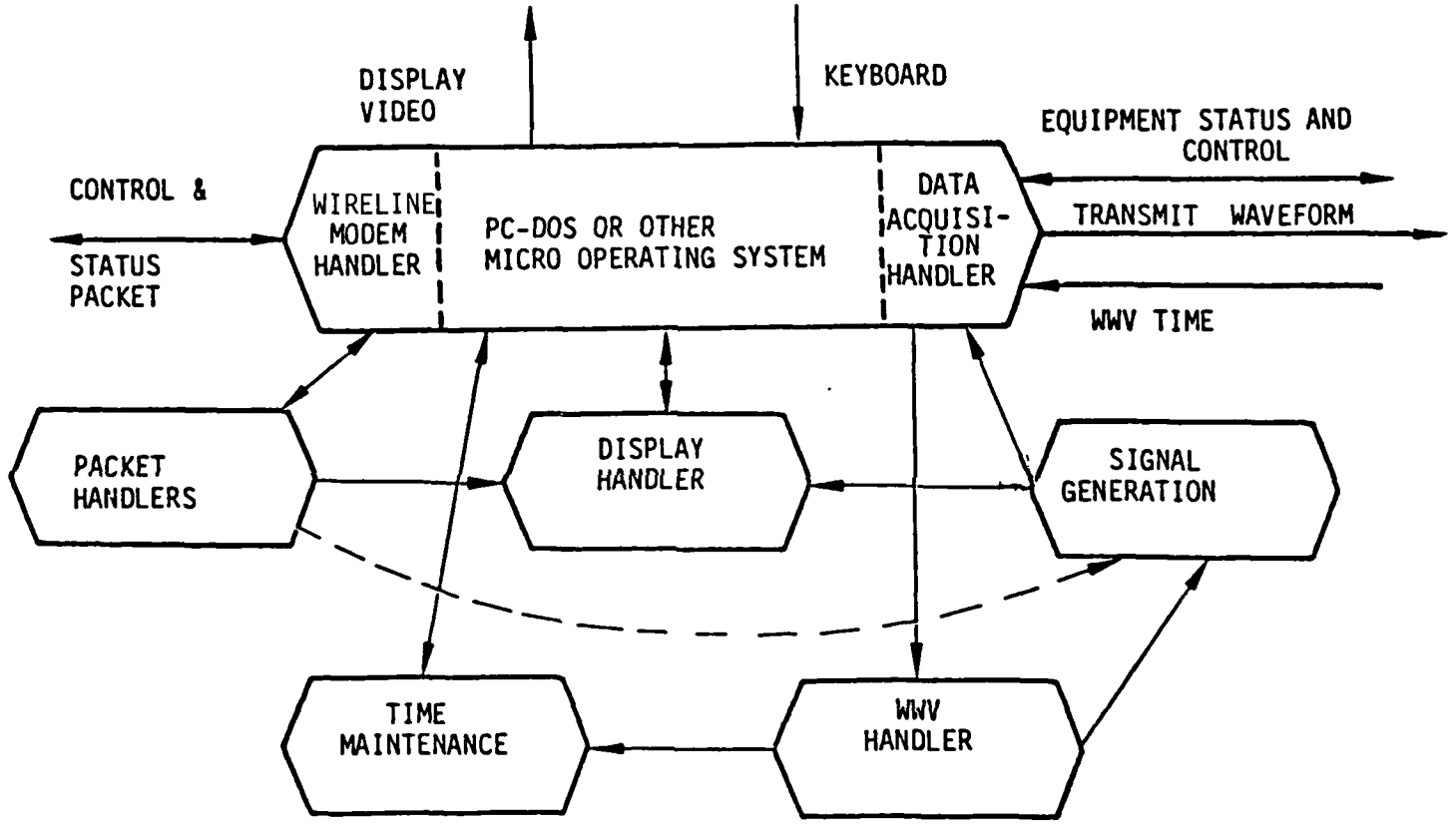

Figure 2.26. Modulator Software Organization

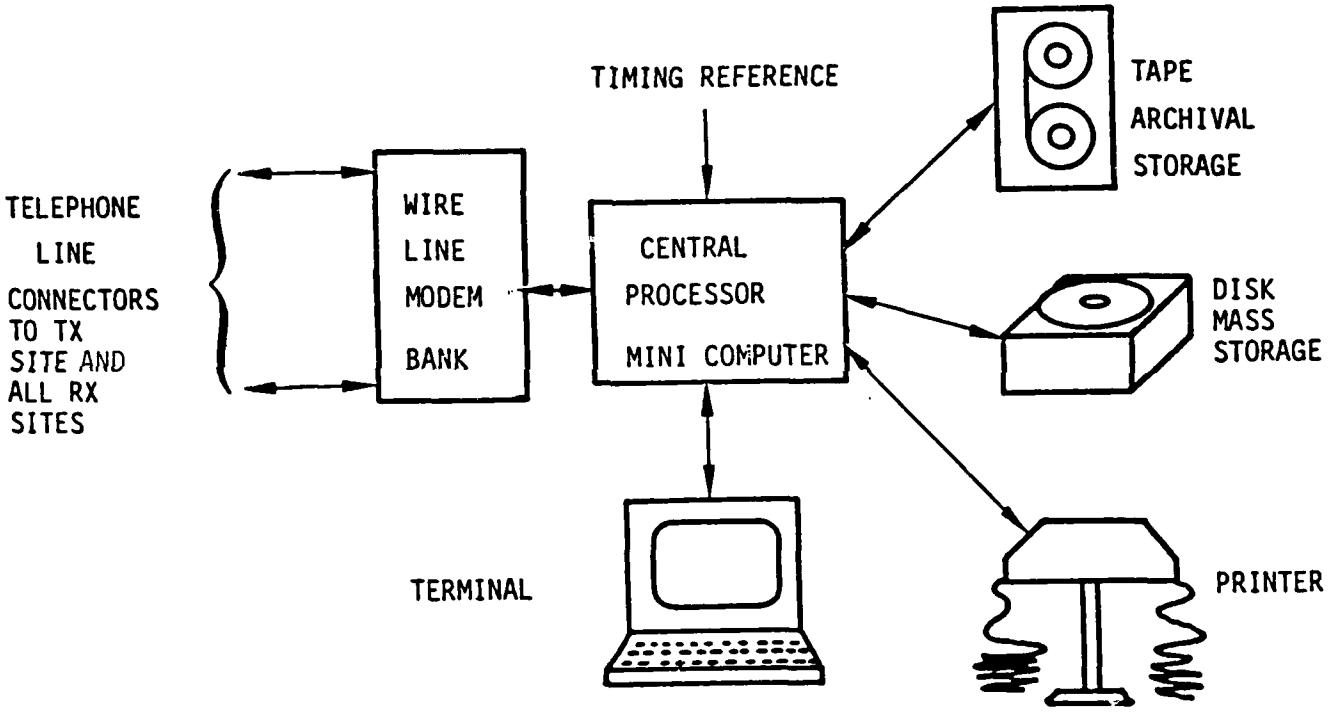

Figure 2.32. Central Processor - Hardware Organization

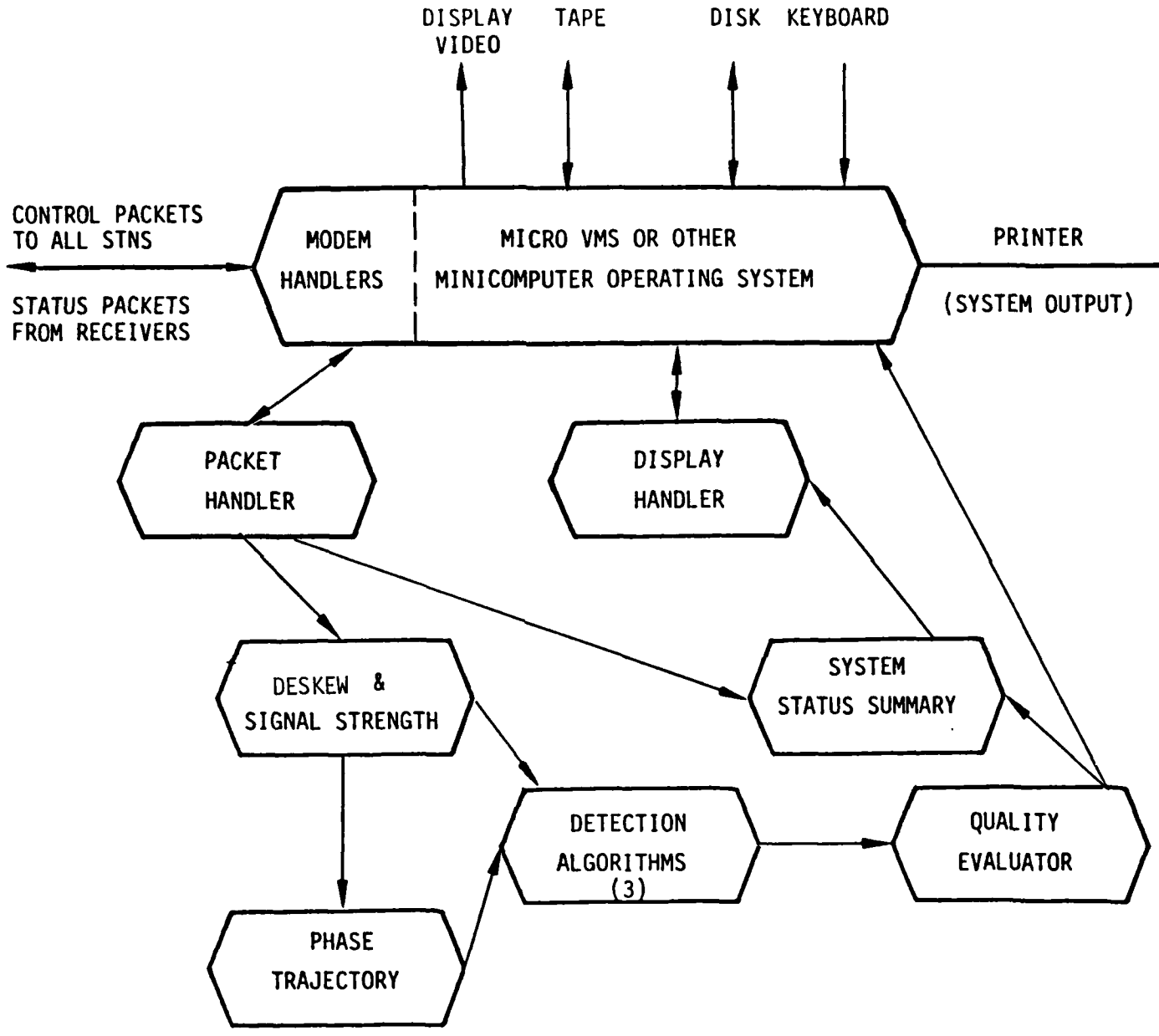

Figure 2.33. Central Processor - Software Organization

2.5 REFERENCES

1. D. K. Bailey, R. Bateman, and R. C. Kirby, "Radio Transmission by Scattering and Other Processes in the Lower Ionosphere," Proc. IRE, 43, pp. 1181-1230, 1955.

2. W. C. Bain, "The Azimuth Distribution of Oblique Reflections from Meteor Trails and its Relation to Meteor Radiant Distributions," Journal of Atmospheric and Terrestial Physics, 17, pp. 188-204, 1960.

3. V. R. Eshleman, "Theory of Radio Reflections from Electron-Ion Clouds," IRE Transactions on Antennas and Propagation, AP-3, pp. 32-39, 1955.

4. V. R. Eshleman, "The Theoretical Length Distribution of Ionized Meteor Trails," Journal of Atmospheric and Terrestial Physics, 10, pp. 57-72, 1957.

5. V. R. Eshleman and L. A. Manning, "Radio Communication by Scattering from Meteoric Ionization," Proc. IRE, 42, pp. 530-536, 1954.

6. J. S. Greenhow and J. E. Hall, "The Variation of Meteor Heights with Velocity and Magnitude," Monthly Notices Royal Astron. Soc., 121, pp. 174-182, 1960.

7. J. S. Greenhow and E. L. Neufeld, "The diffusion of Ionized Meteor Trails in the Upper Atmosphere," J. Atmos. Terr. Phys., 6, p. 133, 1955.

8. E. J. Haakinson, "Meteor Burst Communications Model," NHTIA Report 83-116, U.S. Department of Commerce, February 1983.

9. G. S. Hawkins, "Variations in the Occurrence Rate of Meteors," Astonomical Journal, 61, pp. 386-391, 1956.

10. G. S. Hawkins, "A Radio Survey of Sporadic Meteor Radiants," Monthly Notices of the Royal Astron. Soc., 116, pp. 92-104, 1956b.

11. J. S. Hey and G. S. Stewart, "Derivation of Meteor Stream Radiants by Radio Reflexion methods," Nature, 158, pp. 481-482, 1946.

12. C. O. Hines, "Diurnal Variations in Forward-Scatter Meteor Signals," J. Atmos. Terr. Phys., 9, pp. 229-232, 1956.

13. A. C. B. Lovell and J. A. Clegg, "Characteristics of Radio Echoes from Meteor Trails," Proc. Phys. Soc., 60, p. 491, 1948.

14. L. A. Manning, "The Initial Radius of Meteoric Ionization Trails," Journal of Geophysical Research, 63, pp. 181-196, 1958.

15. D. W. R. McKinley, Meteor Science and Engineering, McGraw-Hill Book Company, New York, NY, 1961.

16. M. L. Meeks, J. C. James, "On the Influence of Meteor-Radiant Distributions in Meteor-Scatter Communications," Proc. IRE, 45, pp. 1724-1733, 1957.

17. M. L. Meeks, J. C. James, "Meteor Radiant Distributions and the Radio-Echo Rates Observed by Forward Scatter," J. Atmos. Terr. Phys., 16, 228-235, 1959.

18. G. F. Montgomery and G. R. Sugar, "The Utility of Meteor Bursts for Intermittent Radio Communication," Proceedings of the IRE, 45, pp. 1684-1693, 1957.

19. Naval Ocean Systems Center, Analysis of Meteor Burst Communications for Navy Strategic Applications, MCC Document 797, Feb. 1980.

20. J. D. Oetting, "An Analysis of Meteor Burst Communications for Military Applications," IEEE Transactions on Communications, COM-28, pp. 1591-1601, 1980.

21. G. W. Pickard, "A Note on the Relation of Meteor Showers and Radio Reception," Proceedings of the IRE, 19, pp. 1166-1170, 1931.

22. G. R. Sugar, "Radio Propagation by Reflections from Meteor Trails," Proceedings of the IEEE, 52, pp. 116-136, 1964.

23. L. Vancil, "VHF Meteor Scatter Communications," Ham Radio, 1984.

24. D. G. Villard, V. R. Eshleman, L. A. Manning, A. M. Peterson, "The Role of Meteors in Extended-Range VHF Propagation," Proc. IRE, 43, pp. 1473-1481, 1955.

3.0 TECHNICAL APPROACH

As mentioned in the introduction, the VHF Reception Program - Phase II is intended to be the simplest that resolves the outstanding physics issues concerning diversity reception of meteor path propagation. These issues are summarized by the following questions.

- Gain vs. Beamwidth

  What is the gain vs. beamwidth tradeoff on a single receiver antenna?

- Angular Diversity

  Can independent meteor propagation paths be obtained at a single location using multiple receiver antennas?

- Spatial Diversity

  What spatial separation is needed to obtain independent paths from a common volume?

We have found that the simplest and least expensive approach to addressing these issues is one suggested to us by Dr. Fred Quelle, the Scientific Officer of the Phase I program. This approach calls for a central receiver site and multiple transmitter sites. The central receiver site contains three Yagi antenna arrays and a single receiver. It should be located where the Phase II program will be principally performed. The transmitter sites should be located at appropriate locations to achieve the necessary spatial and angular diversity. The transmitters should be unattended, and turned on and off by simple telephone commands.

The simplest approach has also been taken for signal processing. To resolve the physics issues of Phase II, the data required is percent copy of each transmitter. Therefore, the simplest signal from each transmitter is continuous, steady transmission at a single frequency. To differentiate the signals from each individual transmitter during simultaneous transmission, each transmitter would operate at a slightly different sideband of the same carrier frequency, such as 40 MHz. Four transmitters might transmit at 40 MHz + 500 Hz, 40 MHz + 800 Hz, 40 MHz + 1100 Hz, and 40 MHz + 1400 Hz. At the receiving site, the principal carrier frequency would be subtracted from the incoming signals, so that the transmitter signals would

produce distinct audible tones at 500 Hz, 800 Hz, 1100 Hz, and 1400 Hz. The data would then be collected on a tape recorder for subsequent analysis.

It is worth reemphasizing that the objective of the Phase II program is not to simulate applications, such as reception of noncooperative tactical VHF communications, but rather to address physics issues that must be resolved in order to develop the capability to design optimal netted diversity reception communications systems. This objective justifies, for example, the use of steady tones as signals, and justifies invoking reciprocity to consider a system with multiple transmitters and a single receiver, even though reciprocity does not strictly hold in meteor burst communications, as explained in Subsection 2.2. The duty cycle differs when a receiver and transmitter exchange locations, owing to asymmetries in the number of meteor bursts over different locations, particularly along east-west paths. The JAYCOR MBCS code accounts for these asymmetries, however, and provides a valid standard against which to compare data from any receiver/transmitter configuration. Therefore, the proposed configuration is just as valid for addressing the physics issues as the more compex and expensive alternatives that have been considered.

One disadvantage of the proposed configuration is that multiple transmitters imply multiple FCC authorizations, and the authorizations must be coordinated in frequency. We have been told, however, that obtaining authorizations for government-sponsored transmissions is a relatively straightforward procedure requiring only 90 to 180 days in many cases. Since the authorizations must be coordinated in frequency and are site-specific, somewhat more time should be allowed for obtaining the authorizations, and ample redundancy should be provided in the number of sites for which one seeks authorizations.

The transmitter sites should be provided by military bases and government property at no cost for land use to the Phase II program. Indications are that military bases will provide land and utilities, but will want the experimenters to provide a shed or trailer for their equipment.

We have received preliminary approval to locate a central receiving site at Camp Elliot, which is in the eastern part of NAS Miramar. Because Camp Elliot is at the northeastern outskirts of San Diego, and the receiving antennas would be looking north and east only, interference by RF noise

from San Diego is expected to be moderate. Housing for the experimental equipment will also be available at Camp Eliot.

This completes the discussion of the strategy of the overall approach to the Phase II program. The rationale behind the specific technical approach to each of the physics issues is summarized in the remainder of this section.

3.1 Gain vs. Beamwidth

To a good approximation, the power in the main lobe of an antenna is inversely proportional to the angular width of the main lobe. This relation allows some flexibility in the design of antennas for meteor-burst communications systems. To date, virtually all meteor-burst communications systems have used wide-beam antennas, with main lobes having 3 dB points typically separated by about 40° or 50°.

An unresolved physics issue is whether it may be advantageous to focus a receiving antenna to a smaller beam at a higher gain. Of course, the smaller beam subtends a smaller field of view and encompasses fewer meteor bursts per hour. But the higher gain of the antenna compensates to some extent by making more reflected signals observable per unit solid angle. Whether there might be a net gain of percent copy by focusing a receiving antenna, and what the optimal gain and beamwidth are for a given transmitter/receiver configuration are the issues to be addressed.

The Monte-Carlo code, MBCS, which was developed in the Phase I program, was exercised to get a preliminary estimate of the gain vs. beamwidth tradeoff. The code simulated the SNOTEL transmitters in Boise, Idaho and Ogden, Utah and a receiver antenna array in San Diego similar to that proposed for the Phase II program.

The receiver antenna array will be capable of producing three beamwidths of 10°, 16°, and 40° with corresponding gains of 18 dB, 16 dB, and 12 dB, respectively. Note the near exact inverse relationship between beamwidth and received power (not gain). Beamwidths smaller than 10° are very difficult to achieve owing to practical limitations on antenna array sizes and the physical effects of the partially conducting ground plane of the earth.

Because the code simulates random arrival of meteors and contains numerous physical effects, each simulation runs 5 to 8 hours on an IBM PC. The present implementation of the code on a microcomputer avoids CPU costs

and is convenient for overnight runs. Available time in the Phase I program did limit, however, the scope of our predictions. We only had time to consider the receiving beam to be aimed directly at each of the transmitters in turn. Had we aimed the receiving beams at the hot spots instead, the results would be expected to look completely different.

The results of the MBCS code are summarized in Table 3.1. Table 3.1 shows the percent probability that a meteor channel is active in a receiver at San Diego from transmitters in Boise and Ogden at 0600 and 1200 for three different gain/beamwidth combinations. The pairs of numbers in parentheses represent the 95% confidence interval about the predicted probability. The last column is the probability of connectivity for two antennas operating simultaneously and looking 10° to either side of the great-circle path between the transmitter and receiver.

The MBCS results clearly indicate that when the receiver antenna is pointed directly at the transmitter, wide low-gain beams have greater probability of connectivity. This result is not too surprising, because the wide beams encompass more of the hot spots on either side of the relatively quiescent great circle path between receiver and transmitter. A more interesting calculation that will be done in Phase II is to focus narrow beams individually on the hot spots. Then we might find an optimal beamwidth perhaps comparable to the width of the hot spots.

The three different gain/beamwidth combinations can be readily achieved by selectively activating only certain antennas in each 8-antenna array. This procedure was shown schematically in Figure 2.19.

The Yagi antenna arrays are cheap, but unwieldy and difficult to move once installed. One should plan to have three 8-antenna arrays at the receiving site. Two of the arrays would be permanently fixed. The third array would be rotated according to the test plan (as infrequently as possible) to perform the gain vs. beamwidth experiments and angular and spatial diversity experiments.

The data from the gain vs. beamwidth experiments should be compared with the MBCS code predictions both to validate the code and to develop a good understanding of the gain vs. beamwidth tradeoffs. The benefits will be the capability to design any meteor-burst communications system with optimal beamwidth.

TABLE 3.1. PERCENT PROBABILITY OF CHANNEL CONNECTIVITY
(AND 95% CONFIENCE INTERVAL)

TRANSMITTER LOCATION	TIME OF DAY	BEAMWIDTH/GAIN			
		10^{o}/18 dB	16^{o}/16 dB	40^{o}/12 dB	2 x 16^{o}/16 dB
Boise	6:00 a.m.	9.7% (7.2,12.4)	11.8% (9.1,14.8)	12.6% (9.8,15.6)	18.8% (15.5,22.4)
	12:00 noon	2.8% (1.5,4.4)	3.5% (2.1,5.3)	4.9% (3.1,6.9)	8.9% (6.5,11.5)
Ogden	6:00 a.m.	8.9% (6.6,11.6)	10.7% (8.1,13.5)	10.1% (7.6,12.9)	17.8% (14.6,21.3)
	12:00 noon	2.7% (1.5,4.4)	4.1% (2.5,6.0)	4.8% (3.1,6.9)	8.2% (6.0,10.8)

3.2 Angular Diversity

If neighboring antenna arrays directed towards different parts of the sky could receive signals uncorrelated with each other, then this would have significant tactical implications for deployment of a meteor burst communications system. It would suggest, for example, that receiving arrays could be colocated and increase the combined percent copy by receiving independent paths.

The COMET system operating in Europe has already shown that wide-beam receiving antennas, when directed at a common volume, do not obtain independent paths, even when separated by 35 km. This result does not address the question, however, of whether narrow-beam antennas, focused on separate hot spots can obtain independent paths. We exercised the Meteor Burst Communications Simulation code to get a preliminary answer.

The results of the MBCS code were surprising, but made sense in retrospect. Since the two hot spots are typically separated by the order of 100 km, and since typical meteor trails are tens of km long, we originally expected that signals received by each of two beams focused on separate hot spots would be uncorrelated. The MBCS code suggests otherwise.

The code was run again to simulate the SNOTEL transmitters in Boise and Ogden and an 8-antenna Yagi array in San Diego. In the simulation, four antennas in the array produced a 16° receiving beam at 16 dB directed 10° to the left of the great circle path to the transmitter, while four other antennas produced a similar beam 10° to the right. The main lobes of the two beams did not overlap within the 3 dB points. The simulation was done first for the transmitter at Boise and then for Ogden. Boise and Ogden subtend an angle of 20° from San Diego.

Table 3.2 shows the results of this simulation. P(L) and P(R) are the probabilities that the left channel (10° to the left of the great circle path) and right channel are active, respectively. P(L/R) is the probability that the left channel is active at any time that the right channel is known to be active. P(R/L) is the reverse. The correlation coefficient is a measure of the correlation of signals between left and right channels. In all cases, the possibility that the left and right channels are uncorrelated in less than one part in one thousand.

TABLE 3.2. PERCENT PROBABILITY OF ACTIVE CHANNELS AND CORRELATIONS OF TWO CHANNELS

		PROBABILITIES OF ACTIVE CHANNELS				CORRELATIONS	
TRANSMITTER LOCATION	TIME OF DAY	P(L)	P(R)	P(L/R)	P(R/L)	CORRELATION COEFFICIENT	PROBABILITY OF NO CORRELATION
Boise	6:00 a.m.	9.4% (7.0,12.1)	11.4% (8.7,14.3)	17.0%	20.1%	0.164	< 0.1%
	12:00 noon	1.6% (0.7,2.9)	8.2% (5.9,10.7)	11.3%	57.3%	0.168	< 0.1%
Ogden	6:00 a.m.	8.4% (6.2,10.0)	12.3% (9.6,15.3)	23.7%	34.6%	0.140	< 0.1%
	12:00 noon	1.9% (0.9,3.3)	6.9% (4.9,9.3)	9.0%	33.0%	0.122	< 0.1%

The reason that the MBCS code shows such strong correlations between beams directed at separate hot spots is that the side lobes of the beams, although down by more than about 10 dB at the location of the other hot spot, still have enough gain to pick up many of the meteor trails in the other hot spot.

The MBCS code, as presently configured assumes a dipole-antenna receiving pattern. A more realistic receiving pattern corresponding to the Yagi antenna array will be put into the code in Phase II, but the results are expected to be qualitatively similar.

The experimental configuration for testing these predictions was shown in Figure 2-20. The gain and beamwidths of the two beams will be the same as in the simulations. The beams will be directed towards the hot spots on either side of the transmitter. Correlations of signals from different transmitters will be observed as the overlapping of the audible tones from each of the two receiving arrays. Tests will be done for transmitters in different directions and at different times of day to include the effects of the diurnal cycle of the hot spot intensities.

Although the code suggests that the signals from the hot spots will be correlated, it also suggests that there may be an advantage of using split receiver beams. The last column of Table 3.1 showed that the highest probability of channel connectivity is achieved by using all eight antennas in the array to produce two beams aimed at separate hot spots. The increase in percent connectivity over the next best configuration, which was a wide beam directed along the great circle path to the transmitter ranged from 50% to 80% in the cases examined.

Perhaps the advantage of the split beam is more clearly displayed in terms of meteor bursts observed per hour. Table 3.3 shows these code results for the same simulation as in Table 3.1. Again, 95% confidence intervals are given. The results show that for a receiving beam directed along the great circle path to the transmitter, wide, low-gain beams are preferable, but a split beam, with each looking at separate hot spots, picks up the most meteors per hour.

This is not to say that a split beam is the optimal configuration. By no means have all likely configurations been tried in the simulations. For example, a single, high-gain narrow beam directed at a single hot spot has not yet been simulated. It is quite conceivable that the optimal

TABLE 3.3. METEOR BURSTS OBSERVED PER HOUR (AND 95% CONFIENCE INTERVAL)

TRANSMITTER LOCATION	TIME OF DAY	BEAMWIDTH/GAIN			
		10^{o}/18 dB	16^{o}/16 dB	40^{o}/12 dB	2 x 16^{o}/16 dB
Boise	6:00 a.m.	449.11 (391.0,515.9)	552.12 (480.7,634.2)	739.70 (644.0,849.7)	1050.38 (964.5,1143.9)
	12:00 a.m. (Noon)	139.60 (128.2,152.0)	197.18 (181.1,214.7)	331.12 (304.0,360.6)	508.75 (467.1,554.1)
Ogden	6:00 a.m.	468.11 (407.5,537.7)	629.24 (547.8,722.8)	771.95 (672.0,886.7)	1077.38 (989.3,1173.3)
	12:00 a.m. (Noon)	151.56 (139.2,165.1)	211.56 (194.3,230.4)	314.90 (289.2,342.9)	443.89 (407.6,483.4)

AD-A159 891 CONCEPTS FOR NEAR CONTINUOUS RECEPTION OF VHF (VERY HIGH FREQUENCY) SIGNA..(U) JAYCOR SAN DIEGO CA F FELBER ET AL. 15 JUL 85 JAYCOR-J200-85-875/2393 2/2

UNCLASSIFIED N00014-84-C-0730 F/G 17/2.1 NL

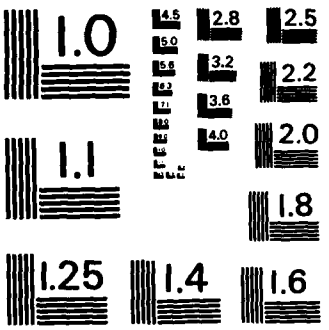

configuration is a single beam that changes direction every twelve hours to focus on the hotter hot spot.

The purpose of the angular diversity experiments would be to develop an understanding of the physics issues determining optimal antenna configurations at a single receiving site through mutually validated experiments and code simulations.

3.3 Spatial Diversity

The issue of spatial diversity considers advantages in a receiving network in terms of percent copy of spatially separated receiving antennas. Alternatively, by reciprocity, one may consider spatially separated transmitting antennas.

Since the MBCS code suggests that colocated receiving antennas directed towards separate hot spots may pick up signals that are stongly correlated, the next question becomes how far apart must the receiving antennas be in order to pick up uncorrelated signals. Some work on this question was done in the COMET network in Europe, but in those experiments the receivers all viewed a common volume. We are more interest in the various configurations that promise higher percent copy by selectively focusing on hot spots. For example, in a two-transmitter system, the optimal percent copy may be achieved by directing one receiving antenna array towards the left hot spot of the left transmitter, and another towards the right hot spot of the right transmitter, and depending on the side lobes to pick up the meteor bursts in the hot spots between. The optimal receiving antenna directions can be expected to be dependent on both angular and spatial separation of the transmitters, beamwidth of the receiving antennas, and time of day.

The experimental configuration to test the correlation of signals obtained by spatially diverse receivers was shown in Figure 2.21. Three receiving antenna arrays would be located at the receiving site. The two arrays pointed at the outermost angular separations would remain fixed. A third would be rotated to point in various directions between the outermost two. This arrangement represents the fewest possible antennas that can address the issue of spatial diversity without requiring impractical amounts of time for reorienting antennas. Similarly, the two transmitters at the outermost angles would remain fixed. A third and possibly a fourth transmitter, which would be operating simultaneously with these two, should

be located at a variety of distances from the receiving site and a variety of directions between the outermost sites.

The diversity achieved in this manner would enable a determination to be made of correlation footprints as functions of range and angle as well as time of day and beamwidth and direction with respect to hot spots. This data is critical to developing the capability to optimize designs of meteor burst communications systems.

Our preliminary designs of the test systems, discussed in Subsection 2.3, were guided by fact that the equipment for the Phase II experiments is simple and cheap, and that the dominating costs are in labor. Where tradeoffs were possible, we have chosen additional equipment to reduce labor costs and overall costs. This is reflected, for example, in the redundancy of receiving antenna arrays.

4.0 PHASE II PROGRAM PLAN

4.1 Phase II Tasks

This subsection discusses the four principal tasks of the VHF Reception Program - Phase II.

TASK 1 - EXPERIMENT PREPARATION

TASK 1.1. Frequency Allocation

The experiment requires the transmission and reception of an RF signal in the low VHF (30-50 MHz) range. It is expected that at any one time, no more than three transmitters will be operating with one central receiver site. Two transmitters will be operating at fixed sites; the third will operate at one of four or five locations. Frequency authorizations will be sought for as many as nine transmitting sites, however, to allow for difficulties in obtaining some authorizations or site use approvals. All sites will be authorized for the same frequency band. A license and frequency authorization to be obtained from the FCC requires the submission of documentation and technical information including specific locations and characteristics of the transmitters and receivers.

TASK 1.2. Facilities Procurement

The use of government space and facilities requires the request for use and coordination of users and hosts to satisfy government or military requirements for support of a government sponsored experiment. Our preliminary discussions indicate that military sites are willing to host experiments provided that the experimenters supply the housing for equipment, such as sheds or trailers.

TASK 1.3. Test Planning

A detailed test plan designed to satisfy the test goals and objectives of the experiment must be developed which provides the general direction and specific instruction for the fielding, operation and data evaluation of the experiment.

TASK 1.4. Test Schedule

A test schedule will identify the sequence of activities based on the definition of milestones and estimates of effort need to accomplish the experiment tasks.

TASK 2 - EXPERIMENT FIELDING

TASK 2.1. Hardware Design

The hardware design will include the selection of commercially available equipment and the integration and, if necessary, design modification needed to perform the experiments defined in the test plan.

TASK 2.2. Procurement

Equipment must be procured based on the equipment specified in the hardware design. A preliminary design should be developed to identify any long-lead items. A cost trade-off should be evaluated to identify the most advantageous buy-rent options based on the hardware design and the test schedule.

TASK 2.3. Fabrication and Assembly

While much of the experiment hardware will be off-the-shelf electronics, the integration and hookup of the interfacing units and the design of selected items will require the fabrication and assembly of the units into an operable system.

TASK 2.4. Installation and Checkout

The installation of the equipment for the VHF reception experiment will require not only the assembly and hookup of the transmitters and receivers and antennas, but will include accurate surveys to establish the accurate pointing of antennas and antennas arrays.

TASK 3 - TEST OPERATIONS

The proposed VHF reception experiment includes three different experimental efforts that use the antenna arrays to evaluate different experimental configurations. The present concept includes the capability to simultaneously receive 3 different signal paths, and includes the options to vary the gain/beamwidth of the antenna arrays. Each experiment will require the specific configuration of transmitters and receiver antenna arrays defined in the test plan. Data will be acquired and recorded on a scheduled basis. Upon completion of each experiment phase, the antennas will have to be reconfigured to the orientation and configuration needed for the next experiment.

Transmitters will be remotely operated (turned on and off) using normal dial-up telephone control from the central receiver site.

The specific test and an evaluation of test results will determine the selection of options to move one or more of the remote transmitters to different authorized and licensed locations.

TASK 4 - TEST RESULTS

An objective of this proposed VHF reception experiment is to validate existing meteor channel computer models and propagation theory. A set of preliminary predictions which model the experiment configurations will be compared to the experimental data acquired during the test operation phase of the program. A continuing analysis effort will be maintained while test operations are in progress. Quick-look analysis will provide an evaluation of the usefulness of the experimental data and will be used to make adjustments to the test plan to optimize the test configuration and data format. An assessment of the test results and a comparison with predictions will be described.

4.2 Statement of Work

A statement of work for the Phase II program has been developed as follows.

TASK 1 - EXPERIMENT PREPARATION

Perform preliminary authorization activities necessary for the VHF Reception Program - Phase II, including preparation of documentation and coordination needed to obtain proper frequency authorization and government licensing of radio transmitters and radio sites, and approval for the installation of transmitters and receivers on government or military property, and use of services and facilities needed for test operations. Develop a detailed test plan and schedule for the performance of the VHF reception experiment. The plan will provide for the sequencing of the experiment parts to ensure that cyclical effects, such as diurnal and seasonal variations, are included in the acquired data base.

TASK 2 - EXPERIMENT FIELDING

Perform the fielding of the experiment, including the design, procurement, fabrication and assembly of the required hardware and electronics. The equipment will be installed and checked out in accordance with the test plan and schedule.

TASK 3 - TEST OPERATIONS

The test operations will be performed in accordance with the test plan. Operations will include control of the remote transmitter sites, receiver operation, and data recording. The test facilities will be reconfigured as scheduled for each of the various experiments.

TASK 4 - TEST RESULTS

Test results will be evaluated by comparing preliminary modeling and prediction efforts to test data. Assessment of these data will be documented in reports.

4.3 Schedule

A detailed test plan which defines exact test configurations: path orientation (surveyed angular measure from true North), antenna combinations, transmit on-off times, and data collection criteria will be developed based on final site locations and analytical requirements. A representative schedule showing estimated hardware design, procurement and fabrication times, allocation of antenna reconfiguration times and a sequence of daily and seasonal experiment data-taking periods is shown in Figure 4.1.

4.4 Manpower Allocation

Estimates of man-months that should be allocated to each activity in Phase II are displayed in Table 4.1.

TABLE 4.1. MAN-MONTHS ALLOCATED TO PROGRAM ACTIVITIES

ACTIVITY	MAN-MONTHS
Program Management	4
Analysis	6
Experiment Design	4
Installation and Maintenance	8
Test Operations	20
Data Reduction	8
Site Selection, Coordination	3
TOTAL	53

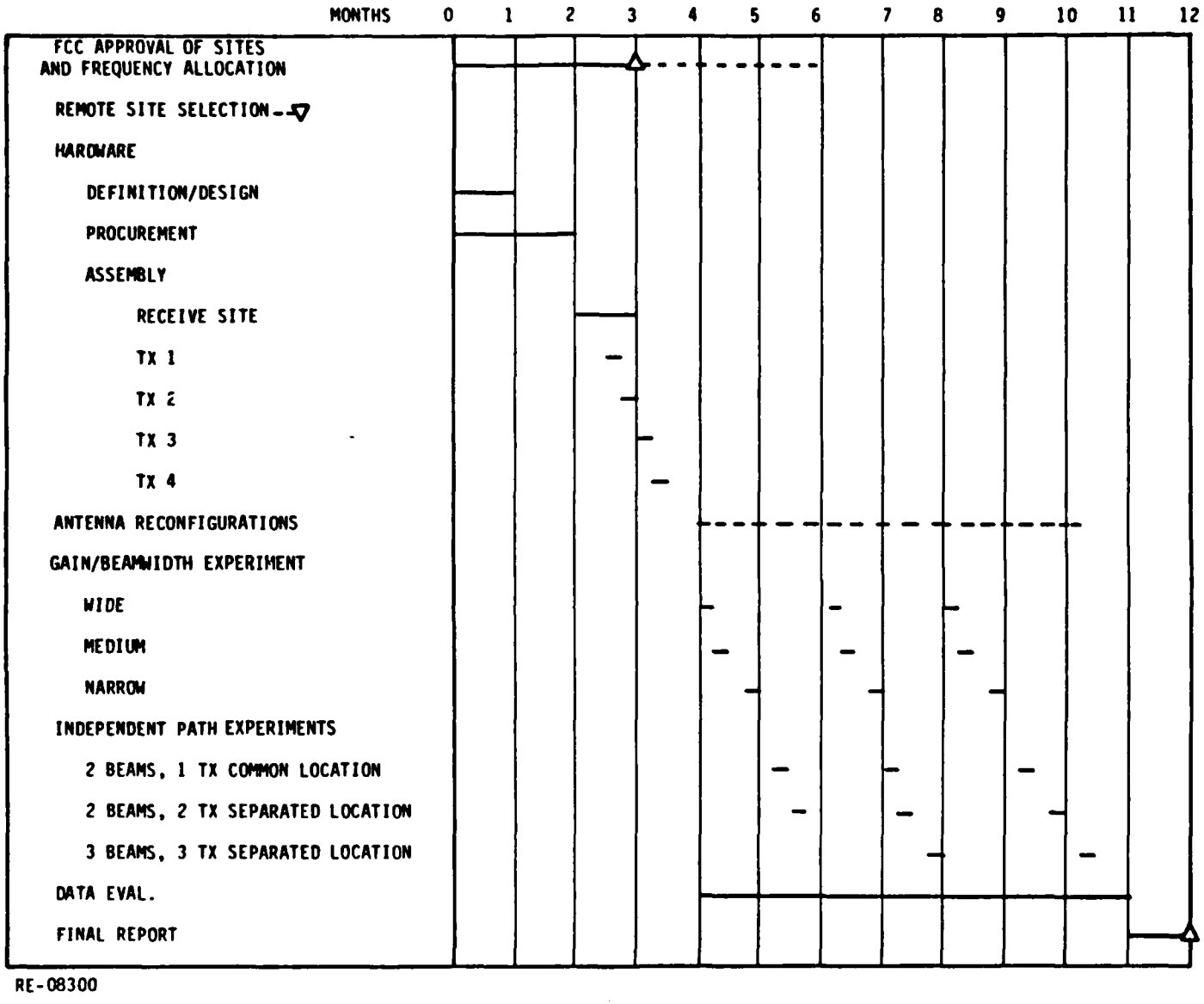

Figure 4.1. Schedule for VHF Reception Program — Phase II

END

FILMED

11-85

DTIC